UNIVERSITÀ DEGLI STUDI DI UDINE
hic sunt futura

www.uniud.it

Corso di dottorato di ricerca in:

"Scienze e Biotecnologie Agrarie"

in convenzione con Fondazione E. Mach

32° Ciclo

Titolo della tesi

"The sociobiology of microbial communities of the plant as an innovative approach to discover new sustainable low impact biofungicides against plant diseases"

in co-tutela con Fondazione E. Mach

Dottoranda: Francesca Brescia

Supervisore: Prof. Paolo Ermacora

Co-supervisore: Prof. Ilaria Pertot

Tutor: Prof. Gerardo Puopolo

Anno di discussione: 2020

Index of contents

Abstract

The ecological role of the genus *Lysobacter* in the plant rhizosphere has received relatively little attention compared to other bacterial genera, such as *Bacillus* and *Pseudomonas*. The aim of this thesis was to analyse the impact of rhizosphere nutrient conditions and of bacteria inhabiting plant-related ecological niches on the physiological traits of *Lysobacter capsici* AZ78 (AZ78), an effective rhizosphere-associated biocontrol agent of phytopathogenic oomycetes.

AZ78 behaviour *in vitro* was studied in two nutrient conditions using a common laboratory growth medium (LBA) and a specific growth medium, the Rhizosphere-Mimicking Agar (RMA). RMA contains artificial root exudates, cellulose, humic acids, lignin, salts and starch. In AZ78 cells grown on RMA, the gene *clp,* involved in biofilm formation and cell motility, was up-regulated compared to LBA. This was reflected in the biofilm formation and production of type IV pili, extracellular appendages involved in cell motility. A metabolomic analysis (MALDI TOF MSI) highlighted an increased production of secondary metabolites in the AZ78 cells grown on RMA compared to LBA. Putative cyclic lipodepsipeptides, cyclic and polycyclic macrolactams and other bioactive secondary metabolites were found exclusively in AZ78 cells grown on RMA. This study revealed AZ78 potential to thrive in the rhizosphere, moving to colonise new niches, forming a biofilm to firmly occupy favourable spaces and producing secondary metabolites to antagonise competitors.

The interactions occurring between AZ78 and rhizosphere-dwelling bacteria represented another part of this thesis. The bacterial strains *Bacillus amyloliquefaciens* S499 (S499) and *Pseudomonas protegens* Pf-5 (Pf-5) were chosen because they belong

to bacterial genera commonly associated to plant rhizosphere. The two- (AZ78 *vs* Pf-5; AZ78 *vs* S499) and three-way interactions (AZ78 *vs* Pf-5 *vs* S499) were studied with a multitechnique approach. The interaction with S499 did not affect negatively AZ78 cell viability, while a slight reduction of AZ78 viable cells was registered during the interaction with Pf-5. However, the decrease in AZ78 viable cells was reduced during the three-way interaction.

During the interaction with S499, AZ78 outer ring was strongly reduced and AZ78 cells were transparent and not motile. In addition, AZ78 inhibitory activity against the phytopathogenic oomycete *Pythium ultimum* was negatively influenced by the presence of S499. A metabolomic analysis highlighted how the presence of S499 negatively modulated the production of secondary metabolites in AZ78. Conversely, the interaction with Pf-5 resulted in an increased AZ78 inhibitory activity both in the two- and three-way interaction. These differences might be linked to the production of pyrrole, a broad-spectrum antibiotic, and cephabacin H1 during the two-way interaction with Pf-5. Moreover, AZ78 produced WAP-8294A1/A2/A4, secondary metabolites toxic against Gram-positive bacteria, during the three-way interaction that may explain the reduced negative effect of S499. A transcriptomic analysis shed light on the strong effect that the presence of S499 was having on AZ78 transcriptome. During all the two- and three-way interactions, AZ78 up-regulated genes involved in a defence response against oxydative stress and in the detoxyfication from antibiotics produced by competitors.

To understand which secondary metabolites produced by S499 were responsible for the negative effects on AZ78, *Bacillus velezensis* (ex. *B. amyloliquefaciens*) FZB42, phylogenetically close to S499, and its mutants deficent for the production of some bioactive secondary metabolites were used. Difficidin and Bacilysin resulted to be the

main secondary metabolites responsible for the negative effects on AZ78 physiology and inhibitory activity.

The overview of AZ78 interactions with the plant-related microbiota was implemented with the study of the effect of grapevine phyllosphere associated bacteria on AZ78 inhibitory activity. The influence of each phyllosphere associated strain on the inhibitory activity of AZ78 was evaluated *in vitro* on LBA. The majority of the Gram-negative strains, in particular belonging to the genus *Pseudomonas,* had a positive effect on AZ78 inhibitory activity against *P. ultimum.* On the other hand, the Gram-positive strains had a negative effect, particularly relevant in the case of *Bacillus* spp. strains. Therefore, the outcome of the interactions was consistent in both the ecological niches of plant rhizosphere and phyllosphere, with the genus *Bacillus* having mainly a negative effect on AZ78.

Overall, this PhD thesis showed that the nutrient conditions and the interactions occurring between *Lysobacter* spp. and the plant microbiota are important factors to be considered in the study of this genus. Indeed, root exudates and microbial interactions may significantly affect the physiological traits linked to competition, to colonisation of ecological niches and to antagonism against plant pathogens

Chapter 1 - Introduction

The Genus Lysobacter

Francesca Brescia[1,2], Ilaria Pertot[1,3], Gerardo Puopolo[1]

[1]Department of Sustainable Ecosystems and Bioresources, Research and Innovation Centre, Fondazione Edmund Mach, 38010 San Michele all'Adige, Italy;[2]PhD school in Agricultural Science and Biotechnology, Department of Agricultural, Food, Environmental and Animal Sciences, University of Udine, 33100 Udine, Italy; [3]Center Agriculture Food Environment, University of Trento, 38122 Trento, Italy.

E-mail address: gerardo.puopolo@fmach.it

Abstract

The genus *Lysobacter* is among the youngest bacterial genera encompassing plant beneficial strains. In the last forty years the number of bacterial species included in this genus increased and the advent of sequencing technologies contributed to shed a light on the characteristics of these bacteria. At this regard, it was proven that the absence of a flagellum is a feature not shared by all the *Lysobacter* species and, moreover, the cell motility of some species mainly relies on the formation of type IV pili. Culture dependent and independent methods revealed that *Lysobacter* members are cosmopolitan bacteria able to colonize different environments and to persist in extreme environments also. Looking at the agroecosystem, strong evidences were provided on the association of these bacteria with plants and their correlation with the phenomenon of soil suppressiveness was also shown. Although their ability to actively colonize plants and soils, the number of *Lysobacter* spp. strains studied for their plant beneficial

potential is still limited. This might be related to the unavailability of growth media specific for the isolation of *Lysobacter* members. In this chapter, a semi-selective growth medium was designed for the isolation of strains belonging to *L. antibioticus*, *L. capsici*, *L. enzymogenes* and *L. gummosus* species, based on their capability to resist antibiotics. Moreover, these species encompass most of the plant beneficial *Lysobacter* spp. strains characterized so far. Their ability to control plant pathogenic bacteria, fungi, nematodes, oomycete and protists mainly relied on various mechanisms of action such as the competition for spaces, the induction of plant defense mechanisms, the predation and the release of antibiotics, lytic enzymes and volatile organic compounds. In the last years, more evidences were provided about the presence of *Lysobacter* spp. in agricultural soils contaminated by heavy metals and petroleum derivatives. Although, in their infancy, several studies proved that bacteria belonging to this genus may be applied for the bioremediation of contaminated agricultural soils. Overall, *Lysobacter* spp. may be considered a valuable reservoir of novel bacterial strains that may be developed to make the future of crop production more sustainable.

Keywords: *Lysobacter*, cell motility, isolation procedure, biological control, lytic enzymes, antibiotics, bioremediation

1. Taxonomy of *Lysobacter*, a forty years old bacterial genus

In the γ-proteobacteria, the Xanthomonadaceae family encompasses a wide variety of bacterial species with diverse ecological functions and significance, from human and plant pathogens to bioremediation and biocontrol agents (Saddler and Bradbury, 2015).

Looking at the bad side of the Xanthomonadaceae family, the genus *Stenotrophomonas,* in particular *S. maltophilia*, is an increasing concern for compromised patients, mostly due to its resistance to many broad-spectrum antibiotics (Adegoke et al., 2017; Osawa et al., 2018). However, it also worth noting that there are some *S. maltophilia* strains with antagonistic potential against plant pathogens, such as *Ralstonia solanacearum*, the causal agent of potato brown rot (Elhalag et al., 2016).

The genera *Xanthomonas* and *Xylella* encompass plant-associated bacteria that may cause serious crop losses. *Xylella fastidiosa*, a xylem limited bacterium causal agent of grapevine (*Vitis vinifera*) Pierce's disease (Van Sluys et al., 2003), is recently threatening the crop production of Mediterranean countries causing losses in olive production (Saponari et al., 2017). Many host-specific phytopathogenic species that cause severe losses in economically important crops are comprised in the genus *Xanthomonas* (Chen et al., 2018b) such as *X. campestris* pv. *campestris*, causal agent of black rot disease of Brassicaceae (Mansfield et al., 2012), *X. euvesicatoria, X. vesicatoria, X. perforans* and *X. gardneri,* causal agents of bacterial spot of tomato and pepper (Horvath et al., 2012; Jones et al., 1995; Kebede et al., 2014, Kim et al., 2010), and *X. oryzae,* causal agent of bacterial blight and bacterial leaf streak of rice (Nino-Liu et al., 2006).

On the other side of the Xanthomonadaceae family, there are bacterial genera that may have a positive impact on the environment, as in the case of the genus

Pseudoxanthomonas. Its first described species, *P. broegbernensis,* was isolated from a biofilter and showed a valuable potential for bioremediation of contaminated sites (Finkmann et al., 2000). Many other members of the genus *Pseudoxanthomonas* have this potential, such as *P. kaohsiungensis* able to produce a biosurfactant that enhances the dissolution of hydrophobic organic contaminants (Biswas et al., 2017) and *Pseudoxanthomonas* sp. YP1 that has potential applications in wastewater nutrient removal, to prevent eutrophication (Wang et al., 2018).

Remaining in the beneficial side of the Xanthomonadaceae family, the genus *Lysobacter* has never been reported to be pathogenic for plants or animals (Christensen and Cook, 1978; Puopolo et al., 2018). This bacterial genus owes its name, literally "the lysing rod", to its ability to lyse many organisms including algae, both Gram-negative and Gram-positive bacteria, fungi, nematodes, oomycetes, and yeasts as well (Christensen, 2015). The genus *Lysobacter* has raised great interest in the last years because of its potential in producing lytic enzymes and novel antimicrobial compounds that can be useful in the war against antibiotic resistance occurring in bacterial human pathogens (Panthee et al., 2016; Puopolo et al., 2018; Xie et al., 2012).

Before the establishment of the genus by Christensen and Cook (1978), *Lysobacter* species were either wrongly assigned to the Myxobacteriales family or misidentified as *Stenotrophomonas* and *Xanthomonas* (Puopolo et al., 2018; Sullivan et al., 2003). Indeed myxobacteria have many characteristics in common with *Lysobacter,* such as gliding motility and high genomic GC content (Reichenbach, 2006). However, differently from myxobacteria, *Lysobacter* cells show higher variability in size and never produce fruiting bodies.

Overall, species belonging to the genus *Lysobacter* are aerobic, Gram-negative thin rods that measure 0.4 – 0.6 × 2-5 μm. The bacterial colonies appear mucoid and in pale colors, ranging from cream-colored, pink, yellow-brownish to brown. Some strains may produce a brown pigment, soluble in water (Christensen and Cook, 1978; Reichenbach, 2006).

Other typical features of this genus are:

- Presence of cells and filaments up to 70 μm long within a population
- High G + C content (65.4 – 70.1%)
- Ubiquinone 8 (Q-8) as the major respiratory quinone
- Oxidase activity
- Optimum temperature for growth at 28°C
- Inability to produce fruiting bodies and microcysts.

Nowadays, there are 48 species belonging to the genus *Lysobacter* (http://www.bacterio.net; Figure 1.1), and their number is constantly increasing also because many previously misidentified bacterial species and assigned to other genera were reclassified as *Lysobacter*, such as the recent reclassification of *Pseudomonas* sp. PB-6250T and *Luteimonas tolerans* as *Lysobacter firmicutimachus* and *Lysobacter tolerans*, respectively (Margesin et al., 2018; Miess et al., 2016).

The increase of the proposal of new *Lysobacter* species was accompanied by the genome sequencing and, at the time of writing, 22 genomes of *Lysobacter* strains are publicly available. Most interest was given to the sequencing of genomes of bacterial strains belonging to *L. antibioticus*, *L. capsici* and *L. enzymogenes*, species that encompass biocontrol agents of phytopathogenic microorganisms. The size of the

sequenced genomes ranged from the 2.54 Mb of *Lysobacter tolerans* UM1^T to the 6.39 of *L. capsici* 55 (Table 1.1).

The availability of the sequenced genomes allowed their comparison with the aim of finding orthologues that may represent the core genome of *Lysobacter* spp.. Liu et al. (2015a) found that the type strains *L. arseniciresistens* ZS79^T, *L. concretionis* Ko07^T, *L. daejeonensins* GH1-9^T, *L. defluvii* IMMIB APB-9^T and the biocontrol agent *L. capsici* AZ78 shared 1,207 genes, a number lower than the one found in the comparison of the genomes of the biocontrol strains belonging to *L. antibioticus*, *L. capsici*, *L. enyzmogenes* and *L. gummosus* species (de Bruijn et al., 2015). Interestingly, the comparison of the genomes of the biocontrol agent *L. capsici* AZ78, the plant pathogen *X. campestris* pv. *campestris* ATCC 33913 and the human pathogen *S. maltophilia* K729a clearly showed the absence of genes known to be involved in infection of humans and plants in *L. capsici* AZ78, this may indicate that *Lysobacter* strains are not harmful bacteria and, as consequence, may be developed as safe biofungicides (Puopolo et al., 2016).

The proposal of new *Lysobacter* species coupled with the genome sequencing allowed to revise a feature thought to be shared by all the members of this bacterial genus. Since the proposal of this genus, *Lysobacter* species have been reported as non-motile by means of flagella but able to glide (Christensen and Cook, 1978). Although the majority of *Lysobacter* species lacks of flagella, exceptions can be found in some recently described *Lysobacter* species, namely *L. spongiicola*, *L. arseniciresistens*, and *L. mobilis*, in which a single polar flagellum was reported (Luo et al., 2012; Romanenko et al., 2008; Yang et al., 2015). Moreover, de Bruijn et al. (2015), comparing four *Lysobacter* species genomes, found that non-functional genes encoding components of the flagellar apparatus were present in the genomes of *L. capsici*, *L. enzymogenes* and *L.*

gummosus. Recently, Tomada et al. (2016) proved that some *Lysobacter* species are characterized by a nutrient-dependent motility and, thus, the non-motile phenotype characterizing *Lysobacter* members may be due to the lack of environmental stimuli that trigger cell motility (Figure 1.2).

Motility in the genus *Lysobacter* mainly relies on the activity of type IV pili and genes encoding components of type IV pili are highly conserved within *Lysobacter* spp. (Chen et al., 2018a; Xia et al., 2018). Cell motility and ability to form biofilm allow *Lysobacter* members to colonize the surface of plant tissues and to efficiently attack their preys since lytic enzymes and antimicrobial compounds can be easily accumulated in the formed biofilm (Xia et al., 2018). Interestingly, *L. capsici* SB-K88, a biocontrol bacterium, was able to perpendicularly attach to the plant root surfaces and to form a strong biofilm by means of brush-like fimbriae (Islam et al., 2005). However, more studies are still required to assess whether this particular way of attachment is a typical feature shared by the members of the genus *Lysobacter*.

2. Ubiquity of *Lysobacter* species and their ecology in the agroecosystem

Before the establishment of the genus *Lysobacter*, several bacterial isolates presumably belonging to this genus were recovered from soil and freshwater samples in works aimed at selecting bacterial strains able to lyse cyanobacteria and algae (Christensen, 2001; Reichenbach, 2006). Accordingly, three of the first four *Lysobacter* species (*L. antibioticus*, *L. enzymogenes* and *L. gummosus*) were isolated from soil, whereas *L. brunescens* DSM 6979^{T}, the type strain of the fourth species, was isolated from a freshwater sample collected in Canada (Christensen and Cook, 1978). In the following

years, other *Lysobacter* species were isolated from sources different than soil and freshwater as the case of *L. spongiicola* isolated from a deep-sea sponge in Philippine Sea (Romanenko et al., 2008).

Lysobacter spp. resulted also associated with other (micro)organisms such as spores of arbuscular mycorrhizal fungi *Glomus geosporum* and *Glomus constrictum* (Roesti et al., 2005), cysts of soybean cyst nematode *Heterodera glycines* (Nour et al., 2003), intestinal apparatus of the fly *Lutzomyia evansi* pupae (Vivero et al., 2016) and the feathers of penguins *Pygoscelis papua* and *Pygoscelis adeliae* in Antarctica (Pereira et al., 2014).

Furthermore, the employment of molecular techniques broadened our knowledge about the range of the habitats colonized by *Lysobacter* members, including extreme environments. For instance, 16S rRNA gene sequences from *Lysobacter* members were retrieved from samples collected from hot mud (87°C) deriving from a hydrothermal spring system (Brito et al., 2014), glacial soils (Liu et al., 2015b; Yang et al., 2016) and bio-aerosols from Antarctica (Bottos et al., 2014). Several new established *Lysobacter* species originated from extreme environmental conditions, as in the case of the type strains *L. thermophilus* YIM 77875^T and *L. oligotrophicus* 107-E2^T, respectively isolated from a geothermal soil and freshwater samples from Antarctica (Fukuda et al., 2013; Wei et al., 2012).

Studies dealing with the characterization of microbial communities inhabiting the agroecosystem clearly showed that *Lysobacter* spp. are common inhabitants of agricultural soils. Indeed, type strains of two *Lysobacter* species were isolated from ginseng soils (Choi et al., 2014; Lee et al., 2006a) while four other species were isolated from greenhouse soils in South Korea (Kim et al., 2016; Weon et al., 2006; 2007).

Soil texture and pH are some environmental factors determining the *Lysobacter* spp. abundance in agricultural soils. Before the establishment of the genus, bacterial strains resembling *Lysobacter* members were commonly isolated from soils with high pH values ranging from 6 to 8.8 (Reichenbach 2006). Accordingly, Postma et al. (2008; 2011) showed that the abundance of *Lysobacter* spp. in soils collected from organic farms positively correlated with pH and clay content. However, *Lysobacter* spp. were found in high abundance also in the rhizosphere of potato plants grown in sandy soils (Turnbull et al., 2012) and in the rhizosphere of *Calystegia soldanella* and *Elymus mollis* plants grown in coastal sand dune (Lee et al., 2006b). The abundance of *Lysobacter* members in agricultural soils is also positively modulated by the presence of biomacromolecules since it was shown that they are actively involved in the degradation of complex compounds and the subsequent release of readily available nutrients in the soil food web (Lueders et al., 2006). The positive effect of complex biomacromolecules on *Lysobacter* spp. abundance was confirmed by the application of bioorganic fertilizers in apple orchard soil, alfalfa in greenhouse soil, and protein-rich waste yeast, or chitin in clay soil from fields deputed to cauliflower production (Huang et al., 2016; Postma and Schilder 2015; Wang et al., 2017).

Regarding the ability to colonize plants, *L. capsici*, *L. fragariae*, *L. oryzae* and *L. solanacearum* type strains were respectively isolated from the rhizosphere of pepper (*Capsicum annuum*), strawberry (*Fragaria* × *ananassa*), rice (*Oryza sativa*) and tomato (*Solanum lycopersicum*) plants (Aslam et al., 2009; Kim et al., 2017; Park et al., 2008; Singh et al., 2015). *Lysobacter* spp. may colonize also other plant tissues and live endophytically inside the plants as in the case of *L. gummosus* L101, an endophyte of Styrian oil pumpkin (*Cucurbita pepo*) plants. The presence of *L. gummosus* L101 cells in Styrian oil pumpkin endosphere contributed to the increase of harvest yields and the

decrease of losses due to the attacks by the fungus *Sphaerotheca fuliginea*, causal agent of powdery mildew of cucurbits (Fürnkranz et al., 2012). Moreover, it was shown that *Lysobacter* spp. represented a dominant taxon of the seed microbiome of 14 Styrian oil pumpkin genotypes (Adam et al., 2016).

Lysobacter 16S rRNA sequences were dominant in the rhizosphere of soybean (Liang et al., 2014), wheat (Qin et al., 2016) and maize plants grown in alkaline soils (pH 8.5) rich in carbonate (García-Salamanca et al., 2013). Recently, Rodrigues et al. (2018) showed that *Lysobacter* spp. was part of the core microbiome of switchgrass rhizosphere by mining the data deriving from 31 switchgrass rhizosphere community habitats collected from different soils and environment using the webtool COREMIC. On the basis of the role played by *Lysobacter* spp. in the degradation of macromolecules with the subsequent release of nutrients available for the soil microflora, it is tempting to speculate that *Lysobacter* spp. may play a key role in the microbiome of plant species including crop plants. Thus, the presence of members of this bacterial genus in the soil may be considered as an indicator of soil fertility.

3. Correlation of *Lysobacter* spp. with soil suppressiveness and isolation of bacterial strains belonging to plant beneficial species

Several studies dedicated to the assessment of microbial taxa associated with disease conducive and suppressive soils showed an interesting correlation between these phenomena and the abundance of *Lysobacter* spp. in soils. Recently, a decrease in *Lysobacter* spp. abundance was observed during tobacco monoculture span and this event was associated with an increase of tobacco bacterial wilt disease caused by *R. solanacearum* (She et al., 2017). A clear positive correlation between abundance of

Lysobacter 16S rRNA gene sequences was observed in fields with naturally occurring suppression of potato common scab caused by *Streptomyces* spp. (Rosenzweig et al., 2012). Similarly, Castillo et al. (2017) found *Lysobacter* spp. 16S rRNA gene sequences in high abundance in potato soils in Colorado. This higher content of *Lysobacter* spp. corresponded in a decrease in the presence of *Meloidogyne chitwoodi* and *Pratylenchus neglectus*, two important pathogenic nematodes potato (*Solanum tuberosum*; Castillo et al., 2017).

Other evidences on the correlation between *Lysobacter* spp. and disease suppressiveness derived from the extensive studies aimed at understanding the causes of the disease suppressiveness against *Rhizoctonia solani* occurring in agricultural soils in The Netherlands. The analysis of agricultural soils of 10 organic farms located in different locations of The Netherlands and multiple regression analysis supported the involvement of *L. antibioticus* and *L. gummosus* antagonistic strains in the control of *R. solani* in clay soils (Postma et al., 2008). *Rhizoctonia*-suppressive clay soils were also characterized by a significant high abundance of *L. capsici* species (Postma et al., 2010a). The correlation between the abundance of *Lysobacter* spp. populations and suppressiveness was further confirmed by quantitative TaqMan PCR detection, that revealed a larger *Lysobacter* spp. population in suppressive than in conducive soils (Postma et al., 2010b). However, further studies showed that *L. antibioticus*, *L. capsici*, *L. enzymogenes* and *L. gummosus* strains are not the unique actors in the control of *R. solani* and future investigation are needed to better understand the role played by these bacteria in suppressive soils (Gómez Expósito et al., 2015; Postma and Schilder, 2015).

To better investigate the role played by *Lysobacter* spp. in the control of soil-borne diseases, there is the need to specifically isolate these bacteria from plant tissues and soils. At the moment, the lack of a selective medium enabling the isolation of

Lysobacter species might undermine the understanding of the real impact that these bacterial species may have on plant health. Indeed, *Lysobacter* strains are slow growers and, on solid microbiological growth media, they may be outcompeted by other fast growing plant associated bacterial species, such as *Bacillus* spp. and *Pseudomonas* spp.. Thus, a semi-selective medium that favors the growth of *Lysobacter* spp. minimizing the competition brought by fast growing bacterial species was designed in order to address this issue.

Most of the type strains of *Lysobacter* spp. associated to plants and inhabiting agricultural soils were isolated using the R2A medium, whereas few exceptions were isolated using Nutrient Agar, Tryptic Soy Agar and Yeast Cell Agar (Table 3.1). Interestingly, *L. erysipheiresistens* RS-LYSO-3^T was isolated using a modified LB medium amended with tobacco root exudates, indicating that the bacterial species has the potential to metabolize the nutrient exuded by tobacco plants in the rhizosphere (Xie et al., 2016). However, based on these works, it is conceivable that R2A has a carbon/nitrogen ratio and a quantity of minerals appropriate for the growth of a large set of *Lysobacter* members.

To design a semi-selective medium for plant beneficial *Lysobacter* spp., R2A was chosen as a standard medium that might be modified to preferentially isolate bacterial strains belonging to *L. antibioticus*, *L. capsici*, *L. enzymogenes* and *L. gummosus*, the species mostly investigated for their correlation with soil suppressiveness (Postma et al., 2008; 2010ab). The evidence that resistance to antibiotics commonly used in molecular cloning techniques is a common trait shared by *Lysobacter* members (Zhang et al., 2017), led to the selection of antibiotics that may be used to reduce the negative impact of fast growing plant associated bacteria at the moment of the dilution plating. The type strains of the *L. antibioticus*, *L. capsici*, *L. enzymogenes* and *L. gummosus* species were

tested for their ability to resist antibiotics according to Puopolo et al. (2016). In this analysis, *B. velezensis* FZB42 (DSM 23117) and *P. protegens* Pf-5 (ATCC BAA 477) were included as representatives of plant associated fast growing bacteria (Fan et al., 2018; Paulsen et al., 2005). The growth of *B. velezensis* FZB42 was inhibited by all the antibiotics tested whereas *P. protegens* Pf-5 growth was inhibited by gentamicin, kanamycin, streptomycin and tobramycin only (Table 3.2).

Within the *Lysobacter* type strains, *L. enzymogenes* DSM 2043^{T} was the most insensitive to antibiotics, being inhibited only by chloramphenicol, gentamicin and vancomycin, whereas *L. capsici* DSM 19286 ^{T} was the most sensitive to the antibiotics tested. However, the four *Lysobacter* type stains used in the analysis shared the same insensitivity to kanamycin, streptomycin and tobramycin (Table 3.2), antibiotics that, at the same time, were toxic to *B. velezensis* FZB42 and *P. protegens* Pf-5. Therefore, a modified R2A containing kanamycin (5 mg/L), streptomycin (10 mg/L) and tobramycin (1 mg/L) was compared with R2A to assess its selectivity towards *Lysobacter* species. Cell suspensions in saline solution (NaCl 0.85%) containing 1 x 10^{8} Colony Forming Units (CFU)/mL were prepared for each bacterial strain and serially diluted (from 10^{-1} to 10^{-7}) and spread onto R2A and R2A amended with antibiotics. After 48 h incubation at 27°C, the counting of CFU clearly indicated that adding the three antibiotics may be a fast and easy method to specifically recover *L. antibioticus*, *L. capsici*, *L. enzymogenes* and *L. gummosus* strains from soils and plant tissues. Indeed, no significant differences in the quantity of CFU counted on R2A and R2A amended with kanamycin, streptomycin and tobramycin were observed in the case of the four *Lysobacter* spp. (Figure 3.1).

On the contrary, no CFU were counted on R2A amended with the selected antibiotics in the case of *B. velezensis* FZB42, whereas a significant reduction of six orders of magnitude in the quantity of counted CFU was registered in the case of *P. protegens* Pf-5 (Figure 3.1). Thus, it is highly conceivable that the use of kanamycin, streptomycin and tobramycin in R2A might represent an advantage for the growth of bacterial strains belonging to *L. antibioticus*, *L. capsici*, L*. enzymogenes* and *L. gummosus* species living in soils or plant tissues. This specific medium may be associated with enrichment phases where lytic properties of *Lysobacter* spp. may be used to increase their number in the soil samples before proceeding with the dilution plating (Christensen and Cook, 1978). At the best of our knowledge, this is the first time that a semi-selective medium for the isolation of plant beneficial *Lysobacter* spp. has been designed and it might be helpful in future works aimed to select new *Lysobacter* strains able to effectively protect crop plants.

4. Plant beneficial role of *Lysobacter* spp. relies on multiple mechanisms of action

The genus *Lysobacter* is a promising source of biocontrol agents of plant diseases because of its broad spectrum activity against diverse plant pathogenic microorganisms. More importantly, it was shown that *Lysobacter* biocontrol agents may act through multiple mechanisms such as competition for spaces, predation, induction of plant resistance mechanisms, production of antibiotics, lytic enzymes and toxic compounds (Table 4.1). This multiple-mechanism mode of action is a very important key feature for a biocontrol agent, since the selection of resistant populations of plant pathogenic microorganisms is less likely to occur (Puopolo et al., 2018).

Mining of *Lysobacter* sequenced genomes has confirmed the presence of an impressive amount of genes encoding different lytic enzymes (Figure 4.1), which have a key role for the degradation of complex macromolecules present in soil as well as for the degradation of the cell wall of plant pathogenic microorganisms (de Bruijn et al., 2015; Puopolo et al., 2016).

Undoubtedly, proteases which catalyze the hydrolysis of peptide bonds are the most studied enzymes produced by members of this bacterial genus due to their biotechnological application and the involvement in the control of plant pathogenic microorganisms. Regarding biotechnological application, cold-adapted proteases received remarkable attention for the possibility to decrease the energy cost of substrate transformation (Joshi and Satyanarayana, 2013). Antarctic *Lysobacter* strains, as *Lysobacter* sp. A03 isolated from penguin feathers in the Antarctic region, are good candidates for the isolation of cold-tolerant proteases (Pereira et al., 2014, 2017). Another important application of proteases is the cleaning of medical and industrial equipment from pathogenic bacteria, as it was proposed for the biofilm degradation activity of *L. gummous* DSM 6980^{T} (Gökçen et al., 2014). In addition, proteases can hydrolyze peptidoglycan, the major component of the bacterial cell wall and, in nature, they are exploited by many bacterial species to antagonize each other. *Lysobacter* sp. XL1 produces proteases that have a broad antimicrobial spectrum and can antagonize not only plant pathogenic bacteria, such as *Erwinia carotovora* and *Erwinia marcescens* (Vasilyeva et al., 2008, 2014), but also fungi and yeasts (Ryazanova et al., 2005). Plant pathogenic nematodes are another target for bacterial proteases, since their cuticle is mainly constituted by proteins. *Lysobacter capsici* YS1215 effectively controlled second-stage juveniles of root-knot nematodes in tomato plants by releasing lytic enzymes such as gelatinases (Lee et al., 2013a, 2015).

Other important enzymes produced by the genus *Lysobacter* are chitinases that can be employed against fungi, insects and, nematodes, as chitin is an important component of their cell wall structures and of nematodes egg shell. For instance, Zhang and Yuen (2000a) showed that *L. enzymogenes* C3 inhibited, both *in vivo* and *in vitro*, the fungal pathogen *Bipolaris sorokiniana* through chitinase production causing the deformation of conidia and the formation of abnormal germ tube. Later, two chitinases of 32 and 48 kDa produced by *L. enzimogenes* C3 were identified (Zhang et al., 2001). However, the biocontrol mechanism of this strain was not exclusively due to these lytic enzymes, as proved by Choi et al. (2012) that compared *L. enzimogenes* C3 wild type and mutants unable to produce chitinases. On the other hand, biocontrol activity of the same strain against *B. sorokiniana* and *Pythium ultimum* was reported to be positively correlated with production of glucanases (Palumbo et al., 2005). The β-1,3-glucanases produced by *L. enzymogenes* C3 and N4-7 were purified and characterized and the genes, namely *gluA, gluB* and *gluC,* involved in their production were identified (Palumbo et al., 2003, 2005).

Besides fungal pathogens, chitinases produced by *Lysobacter* members can effectively control root-knot nematodes and thus promote the plant growth (Lee et al., 2013a, 2015). *Lysobacter enzymogenes* C3 consistently reduced the hatching of nematodes but had also a negative effect on their reproduction (Chen et al. 2006). Since chitin is part of the egg shell of nematodes but it is absent in the adult cuticle, Chen et al. (2006) hypothesized that *L. enzymogenes* C3 was controlling nematodes both by means of chitinases and by releasing toxic compounds molecules as well. This hypothesis was recently proved by Yuen et al. (2018) that showed the ability of *L. enzymogenes* C3 to suppress nematodes by releasing the heat stable antifungal factor (HSAF).

The genus *Lysobacter* is well known for its potential as a producer of antimicrobial compounds and its bioactive natural products were widely reviewed also with a focus on the antibiotics active against phytopathogenic (micro)organisms (Panthee et al.,2016; Puopolo et al., 2018; Xie et al., 2012).

The HSAF is included in the family of polycyclic tetramate macrolactams and it is a promising broad spectrum antifungal compound. It interfered with different cell metabolisms as the biosynthesis of sphingolipids in *Aspergillus nidulans* with the result of blocking hyphal growth (Li et al., 2009). Moreover, HSAF negatively affected tricarboxylic acid cycle, nitrogen metabolism and cell wall synthesis in *Alternaria alternata* (He et al., 2018) and it triggered reactive oxygen species accumulation with the subsequent apoptosis in *Candida albicans* (Ding et al., 2016b). Moreover, HSAF produced by *L. enzymogenes* C3 and OH11 inhibited the conidial germination of *B. sorokiniana* and degraded the hyphae of both *Fusarium graminearum* and *Fusarium verticillioides* (Lou et al., 2011; Odhiambo et al., 2017; Yu et al., 2007). Other polycyclic tetramate macrolactams, Xanthobaccins A, B and C produced by *L. capsici* SB-K88 inhibited plant pathogenic oomycetes, such as *Pythium* and *Aphanomyces*, and showed lytic activity against the zoospores of *Peronosporomycetes* (Islam et al., 2005; Nakayama et al., 1999). Their mechanism of action seems to be based on the disruption of actin organization in the hyphae and zoospores (Islam, 2008).

Recently, it was shown that *Lysobacter enzymogenes* C3 is able to produce also other polycyclic tetramate macrolactams, namely alteramide A, lysobacteramide A and B that, interestingly, showed toxicity against human carcinoma (Xu et al., 2015), while alteramide B drastically reduced the growth of yeasts by inhibiting the tubulin polymerization (Ding et al., 2016a).

Given these recent findings, polycyclic tetramate macrolactams may be also applied in medicine as new drugs. Unfortunately, the broad-scale production of HSAF can be considered as a drawback for this aim, since the low yield obtained using *L. enzymogenes* producer strains. However, current research is focusing on its biosynthesis and on methods to enhance its production (Li et al., 2018; Su et al., 2018; Tang et al., 2018a,b).

In the group of the cyclic lipodepsipeptides, the mode of action of WAP-8294A family was still not clear until Itoh et al. (2018) showed that WAP-8294A2 and its deoxy analogue could kill bacterial cells by disrupting their membrane, having as molecular target the menaquinone, an essential component of the bacterial respiratory chain. Moreover, Yu et al. (2018) remarkably increased WAP-8294A production in *L. enzymogenes* OH11 using CRISPR/dCas9-ω3 system. Similar to WAP-8294A, with an analogous mode of action, Lysocin E was recently isolated and characterized from a culture of *Lysobacter* sp. strain RH2180-5 (Hamamoto et al., 2015).

Another important antibiotic compound produced by *Lysobacter* spp. is represented by the phenazine N-oxyde myxin, highly toxic both towards prokaryotes and eukaryotes due to the inhibition of DNA synthesis (Lesley and Behki, 1967). Recently, Jiang et al. (2018) identified the gene in *L. antibioticus* OH13 deputed to the biosynthesis of myxin starting from the phenazine 1,6-dicarboxylic acid, its direct precursor.

An additional broad spectrum toxic compound is represented by 4-hydroxyphenylacetic acid isolated from *L. antibioticus* HS124 and active against *Phytophthora* (*Ph.*) *capsici* and plant pathogenic nematodes (Ko et al., 2009; Lee et al., 2013a). A proline derivative of the 2,5-diketopiperazine family, namely cyclo(L-Pro-L-Tyr), was isolated from *L. capsici* AZ78 (Cimmino et al., 2014) and showed toxic effect against the sporangia of

Phytophthora (*Ph.*) *infestans* and *Plasmopara* (*Pl.*) *viticola*, the causal agents of potato late blight and grapevine downy mildew respectively (Puopolo et al., 2014a).

In addition, *Lysobacter* spp. strains can emit volatile organic compounds (VOCs) that are toxic to plat pathogenic fungi and oomycetes. For example *L. enzymogenes* ISE13 produced the VOC 2,4-di-tert-butylphenol that inhibited the growth of *Colletotrichum acutatum* and *Ph. capsici* (Sang et al., 2011). Consistently with these results, Lazazzara et al. (2017) showed that the type strains of *L. antibioticus*, *L. capsici*, *L. enzymogenes* and *L. gummosus* species inhibit the mycelial growth of *Ph. infestans in vitro* through the release of VOCs, such as 2,5-dimethyl pyrazine, 2-methoxy-3-methyl pyrazine, decanal and pyrrole. Interestingly, the production of toxic VOCs was nutrient dependent and was enhanced when the bacterial strains were grown on a protein-rich medium (Lazazzara et al., 2017), thus it is tempting to speculate that the production of toxic VOCs by *Lysobacter* spp. in agricultural soils may be enhanced through the application of low cost protein-rich wastes.

The production of antimicrobial compounds and lytic enzymes is consistent with the hypothesis of the facultative predatory behavior of the genus *Lysobacter.* In particular, they are supposed to perform a special type of group predation named "wolf-pack predation", in which a "pack" constituted by a sufficient number of predatory cells produces hydrolytic enzymes and toxic compounds that kill and degrade other microorganisms (Martin, 2002; Seccareccia et al., 2015). Islam (2010) described for the first time the *Lysobacter* wolf-pack predation behavior on eukaryotic microorganisms. *Lysobacter capsici* SB-K88 was reported to attach in a perpendicular way, by means of brush-like fimbriae, to the hyphae and cytospores of *Aphanomyces cochlioides,* thus starting the degradation of the pathogen.

Besides directly killing plant pathogens through the release of antibiotics and lytic enzymes, *Lysobacter* can also act in indirect ways, such as competition for ecological niche colonization. Indeed, *L. capsici* SB-K88 vigorously and densely colonized seeds and roots of sugar beet, spinach, tomato, *Arabidopsis thaliana* and *Amaranthus gangeticus* (Islam et al., 2005). Interestingly, the roots colonized by SB-K88 were less attractive to the zoospores of *A. cochlioides*, and the zoospores that were approaching the roots were immobilized (Islam, 2010).

It was also proved that *Lysobacter* spp. can protect plants from pathogenic microorganisms by eliciting plant resistance mechanisms. For instance, heat-killed cells of *L. enzymogenes* C3 applied to wheat inhibited the pathogen *B. sorokiniana in planta* but not *in vitro*. Indeed, this biocontrol strain was able to trigger systemic resistance in tall fescue when applied to roots and localized resistance when applied to leaves (Kilic-Ekici and Yuen, 2003). However, *L. enzymogenes* N4-7 was not able to induce resistance in tall fescue when applied to roots, thus it should not be assumed that the ability to trigger a defense response in plants is a feature shared by all the members of the *Lysobacter* genus (Kilic-Ekici and Yuen, 2003).

On the other hand, the studies involving the biocontrol activity of *Lysobacter* against other plant pathogens are abundant and *L. enzymogenes* is the species that has been studied the most extensively. For instance, *L. enzymogenes* C3 was able to control plant pathogenic fungi (*B. sorokiniana*, *F. graminearum*, *Magnaporthe poae*, *R. solani* and *Uromyces appendiculatus*), nematodes (*Aphelenchoides fragariae*, *Heterodera schachtii*, *Meloidogyne javanica* and *Pratylenchus penetrans*) and the oomycete *P. ultimum* var. *ultimum* (Chen et al., 2006; Giesler and Yuen, 1998; Jochum et al., 2006; Kilic-Ekici and Yuen, 2003, 2004; Kobayashi et al., 2005; Kobayashi and Yuen, 2005; Palumbo et al., 2005; Yuen et al., 2001; Zhang and Yuen, 1999, 2000a; Zhang et al.,

2001). Within the other *L. enzymogenes* biocontrol strains studied so far, *L. enzymogenes* 3.1T8 controlled the damping-off of cucumber caused by *Pythium aphanidermatum* (Folman et al., 2003, 2004; Postma et al., 2009), while *L. enzymogenes* OH11 was tested *in vitro* for its capacity to inhibit the growth of the fungi *Fusarium oxysporum*, *Fusarium solani*, *R. solani*, *Rhizopus stolonifer* and *Sclerotinia sclerotiorum* and the oomycetes *Ph. capsici* and *P. aphanidermatum* (Qian et al., 2009).

Other *Lysobacter* strains belonging to other species were reported as biocontrol agents. For instance, Zhou et al. (2014) characterized two *L. antibioticus* strains able to control the obligate biotroph protist *Plasmodiophora brassicae*, the causal agent of clubroot disease of brassica species, in greenhouse conditions and, interestingly, the application of their cell-free culture filtrates could control the disease in two field trials. The strains *L. antibioticus* HS124 and MAD009 effectively inhibited the phytopathogenic oomycetes *Ph. capsici* and *Pythium torulosum* and the phytopathogenic fungus *F. oxysporum* f. sp. *lycopersici* (Ko et al., 2009; Rondon et al., 1999) whereas *L. antibioticus* 13-1 t successfully controlled in field *X. oryzae* pv. *oryzae,* the causal agent of bacterial leaf blight (Ji et al., 2008).

Furthermore, also *L. capsici* members were found to be effective as biocontrol agents, such as *L. capsici* SBK88 able to inhibit phytopathogenic oomycetes (*Aphanomyces cochlioides* and *Pythium* sp.) on sugar beets (Islam, 2008; Islam et al., 2005; Nakayama et al., 1999) and *L. capsici* ZST1-2 that was effective in controlling *P. brassicae* attacks on Chinese cabbage (Fu et al., 2018). Moreover, *L. capsici* members are also able to control plant pathogenic fungi, such as *F. oxysporum* f. sp. *radicis-lycopersici* on tomato controlled by *L. capsici* PG4 in greenhouse trials (Puopolo et al., 2010). Moreover, *L. capsici* AZ78 was effective in controlling the phytopathogenic oomycetes *Ph. infestans* and *Pl. viticola* respectively on tomato and grapevine under greenhouse

conditions (Puopolo et al., 2014a). Recently, Tomada et al. (2017) dissected the molecular patterns that characterize the interaction between *L. capsici* AZ78 and *Ph. infestans* through a dual RNA-Seq approach. Results clearly showed that the transcriptional profiles of *L. capsici* AZ78 were characterized by the up-regulation of the genes involved in the type IV pilus formation and lytic enzymes production, revealing its colonization of the pathogen mycelium with the subsequent attack of its cell walls. These mechanisms were coupled with the up-regulation of *L. capsici* AZ78 genes involved in antibiotic biosynthesis, which brought to the overall down-regulation of *Ph. infestans* primary metabolism and its consecutive cell death (Figure 4.2).

Interestingly, Puopolo et al. (2014b) showed that *L. capsici* AZ78 is resistant to copper (Figure 4.3) and this resistance made possible its combination with low doses of copper based fungicides for controlling *Pl. viticola* on grapevine. The combination determined a more effective control of the plant pathogenic microorganism compared to the solo application of *L. capsici* AZ78 and copper based fungicides at doses commonly used in viticulture (Puopolo et al. 2014b). These results may pave the way to new plant disease management strategies were this biocontrol *Lysobacter* strain might be applied in combination with copper, with the final aim of reducing the input of this heavy metal in agriculture.

The genus *Lysobacter* is thus very ductile and has a great potential for a wide spectrum of applications. However, in our opinion the recent findings achieved using omics technologies regarding the presence of genes potentially involved in the biosynthesis of still unidentified bioactive secondary metabolites (de Bruijn et al., 2015; Takami et al., 2017; Zhang et al., 2014) indicate that more studies are needed to better unearthing their potential in the control of plant diseases.

5. Potential of *Lysobacter* members for the bioremediation of contaminated soils

Evidences of resistance to heavy metals and recent results on the ability to degrade soil contaminants showed that *Lysobacter* may play a major role also in the bioremediation of polluted sites. Clear examples of the presence of *Lysobacter* species in soil contaminated by heavy metals are represented by the establishment of the *L. arseniciresistens* and *L. mobilis* species, which type strains were respectively resistant to arsenic (Luo et al., 2012) and isolated from abandoned lead-zinc ore (Yang et al., 2015). In addition, the presence of *Lysobacter*, together with *Bacillus*, was dominant in industrial wastes characterized by high pH, salinity and strong contamination by heavy metals, such as chromium and iron (Brito et al., 2013). Recently, the analysis of the microbiome of agricultural soils contaminated by cadmium revealed an increase on the presence of *Lysobacter* 16S rRNA gene sequences in response to this heavy metal (An et al. 2018) and, similarly, an increase of this bacterial genus was also observed in the case of soils treated with copper, lead and zinc (Kou et al., 2018).

Lysobacter members may be involved also in the remediation of soils contaminated with petroleum derivatives, as in the case of *L. gummosus* ITP09 that was resistant and able to degrade 2,4,6-trichlorophenol (Caliz et al., 2011). Accordingly, Chen et al. (2014) reported that the presence of *Lysobacter* was positively correlated with the hypoxic degradation of octachlorodibenzofuran, a toxic contaminant with high bioaccumulation potential. In addition, Cervantes-Gonzalez et al. (2008) showed the presence of *Lysobacter* members in hydrocarbon polluted soils and proved that adding a keratinous waste (chicken-feathers) may increase their ability in oil removal, proposing a new strategy for the improvement of the bioremediation of hydrocarbon polluted soils.

Moreover, plant beneficial bacteria may play a positive role in the bioremediation of contaminated soils by enhancing the capacity of plants to absorb contaminants. At this regard, *Lysobacter* was found in a bacterial guild that positively correlated with petroleum hydrocarbons removal through phytoremediation (Hou et al., 2015). In future, the availability of the sequenced genomes of *Lysobacter* species will allow to determine the genes involved in the absorption and degradation of heavy metals and oil contaminants. This information will be a sound basis to make the application of *Lysobacter* strains more efficient in the bioremediation of contaminated soils.

References

Adam, E., Bernhart, M., Muller, H., Winkler, J., Berg, G., 2016. The *Cucurbita pepo* seed microbiome: genotype-specific composition and implications for breeding. Plant Soil 422, 35–49.

An, F., Li, H., Diao, Z., Lv, J., 2018. The soil bacterial community in cropland is vulnerable to Cd contamination in winter rather than in summer. Environ. Sci. Pollut. Res. Int. doi: 10.1007/s11356-018-3531-8

Adegoke, A.A., Stenstrom, T.A., Okoh, A.I., 2017. *Stenotrophomonas maltophilia* as an emerging ubiquitous pathogen: looking beyond contemporary antibiotic therapy. Front. Microbiol. 8, 2276.

Aslam, Z., Yasir, M., Jeon, C.O., Chung, Y.R., 2009. *Lysobacter oryzae* sp. nov., isolated from the rhizosphere of rice (*Oryza sativa* L.). Int. J. Syst. Evol. Microbiol. 59, 675–680.

Biswas, B., Chakraborty, A., Sarkar, B., Naidu, R., 2017. Structural changes in smectite due to interaction with a biosurfactant–producing bacterium *Pseudoxanthomonas kaohsiungensis*. Appl. Clay Sci. 136, 51–57.

Bottos, E.M., Woo, A.C., Zawar–Reza, P., Pointing, S.B. and Cary, S.C. 2014. Airborne bacterial populations above desert soils of the McMurdo Dry Valleys, Antarctica. Microb. Ecol. 67, 120–128.

Brito, E.M.S., Piñón–Castillo, H.A., Guyoneaud, R., Caretta, C.A., Gutiérrez–Corona, J.F., Duran, R. et al., 2013. Bacterial biodiversity from anthropogenic extreme environments: a hyper–alkaline and hyper–saline industrial residue contaminated by chromium and iron. Applied Microbiology and Biotechnology 97, 369–378.

Brito, E.M., Villegas-Negrete, N., Sotelo-González, I.A., Caretta, C.A., Goñi-Urriza, M., Gassie, C., et al., 2014. Microbial diversity in Los Azufres geothermal field (Michoacán, Mexico) and isolation of representative sulfate and sulfur reducers. Extremophiles 18, 385–398.

Caliz, J., Vila, X., Marti, E., Sierra, J., Nordgren, J., Lindgren, P.E. et al., 2011. The microbiota of an unpolluted calcareous soil faces up chlorophenols: Evidences of resistant strains with potential for bioremediation. Chemosphere 83, 104–116.

Castillo, J.D., Vivanco, J.M., Manter, D.K., 2017. Bacterial microbiome and nematode occurrence in different potato agricultural soils. Microb. Ecol. 74, 888–900.

Cervantes–Gonzalez, E., Rojas–Avelizapa, N.G., Cruz–Camarillo, R., Garcia–Mena, J., Rojas–Avelizapa, L.I., 2008. Oil–removal enhancement in media with keratinous or chitinous wastes by hydrocarbon–degrading bacteria isolated from oil–polluted soils. Environ. Technol. 29, 171–182.

Chen, J., Moore, W.H., Yuen, G.Y., Kobayashi, D., Caswell–Chen, E.P., 2006. Influence *of Lysobacter enzymogenes* strain C3 on nematodes. J. Nematol. 38, 233–239.

Chen, J., Shen, D., Odhiambo, B.O., Xu, D., Han, S., Chou, S.–H., et al., 2018a. Two direct gene targets contribute to Clp–dependent regulation of type IV pilus–mediated twitching motility *in Lysobacter enzymogenes* OH11. Appl. Microbiol. Biot. 102, 7509–7519.

Chen, N.W.G., Serres–Giardi, L., Ruh, M., Briand, M., Bonneau, S., Darrasse, A., et al., 2018b. Horizontal gene transfer plays a major role in the pathological convergence of *Xanthomonas* lineages on common bean. BMC Genomics 19, 606.

Chen, W.Y., Wu, J.H.,Chang, J.E., 2014. Pyrosequencing analysis reveals high population dynamics of the soil microcosm degrading octachlorodibenzofuran. Microbes Environ. 29, 393–400.

Choi, H., Kim, H.J., Lee, J.H., Kim, J.S., Park, S.K., Kim, I.S., et al., 2012. Insight into genes involved in the production of extracellular chitinase in a biocontrol bacterium *Lysobacter enzymogenes* C–3. Plant Pathology J. 28, 439–445.

Choi, J.H., Seok, J.H., Cha, J.H., Cha, C.J., 2014. *Lysobacter panacisoli* sp. nov., isolated from ginseng soil. Int. J. Syst. Evol. Microbiol. 64, 2193–2197.

Christensen, P., 2001. Genus IV *Lysobacter* Christensen and Cook 1978. In Bergey's Manual of Systematic Bacteriology ed. Brenner, D.J., Krieg, N.R. and Staley, J.T. pp. 95–101. New York: Springer.

Christensen, P., 2015. *Lysobacter*. Bergey's Manual of Systematics of Archaea and Bacteria. 1–11.

Christensen, P., Cook, F.D., 1978. *Lysobacter*, a New Genus of Nonfruiting, Gliding Bacteria with a High Base Ratio. Int. J. Syst. Evol. Microbiol. 28, 367–393.

Cimmino, A., Puopolo, G., Perazzolli, M., Andolfi, A., Melck, D., Pertot, I., et al., 2014. Cyclo(L–PRO–L–TYR), the fungicide isolated from *Lysobacter capsici* AZ78: a structure–activity relationship study. Chem. Heterocycl. Comp. 50, 290–295.

de Bruijn, I., Cheng, X., de Jager, V., Expósito, R.G., Watrous, J., Patel, N. et al., 2015. Comparative genomics and metabolic profiling of the genus *Lysobacter*. BMC Genomics 16, 991.

Ding, Y., Li, Y., Li, Z., Zhang, J., Lu, C., Wang, H. et al., 2016a. Alteramide B is a microtubule antagonist of inhibiting *Candida albicans.* Biochim. Biophys. Acta 1860, 2097–2106.

Ding, Y., Li, Z., Li, Y., Lu, C., Wang, H., Shen, Y. et al., 2016b. HSAF–induced antifungal effects in *Candida albicans* through ROS–mediated apoptosis. RSC Adv. 6, 30895–30904.

Elhalag, K.M., Messiha, N.A., Emara, H.M., Abdallah, S.A., 2016. Evaluation of antibacterial activity of *Stenotrophomonas maltophilia* against *Ralstonia solanacearum* under different application conditions. J. Appl. Microbiol. 120, 1629–1645.

Fan, B., Wang, C., Song, X., Ding, X., Wu, L., Wu, H., et al., 2018. *Bacillus velezensis* FZB42 in 2018: The Gram-positive model strain for plant growth promotion and biocontrol. Front. Microbiol. 9, 2491.

Felsenstein, J., 1985. Confidence limits on phylogenies: an approach using the Bootstrap. Evolution 39, 783–791.

Finkmann, W., Altendorf, K., Stackebrandt, E., Lipski, A., 2000. Characterization of N_2O–producing *Xanthomonas*–like isolates from biofilters as *Stenotrophomonas nitritireducens* sp. nov., *Luteimonas mephitis* gen. nov., sp. nov. and *Pseudoxanthomonas broegbernensis* gen. nov., sp. nov. Int. J. Syst. Evol. Microbiol. 50, 273–282.

Folman, L.B., De Klein, M.J.E.M., Postma, J.,van Veen, J.A., 2004. Production of antifungal compounds by *Lysobacter enzymogenes* isolate 3.1T8 under different conditions in relation to its efficacy as a biocontrol agent of *Pythium aphanidermatum* in cucumber. Biol. Control 31, 145–154.

Folman, L.B., Postma, J., van Veen, J.A., 2003. Characterisation of *Lysobacter enzymogenes* (Christensen and Cook 1978) strain 3.1T8, a powerful antagonist of fungal diseases of cucumber. Microbiol. Res. 158, 107–115.

Fu, L., Li, H., Wei, L., Yang, J., Liu, Q., Wang, Y., et al., 2018. Antifungal and biocontrol evaluation of four *Lysobacter* strains against clubroot disease. Indian J. Microbiol. 58, 353–359.

Fukuda, W., Kimura, T., Araki, S., Miyoshi, Y., Atomi, H., Imanaka, T., 2013. *Lysobacter oligotrophicus* sp. nov., isolated from an Antarctic freshwater lake in Antarctica. Int. J. Syst. Evol. Microbiol. 63, 3313–3318.

Fürnkranz, M., Adam, E., Muller, H., Grube, M., Huss, H., Winkler, J., et al., 2012. Promotion of growth, health, and stress tolerance of Styrian oil pumpkins by bacterial endophytes. Eur. J. Plant. Pathol. 143, 509–519.

García-Salamanca, A., Molina-Henares, M.A., van Dillewijn, P., Solano, J., Pizarro-Tobías, P., Roca, A., et al., 2013. Bacterial diversity in the rhizosphere of maize and the surrounding carbonate-rich bulk soil. Microb. Biotechnol. 6, 36–44.

Giesler, L.J., Yuen, G.Y., 1998. Evaluation of *Stenotrophomonas maltophilia* strain C3 for biocontrol of brown patch disease. Crop Prot. 17, 509–513.

Gökçen, A., Vilcinskas, A., Wiesner, J., 2014. Biofilm–degrading enzymes from *Lysobacter gummosus*. Virulence 5, 378–387.

Gómez Expósito, R., Postma, J., Raaijmakers, J.M., de Bruijn, I., 2015. Diversity and activity of *Lysobacter* species from disease suppressive soils. Front. Microbiol. 6, 1243.

Hamamoto, H., Urai, M., Ishii, K., Yasukawa, J., Paudel, A., Murai, M. et al., 2015. Lysocin E is a new antibiotic that targets menaquinone in the bacterial membrane. Nat. Chem. Biol. 11, 127–133.

He, F., Li, B., Ai, G., Kange, A.M., Zhao, Y., Zhang, X., et al., 2018. Transcriptomics analysis of the chinese pear pathotype of *Alternaria alternata* gives insights into novel mechanisms of HSAF antifungal activities. Int. J. Mol. Sci. 19, pii: E1841.

Hernández, I., Fernàndez, C., 2017. Draft genome sequence and assembly of a *Lysobacter enzymogenes* strain with biological control activity against root knot nematodes. Genome Announc. 5, e00271-17.

Horvath, D.M., Stall, R.E., Jones, J.B., Pauly, M.H., Vallad, G.E., Dahlbeck, D. et al., 2012. Transgenic resistance confers effective field level control of bacterial spot disease in tomato. PLoS ONE, 7, e42036.

Hou, J., Liu, W., Wang, B., Wang, Q., Luo, Y., Franks, A.E., 2015. PGPR enhanced phytoremediation of petroleum contaminated soil and rhizosphere microbial community response. Chemosphere 138, 592–598.

Hu, W., Samac, D.A., Liu, X., Chen, S., 2017. Microbial communities in the cysts of soybean cyst nematode affected by tillage and biocide in a suppressive soil. Appl. Soil Ecol. 119, 396–406.

Huang, X., Liu, L., Wen, T., Zhang, J., Wang, F., Cai, Z., 2016. Changes in the soil microbial community after reductive soil disinfestation and cucumber seedling cultivation. Appl. Microbiol. Biotechnol. 100, 5581–5593.

Islam, M.T., 2008. Disruption of ultrastructure and cytoskeletal network is involved with biocontrol of damping–off pathogen *Aphanomyces cochlioides* by *Lysobacter* sp. strain SB–K88. Biol. Control 46, 312–321.

Islam, M.T., 2010. Mode of antagonism of a biocontrol bacterium *Lysobacter* sp. SB–K88 toward a damping–off pathogen *Aphanomyces cochlioides*. World J. Microb. Biot. 26, 629–637.

Islam, M.T., Hashidoko, Y., Deora, A., Ito, T., Tahara, S., 2005. Suppression of damping–off disease in host plants by the rhizoplane bacterium *Lysobacter* sp. strain SB–K88 is linked to plant colonization and antibiosis against soilborne Peronosporomycetes. Appl. Environ. Microb. 71, 3786–3796.

Itoh, H., Tokumoto, K., Kaji, T., Paudel, A., Panthee, S., Hamamoto, H., et al., 2018. Total synthesis and biological mode of action of WAP–8294A2: a menaquinone–targeting antibiotic. J. Org. Chem. 83, 6924–6935.

Ji, G.H., Wei, L.–F., He, Y.–Q., Wu, Y.P., Bai, X.–H., 2008. Biological control of rice bacterial blight by *Lysobacter antibioticus* strain 13–1. Biol. Control 45, 288–296.

Jiang, J., Guiza Beltran, D., Schacht, A., Wright, S., Zhang, L., Du, L., 2018. Functional and structural analysis of phenazine o–methyltransferase LaPhzM from *Lysobacter antibioticus* OH13 and one–pot enzymatic synthesis of the antibiotic myxin. ACS Chem. Biol. 13, 1003–1012.

Jochum, C., Osborne, L.E., Yuen, G., 2006. *Fusarium* head blight biological control with *Lysobacter enzymogenes* strain C3. Biol. Control 39, 336–344.

Joshi, S., Satyanarayana, T., 2013. Biotechnology of cold–active proteases. Biology 2, 755–783.

Jones, J., Stall, R., Scott, J., Somodi, G., Bouzar, H. and Hodge, N., 1995. A third tomato race of *Xanthomonas campestris* pv. *vesicatoria*. Plant Dis. 79, 395–398.

Jung, H.M., Ten, L.N., Im, W.T., Yoo, S.A., Lee, S.T., 2008. *Lysobacter ginsengisoli* sp. nov., a novel species isolated from soil in Pocheon Province, South Korea. J. Microbiol. Biotechn. 18, 1496–1499.

Kebede, M., Timilsina, S., Ayalew, A., Admassu, B., Potnis, N., Minsavage, G.V. et al., 2014. Molecular characterization of *Xanthomonas* strains responsible for bacterial spot of tomato in Ethiopia. Eur. J. Plant Pathol. 140, 677–688.

Kilic–Ekici, O., Yuen, G.Y., 2003. Induced resistance as a mechanism of biological control by *Lysobacter enzymogenes* strain C3. Phytopathology 93, 1103–1110.

Kilic–Ekici, O., Yuen, G.Y., 2004. Comparison of strains of *Lysobacter enzymogenes* and PGPR for induction of resistance against *Bipolaris sorokiniana* in tall fescue. Biol. Control 30, 446–455.

Kim, S.J., Ahn, J.H., Weon, H.Y., Hong, S.B., Seok, S.J., Kim, J.S., et al., 2016. *Lysobacter terricola* sp. nov., isolated from greenhouse soil. Int. J. Syst. Evol. Microbiol. 66, 1401–1406.

Kim, S.J., Ahn, J.H., Weon, H.Y., Joa, J.H., Hong, S.B., Seok, S.J., et al., 2017. *Lysobacter solanacearum* sp. nov., isolated from rhizosphere of tomato. Int. J. Syst. Evol. Microbiol. 67, 1102–1106.

Kim, S.H., Olson, T.N., Peffer, N.D., Nikolaeva, E.V., Park, S. and Kang, S., 2010. First report of bacterial spot of tomato caused by *Xanthomonas gardneri* in Pennsylvania. Plant Dis. 94, 638.

Kimura, M., 1980. A simple method for estimating evolutionary rates of base substitutions through comparative studies of nucleotide sequences. J. Mol. Evol. 16, 111–120.

Ko, H.S., Jin, R.D., Krishnan, H.B., Lee, S.B., Kim, K.Y., 2009. Biocontrol ability of *Lysobacter antibioticus* HS124 against *Phytophthora* blight is mediated by the production of 4–hydroxyphenylacetic acid and several lytic enzymes. Curr. Microbiol. 59, 608–615.

Kobayashi, D.Y., Reedy, R.M., Palumbo, J.D., Zhou, J.M., Yuen, G.Y., 2005. A clp gene homologue belonging to the Crp gene family globally regulates lytic enzyme production, antimicrobial activity, and biological control activity expressed by *Lysobacter enzymogenes* strain C3. Appl. Environ. Microb. 71, 261–269.

Kobayashi, D.Y., Yuen, G.Y., 2005. The role of clp–regulated factors in antagonism against *Magnaporthe poae* and biological control of summer patch disease of Kentucky bluegrass by *Lysobacter enzymogenes* C3. Can. J. Microbiol. 51, 719–723.

Kou, S., Vincent G., Gonzalez, E., Pitre, F.E., Labrecque, M., Brereton, N.J.B., 2018. The response of a 16S ribosomal RNA gene fragment amplified community to lead, zinc, and copper pollution in a Shanghai field trial. Front. Microbiol. 9, 366.

Kumar, S., Stecher, G., Tamura, K., 2016. MEGA7: Molecular Evolutionary Genetics Analysis Version 7.0 for Bigger Datasets. Mol. Biol. Evol. 33, 1870–1874.

Kwak, M.-J., Kwon, S.-K., Yoon, J.-H., Kim, J.F., 2015. Genome sequence of *Lysobacter dokdonensis* DS-58^{T}, a gliding bacterium isolated from soil in Dokdo, Korea. Stand. Genomic Sci. 10, 123.

Lazazzara, V., Perazzolli, M., Pertot, I., Biasioli, F., Puopolo, G., Cappellin, L., 2017. Growth media affect the volatilome and antimicrobial activity against *Phytophthora infestans* in four *Lysobacter* type strains. Microbiol. Res. 201, 52–62.

Lee, J.W., Im, W.T., Kim, M.K., Yang, D.C., 2006a. *Lysobacter koreensis* sp. nov., isolated from a ginseng field. Int. J. Syst. Evol. Microbiol. 56, 231–235.

Lee, M.S., Do, J.O., Park, M.S., Jung, S., Lee, K.H., Bae, K.S., Park, S.J., Kim, S.B., 2006b. Dominance of *Lysobacter* sp. in the rhizosphere of two coastal sand dune plant species, *Calystegia soldanella* and *Elymus mollis*. Ant.Van Leeuw. **90**, 19–27.

Lee, Y.S., Anees, M., Hyun, H.N., Kim, K.Y., 2013. Biocontrol potential of HS124 against the root–knot nematode, causing disease in tomato. Nematology 15, 545–555.

Lee, Y.S., Anees, M., Park, Y.S., Kim, S.B., Jung, W.J., Kim, K.Y., 2014a. Purification and properties of a *Meloidogyne*–antagonistic chitinase from *Lysobacter capsici* YS1215. Nematology 16, 63–72.

Lee, Y.S., Naning, K.W., Nguyen, X.H., Kim, S.B., Moon, J.H., Kim, K.Y., 2014b. Ovicidal activity of lactic acid produced by *Lysobacter capsici* YS1215 on eggs of root–knot nematode, *Meloidogyne incognita*. J. Microbiol. Biotechn. 24, 1510–1515.

Lee, Y.S., Nguyen, X.H., Naing, K.W., Park, Y.S., Kim, K.Y., 2015. Role of lytic enzymes secreted *by Lysobacter capsici* YS1215 in the control of root–knot nematode of tomato plants. Indian J. Microbiol. 55, 74–80.

Lee, Y.S., Park, Y.S., Anees, M., Kim, Y.C., Kim, Y.H., Kim, K.Y., 2013b. Nematicidal activity of *Lysobacter capsici* YS1215 and the role of gelatinolytic proteins against root–knot nematodes. Biocontrol Sci. Techn. 23, 1427–1441.

Lesley, S.M., Behki, R.M., 1967. Mode of action of myxin on *Escherichia coli*. J. Bacteriol. 94, 1837–1845.

Li, S., Calvo, A.M., Yuen, G.Y., Du, L., Harris, S.D., 2009. Induction of cell wall thickening by the antifungal compound dihydromaltophilin disrupts fungal growth and is mediated by sphingolipid biosynthesis. J. Eukaryot. Microbiol. 56, 182–187.

Li, Y., Wang, H., Liu, Y., Jiao, Y., Li, S., Shen, Y. et al., 2018. Biosynthesis of the polycyclic system in the antifungal HSAF and analogues from *Lysobacter enzymogenes*. Angew. Chem. Int. Edit. 57, 6221–6225.

Liang, J., Sun, S., Ji, J., Wu, H., Meng, F., Zhang, M., et al., 2014. Comparison of the rhizosphere bacterial communities of Zigongdongdou soybean and a high–methionine transgenic line of this cultivar. PLoS One 9, e103343.

Lin, S.Y., Hameed, A., Wen, C.Z., Liu, Y.C., Hsu, Y.H., Lai, W.A., et al., 2015. *Lysobacter lycopersici* sp. nov., isolated from tomato plant *Solanum lycopersicum*. Ant. Van Leeuw.107, 1261–1270.

Liu, L., Zhang, S., Luo, M., Wang, G., 2015a. Genomic information of the arsenic-resistant bacterium *Lysobacter arseniciresistens* type strain ZS79^{T} and comparison of *Lysobacter* draft genomes. Stand. Genomic Sci. 10, 88.

Liu, Q., Zhou, Y.G., Xin, Y.H., 2015b. High diversity and distinctive community structure of bacteria on glaciers in China revealed by 454 pyrosequencing. Syst. Appl. Microbiol. 38, 578–585.

Lou, L., Qian, G., Xie, Y., Hang, J., Chen, H., Zaleta–Rivera, K., et al., 2011. Biosynthesis of HSAF, a tetramic acid–containing macrolactam from *Lysobacter enzymogenes*. J. Am. Chem. Soc. 133, 643–645.

Lueders, T., Kindler, R., Miltner, A., Friedrich, M.W., Kaestner, M., 2006. Identification of bacterial micropredators distinctively active in a soil microbial food web. Appl. Environ. Microbiol .72, 5342–5348.

Luo, G., Shi, Z., Wang, G., 2012. *Lysobacter arseniciresistens* sp. nov., an arsenite–resistant bacterium isolated from iron–mined soil. Int. J. Syst. Evol. Microbiol. 62, 1659–1665.

Mansfield, J., Genin, S., Magori, S., Citovsky, V., Sriariyanum, M., Ronald, P., et al., 2012. Top 10 plant pathogenic bacteria in molecular plant pathology. Mol. Plant Pathol. 13, 614–629.

Margesin, R., Zhang, D.C., Albuquerque, L., Froufe, H.J.C., Egas, C., da Costa, M.S., 2018. *Lysobacter silvestris* sp. nov., isolated from alpine forest soil, and reclassification

of *Luteimonas tolerans* as *Lysobacter tolerans* comb. nov. Int. J. Syst. Evol. Microbiol. 68, 1571–1577.

Martin, M.O., 2002. Predatory prokaryotes: an emerging research opportunity. J. Mol. Microb. Biotech. 4, 467–477.

McSpadden Gardener, B.B., Kim, I.S., Kim, K.Y., Kim, Y.C. (2014) Draft genome sequence of a chitinase-producing biocontrol bacterium, *Lysobacter antibioticus* HS124. Res. Plant. Dis. 20, 216–218.

Miess, H., van Trappen, S., Cleenwerck, I., De Vos, P., Gross, H., 2016. Reclassification of *Pseudomonas* sp. PB–6250T as *Lysobacter firmicutimachus* sp. nov.. Int. J. Syst. Evol. Microbiol. 66, 4162–4166.

Nakayama, T., Homma, Y., Hashidoko, Y., Mizutani, J., Tahara, S., 1999. Possible role of xanthobaccins produced by *Stenotrophomonas* sp. strain SB-K88 in suppression of sugar beet damping–off disease. Appl. Environ. Microb. 65, 4334–4339.

Nino–Liu, D.O., Ronald, P.C., Bogdanove, A.J., 2006. *Xanthomonas oryzae* pathovars: model pathogens of a model crop. Mol. Plant Pathol. 7, 303–324.

Nour, S.M., Lawrence, J.R., Zhu, H., Swerhone, G.D., Welsh, M., Welacky, T.W., Topp, E., 2003. Bacteria associated with cysts of the soybean cyst nematode (*Heterodera glycines*). Appl. Environ. Microbiol. 69, 607–615.

Odhiambo, B.O., Xu, G., Qian, G., Liu, F., 2017. Evidence of an unidentified extracellular Heat–Stable Factor produced by *Lysobacter enzymogenes* (OH11) that degrade *Fusarium graminearum* PH1 hyphae. Curr. Microbiol. 74, 437–448.

Osawa, K., Shigemura, K., Kitagawa, K., Tokimatsu, I., Fujisawa, M., 2018. Risk factors for death from *Stenotrophomonas maltophilia* bacteremia. J. Infect. Chemother. 24, 632–636.

Palumbo, J.D., Sullivan, R.F., Kobayashi, D.Y., 2003. Molecular characterization and expression in *Escherichia coli* of three β–1,3–Glucanase Genes from *Lysobacter enzymogenes* strain N4–7. J. Bacteriol. 185, 4362–4370.

Palumbo, J.D., Yuen, G.Y., Jochum, C.C., Tatum, K., Kobayashi, D.Y., 2005. Mutagenesis of β–1,3–glucanase genes in *Lysobacter enzymogenes* strain C3 results in reduced biological control activity toward *Bipolaris* leaf spot of tall fescue and *Pythium* damping–off of sugar beet. Phytopathology 95, 701–707.

Panthee, S., Hamamoto, H., Paudel, A., Sekimizu, K., 2016. *Lysobacter* species: a potential source of novel antibiotics. Arch. Microbiol. 198, 839–845.

Park, J.H., Kim, R., Aslam, Z., Jeon, C.O., Chung, Y.R., 2008. *Lysobacter capsici* sp. nov., with antimicrobial activity, isolated from the rhizosphere of pepper, and emended description of the genus *Lysobacter*. Int. J. Syst. Evol. Microbiol. 58, 387–392.

Paulsen, I.T., Press, C.M., Ravel, J., Kobayashi, D.Y., Myers, G.S., Mavrodi, D.V., et al. 2005. Complete genome sequence of the plant commensal *Pseudomonas fluorescens* Pf-5. Nat. Biotechnol. 23, 873–878.

Pereira, J.Q., Ambrosini, A., Sant'Anna, F.H., Tadra-Sfeir, M., Faoro, H., Pedrosa, F.O., et al., 2015. Whole-genome shotgun sequence of the keratinolytic bacterium *Lysobacter* sp. A03, isolated from the Antarctic environment. Genome Announc. 3, e00246-15.

Pereira, J.Q., Ambrosini, A., Passaglia, L.M.P., Brandelli, A., 2017. A new cold–adapted serine peptidase from Antarctic *Lysobacter* sp. A03: Insights about enzyme activity at low temperatures. Int. J. Biol. Macromol. 103, 854–862.

Pereira, J.Q., Lopes, F.C., Petry, M.V., Medina, L.F.d.C., Brandelli, A., 2014. Isolation of three novel Antarctic psychrotolerant feather–degrading bacteria and partial purification of keratinolytic enzyme from *Lysobacter* sp. A03. Inter. Biodeter. Biodegr. 88, 1–7.

Postma, J., Nijhuis, E.H., Yassin, A.F., 2010a. Genotypic and phenotypic variation among *Lysobacter capsici* strains isolated from *Rhizoctonia* suppressive soils. Syst. Appl. Microbiol. 33, 232–235.

Postma, J., Scheper, R.W.A., Schilder, M.T., 2010b. Effect of successive cauliflower plantings and *Rhizoctonia solani* AG 2–1 inoculations on disease suppressiveness of a suppressive and a conducive soil. Soil Biol. Biochem. 42, 804–812.

Postma, J., Schilder, M.T., 2015. Enhancement of soil suppressiveness against *Rhizoctonia solani* in sugar beet by organic amendments. Appl. Soil Ecol. 94, 72–79.

Postma, J., Schilder, M.T., Bloem, J., van Leeuwen–Haagsma, W.K., 2008. Soil suppressiveness and functional diversity of the soil microflora in organic farming systems. Soil Biol. Biochem. 40, 2394–2406.

Postma, J., Schilder, M.T., van Hoof, R.A., 2011. Indigenous populations of three closely related *Lysobacter* spp. in agricultural soils using real-time PCR. Microb. Ecol. 62, 948–958.

Postma, J., Stevens, L.H., Wiegers, G.L., Davelaar, E., Nijhuis, E.H., 2009. Biological control of *Pythium aphanidermatum* in cucumber with a combined application of *Lysobacter enzymogenes* strain 3.1T8 and chitosan. Biol. Control 48, 301–309.

Puopolo, G., Cimmino, A., Palmieri, M.C., Giovannini, O., Evidente, A., Pertot, I., 2014a. *Lysobacter capsici* AZ78 produces cyclo(l–Pro–l–Tyr), a 2,5–diketopiperazine with toxic activity against sporangia of *Phytophthora infestans* and *Plasmopara viticola*. J. Appl. Microbiol. 117, 1168–1180.

Puopolo, G., Giovannini, O., Pertot, I., 2014b. *Lysobacter capsici* AZ78 can be combined with copper to effectively control *Plasmopara viticola* on grapevine. Microbiol. Res. 169, 633–642.

Puopolo, G., Raio, A., Zoina, A., 2010. Identification and characterization of *Lysobacter capsici* strain PG4: a new plant health–promoting rhizobacterium. J. Plant Pathol. 92, 157–164.

Puopolo, G., Tomada, S., Pertot, I., 2018. The impact of the omics era on the knowledge and use of *Lysobacter* species to control phytopathogenic micro–organisms. J. Appl. Microbiol. 124, 15–27.

Puopolo, G., Tomada, S., Sonego, P., Moretto, M., Engelen, K., Perazzolli, M. et al., 2016. The *Lysobacter capsici* AZ78 genome has a gene pool enabling it to interact successfully with phytopathogenic microorganisms and environmental factors. Front.Microbiol. 7, 96.

Qin, Y., Fu, Y., Dong, C., Jia, N., Liu, H., 2016. Shifts of microbial communities of wheat (*Triticum aestivum* L.) cultivation in a closed artificial ecosystem. Appl. Microbiol. Biotechnol. 100, 4085–4095.

Qian, G.L., Hu, B.S., Jiang, Y.H., Liu, F.Q., 2009. Identification and characterization of *Lysobacter enzymogenes* as a biological control agent against some fungal pathogens. Agr. Sci. China 8, 68–75.

Reichenbach, H., 2006. The Genus *Lysobacter*. The Prokaryotes 939–957.

Rodrigues, R.R., Rodgers, N.C., Wum X., Williams, M.A. 2018. COREMIC: a web-tool to search for a niche associated CORE MICrobiome. Peer J. 6, e4395.

Roesti, D., Ineichen, K., Braissant, O., Redecker, D., Wiemken, A., Aragno, M., 2005. Bacteria associated with spores of the arbuscular mycorrhizal fungi *Glomus geosporum* and *Glomus constrictum*. Appl. Environ. Microbiol. 71, 6673–6679.

Romanenko, L.A., Uchino, M., Tanaka, N., Frolova, G.M., Mikhailov, V.V., 2008. *Lysobacter spongiicola* sp. nov., isolated from a deep–sea sponge Int. J. Syst. Evol. Microbiol. 58, 370–374.

Rondon, M.R., Borlee, B.R., Brady, S.F., Gross, J.A., Guenthner, B.J., Manske, B., et al., 1999. Biocontrol and root colonization by the gliding bacterium *Lysobacter antibioticus*. Phytopathology 89.

Rosenzweig, N., Tiedje, J.M., Quensen, J.F., Meng, Q., Hao, J.J., 2011. Microbial communities associated with potato common scab–suppressive soil determined by pyrosequencing analyses. Plant Dis. 96, 718–725.

Ryazanova, L.P., Stepnaya, O.A., Suzina, N.E., Kulaev, I.S., 2005. Antifungal action of the lytic enzyme complex from *Lysobacter* sp. XL1. Process Biochem. 40, 557–564.

Saddler, G.S., Bradbury, J.F., 2015. Xanthomonadaceae fam. nov. Bergey's Manual of Systematics of Archaea and Bacteria, 1–3.

Saitou, N., Nei, M., 1987. The neighbor–joining method: a new method for reconstructing phylogenetic trees. Mol. Biol. Evol. 4, 406–25.

Sang, M.K., Kim, J.D., Kim, B.S., Kim, K.D., 2011. Root treatment with rhizobacteria antagonistic to *Phytophthora* blight affects anthracnose occurrence, ripening, and yield of pepper fruit in the plastic house and field. Phytopathology 101, 666–678.

Saponari, M., Boscia, D., Altamura, G., Loconsole, G., Zicca, S., D'Attoma, G., et al., 2017. Isolation and pathogenicity of *Xylella fastidiosa* associated to the olive quick decline syndrome in southern Italy. Sci. Rep. 7, 17723.

Seccareccia, I., Kost, C., Nett, M., 2015. Quantitative analysis of *Lysobacter* predation. Appl. Environ. Microb. 81, 7098–7105.

She, S., Niu, J., Zhang, C., Xiao, Y., Chen, W., Dai, L. et al., 2017. Significant relationship between soil bacterial community structure and incidence of bacterial wilt disease under continuous cropping system. Arch. Microbiol. 199, 267–275.

Singh, H., Du, J., Ngo, H.T., Won, K., Yang, J.E., Kim, K.Y., et al., 2015a. *Lysobacter fragariae* sp. nov. and *Lysobacter rhizosphaerae* sp. nov. isolated from rhizosphere of strawberry plant. Ant. Van Leeuw.107, 1437–1444.

Singh, H., Won, K., Du, J., Yang, J.E., Akter, S., Kim, K.Y., et al., 2015b. *Lysobacter agri* sp. nov., a bacterium isolated from soil. Ant. Van Leeuw.108, 553–561.

Srinivasan, S., Kim, M.K., Sathiyaraj, G., Kim, H.B., Kim, Y.J., Yang, D.C., 2010. *Lysobacter soli* sp. nov., isolated from soil of a ginseng field. Int. J. Syst. Evol. Microbiol. 60, 1543–1547.

Su, Z., Han, S., Fu, Z.Q., Qian, G., Liu, F., 2018. Heat–Stable Antifungal Factor (HSAF) biosynthesis in *Lysobacter enzymogenes* is controlled by the interplay of two transcription factors and a diffusible molecule. Appl. Environ. Microb. 84, pii: e01754-17.

Sullivan, R.F., Holtman, M.A., Zylstra, G.J., White, J.F., Kobayashi, D.Y., 2003. Taxonomic positioning of two biological control agents for plant diseases as *Lysobacter enzymogenes* based on phylogenetic analysis of 16S rDNA, fatty acid composition and phenotypic characteristics. J. Appl. Microbiol. 94, 1079–1086.

Takami, H., Toyoda, A., Uchiyama, I., Itoh, T., Takaki, Y., Arai, W. et al., 2017. Complete genome sequence and expression profile of the commercial lytic enzyme producer *Lysobacter enzymogenes* M497–1. DNA Res. 24, 169–177.

Tang, B., Sun, C., Zhao, Y., Xu, H., Xu, G.Liu, F., 2018a. Efficient production of heat–stable antifungal factor through integrating statistical optimization with a two–stage temperature control strategy in *Lysobacter enzymogenes* OH11. BMC Biotechnol. 18, 69.

Tang, B., Zhao, Y.C., Shi, X.–M., Xu, H.Y., Zhao, Y.Y., Dai, C.C. et al., 2018b. Enhanced heat stable antifungal factor production by *Lysobacter enzymogenes* OH11 with cheap feedstocks: medium optimization and quantitative determination. Lett. Appl. Microbiol. 66, 439–446.

Tomada, S., Puopolo, G., Perazzolli, M., Musetti, R., Loi, N., Pertot, I., 2016. Pea broth enhances the biocontrol efficacy of *Lysobacter capsici* AZ78 by triggering cell motility associated with biogenesis of type IV pilus. Front. Microbiol. 7, 1136.

Tomada, S., Sonego, P., Moretto, M., Engelen, K., Pertot, I., Perazzolli, M. et al., 2017. Dual RNA–Seq of *Lysobacter capsici* AZ78 – *Phytophthora infestans* interaction shows the implementation of attack strategies by the bacterium and unsuccessful oomycete defense responses. Environ. Microbiol. 19, 4113–4125.

Turnbull, A.L., Liu, Y., Lazarovits, G., 2012. Isolation of bacteria from the rhizosphere and rhizoplane of potato (*Solanum tuberosum*) grown in two distinct soils using semi selective media and characterization of their biological properties. Am. J. Pot. Res. 89, 294–305.

Van Sluys, M.A., de Oliveira, M.C., Monteiro–Vitorello, C.B., Miyaki, C.Y., Furlan, L.R., Camargo, L.E.A., et al., 2003. Comparative analyses of the complete genome sequences of Pierce's disease and citrus variegated chlorosis strains of *Xylella fastidiosa*. J. Bacteriol. 185, 1018–1026.

Vasilyeva, N.V., Shishkova, N.A., Marinin, L.I., Ledova, L.A., Tsfasman, I.M., Muranova, T.A. et al., 2014. Lytic peptidase L5 of *Lysobacter* sp. XL1 with broad antimicrobial spectrum. J. Mol. Microb. Biotech. 24, 59–66.

Vasilyeva, N.V., Tsfasman, I.M., Suzina, N.E., Stepnaya, O.A., Kulaev, I.S., 2008. Secretion of bacteriolytic endopeptidase L5 of *Lysobacter* sp. XL1 into the medium by means of outer membrane vesicles. FEBS J. 275, 3827–3835.

Vivero, R.J., Jaramillo, N.G., Cadavid-Restrepo, G., Soto, S.I., Herrera, C.X. 2016. Structural differences in gut bacteria communities in developmental stages of natural populations of *Lutzomyia evansi* from Colombia's Caribbean coast. Parasit. Vectors 9, 496.

Wang, L., Li, J., Yang, F.E.Y., Raza, W., Huang, Q., Shen, Q., 2017. Application of bioorganic fertilizer significantly increased apple yields and shaped bacterial community structure in orchard soil. Microb. Ecol. 73, 404–416.

Wang, H., Zhang, W., Ye, Y., He, Q., Zhang, S., 2018. Isolation and characterization of *Pseudoxanthomonas* sp. strain YP1 capable of denitrifying phosphorus removal (DPR). Geomicrobiol. J. 35, 537–543.

Wei, D.Q., Yu, T.T., Yao, J.C., Zhou, E.M., Song, Z.Q., Yin, Y.R., et al., 2012. *Lysobacter thermophilus* sp. nov., isolated from a geothermal soil sample in Tengchong, south–west China. Ant. Van Leeuw. 102, 643–651.

Weon, H.Y., Kim, B.Y., Baek, Y.K., Yoo, S.H., Kwon, S.W., Stackebrandt, E., et al., 2006. Two novel species, *Lysobacter daejeonensis* sp. nov. and *Lysobacter yangpyeongensis* sp. nov., isolated from Korean greenhouse soils. Int. J. Syst. Evol. Microbiol. 56, 947–951.

Weon, H.Y., Kim, B.Y., Kim, M.K., Yoo, S.H., Kwon, S.W., Go, S.J., et al., 2007. *Lysobacter niabensis* sp. nov. and *Lysobacter niastensis* sp. nov., isolated from greenhouse soils in Korea. Int. J. Syst. Evol. Microbiol. 57, 548–551.

Xia, J., Chen, J., Chen, Y., Qian, G., Liu, F., 2018. Type IV pilus biogenesis genes and their roles in biofilm formation in the biological control agent *Lysobacter enzymogenes* OH11. Appl. Microbiol. Biotechnol. 102, 833–846.

Xie, B., Li, T., Lin, X., Wang, C.J., Chen, Y.J., Liu, W.J. et al., 2016. *Lysobacter erysipheiresistens* sp. nov., an antagonist of powdery mildew, isolated from tobacco–cultivated soil. Int. J. Syst. Evol. Microbiol. 66, 4016–4021.

Xie, Y., Wright, S., Shen, Y., Du, L., 2012. Bioactive natural products from *Lysobacter*. Nat. Prod. Rep. 29, 1277–1287.

Xu, L., Wu, P., Wright, S.J., Du, L., Wei, X., 2015. Bioactive polycyclic tetramate macrolactams from *Lysobacter enzymogenes* and their absolute configurations by theoretical ECD calculations. J. Nat. Products 78, 1841–1847.

Yan, Z.F., Trinh, H., Moya, G., Lin, P., Li, C.T., Kook, M.C., et al., 2016. *Lysobacter rhizophilus* sp. nov., isolated from rhizosphere soil of mugunghwa, the national flower of South Korea. Int. J. Syst. Evol. Microbiol. 66, 4754–4759.

Yang, S.Z., Feng, G.D., Zhu, H.H., Wang, Y.H., 2015. *Lysobacter mobilis* sp. nov., isolated from abandoned lead–zinc ore. Int. J. Syst. Evol. Microbiol. 65, 833–837.

Yang, G.L., Hou, S.G., Le Baoge, R., Li, Z.G., Xu, H., Liu, Y.P., et al., 2016. Differences in bacterial diversity and communities between glacial snow and glacial soil on the Chongce ice cap, West Kunlun mountains. Sci. Rep. 6, 36548.

Yi, J.L., Wang, J., Li, Q., Liu, Z.X., Zhang, L., Liu, A.X., et al., 2015. Draft genome sequence of the bacterium *Lysobacter capsici* X2-3, with a broad spectrum of antimicrobial activity against multiple plant-pathogenic microbes. Genome Announc 3, e00589-15.

Yu, F., Zaleta–Rivera, K., Zhu, X., Huffman, J., Millet, J.C., Harris, S.D., et al., 2007. Structure and biosynthesis of Heat–Stable Antifungal Factor (HSAF), a broad–spectrum antimycotic with a novel mode of action. Antimicrob. Agents Ch. 51, 64–72.

Yu, L., Su, W., Fey, P.D., Liu, F., Du, L., 2018. Yield improvement of the anti–MRSA antibiotics WAP–8294A by CRISPR/dCas9 combined with refactoring self–protection genes in *Lysobacter enzymogenes* OH11. ACS Synth. Biol. 7, 258–266.

Yuen, G.Y., Broderick, K.C., Jochum, C.C., Chen, C.J., Caswell–Chen, E.P., 2018. Control of cyst nematodes by *Lysobacter enzymogenes* strain C3 and the role of the antibiotic HSAF in the biological control activity. Biol. Control 117, 158–163.

Yuen, G.Y., Jochum, C.C., Osborne, L.E., Jin, Y., 2003. Biocontrol of Fusarium head blight in wheat by *Lysobacter enzymogenes* C3. Phytopathology 93, S93.

Yuen, G.Y., Steadman, J.R., Lindgren, D.T., Schaff, D., Jochum, C., 2001. Bean rust biological control using bacterial agents. Crop Prot. 20, 395–402.

Zhang, J., Du, L., Liu, F., Xu, F., Hu, B., Venturi, V. et al., 2014. Involvement of both PKS and NRPS in antibacterial activity in *Lysobacter enzymogenes* OH11. FEMS Microbiol. Lett. 355, 170–176.

Zhang, W., Huffman, J., Li, S., Shen, Y., Du, L., 2017. Unusual acylation of chloramphenicol in *Lysobacter enzymogenes*, a biocontrol agent with intrinsic resistance to multiple antibiotics. BMC Biotechnol. 17, 59.

Zhang, Z., Yuen, G.Y., 1999. Biological control of *Bipolaris sorokiniana* on tall fescue by *Stenotrophomonas maltophilia* strain C3. Phytopathology 89, 817–822.

Zhang, Z., Yuen, G.Y., 2000a. The role of chitinase production by *Stenotrophomonas maltophilia* strain C3 in biological control of *Bipolaris sorokiniana*. Phytopathology 90, 384–389.

Zhang, Z., Yuen, G.Y., 2000b. Effects of culture fluids and preinduction of chitinase production on biocontrol of *Bipolaris* leaf spot by *Stenotrophomonas maltophilia* C3. Biol. Control 18, 277–286.

Zhang, Z., Yuen, G.Y., Sarath, G., Penheiter, A.R., 2001. Chitinases from the plant disease biocontrol agent, *Stenotrophomonas maltophilia* C3. Phytopathology 91, 204–211.

Zhou, L., Li, M., Yang, J., Wei, L., Ji, G., 2014. Draft genome sequence of antagonistic agent *Lysobacter antibioticus* 13–6. Genome Announc. 2, e00566–00514.

Figure legends

Figure 1.1. Phylogenetic tree resulting from analysis of the 16S rRNA gene sequences of *Lysobacter* species. GenBank was used to collect genes encoding 16S rRNA from *Lysobacter* species enlisted on the website http://www.bacterio.net at the time of writing. Once aligned by ClustalW, the alignment profile was used to construct the optimal phylogenetic tree using the Neighbour-Joining method (Saitou and Nei, 1987) and the evolutionary distances were computed using the Kimura's two-parameter model (Kimura, 1980). Bootstrap values (1000 replicates) higher than 70 are shown next to the branches (Felsenstein, 1985). All the phylogenetic analyses were carried out using MEGA7 (Kumar et al., 2016).

Figure 1.2. Visualization of type IV pili of *Lysobacter capsici* AZ78 using Transmission Electron Microscopy. Pilus-like structures (arrows) emerge at the pole of *L. capsici* AZ78 cells grown on Pea Agar Medium amended with 0.5% Agar (w/v; A, C) and these structures are absent in cells grown on Luria Bertani Agar amended with 0.5% Agar (w/v; B, D). A and B, magnification X-19000, black bar 500 nm. (C, D), magnification X-64000, white bar 150 nm.

CREDIT: Tomada et al. (2016)

Figure 3.1. Evaluation of a semi-selective growth medium for the isolation of plant beneficial *Lysobacter* spp.. Concentrations of bacterial cells recovered on the growth media were determined through dilution plating. Bars indicate mean ± standard deviation. White bars: R2A medium, Black bars: R2A medium amended with kanamycin 5 mg/L, streptomycin 10 mg/L and tobramycin 1 mg/L. Three replicates

(Petri dishes) were used for each dilution and experiments were repeated. Bars with asterisks differ significantly according to Student's t-test ($\alpha = 0.05$).

Figure 4.1. *Lysobacter capsici* AZ78 production of enzymes. *Lysobacter capsici* AZ78 produces (A) cellulases; (B) β-glucanases; (C) chitinases, and (D) siderophores.

CREDIT: Puopolo et al. (2016).

Figure 4.2. Schematic overview of *Lysobacter capsici* AZ78 and *Phytophthora infestans* interaction. The diagram shows microorganism interaction as interpreted from transcriptional profiling of both partners.

CREDIT: Tomada et al. (2017).

Figure 4.3. Resistance to copper in *Lysobacter capsici* strains. Growth of bacterial strains onto LBA growth medium amended with $CuSO_4$ 400 μg/mL. A) *Lysobacter capsici* DSM 19286^T; B) *Lysobacter capsici* AZ78; C) *Lysobacter capsici* M143.

CREDIT: Puopolo et al. (2014b).

Table 1 Sequenced genomes of *Lysobacter* strains

Bacterial strains	Genome size*	CDS**	Accession Number	References
Lysobacter sp. A03	2.87	2,615	JXSS00000000	Pereira et al., 2015
Lysobacter antibioticus 13-6	5.53	4,521	JMTZ00000000	Zhou et al., 2014
Lysobacter antibioticus 76	5.91	5,143	CP011129	de Bruijn et al., 2016
Lysobacter antibioticus ATCC 29479	5.77	5,178	CP013141	de Bruijn et al., 2016
Lysobacter antibioticus HS124	5.14	4,597	GCA_000336385	McSpadden Gardener et al., 2014,
Lysobacter arseniciresistens ZS79^T	3.09	2,363	AVPT00000000	Liu et al., 2015°
Lysobacter capsici 55	6.39	5,685	CP011130	de Bruijn et al., 2016
Lysobacter capsici AZ78	6.27	5,292	JAJA00000000.2	Puopolo et al., 2016
Lysobacter capsici X2-3	6.13	4,880	LBMI00000000	Yi et al., 2015
Lysobacter concretionis Ko07^T	3.03	2,232	AVPS00000000	Liu et al., 2015a
Lysobacter daejeonensis GH1-9^T	3.28	2,570	AVPU00000000	Liu et al., 2015a
Lysobacter defluvii IMMIB APB-9^T	2.72	2,443	AVBH00000000	Liu et al., 2015a
Lysobacter dokdonensis DS-58^T	3.27	3,155	JRKJ00000000	Kwak et al., 2015
Lysobacter enzymogenes C3	6.16	5,547	CP013140	de Bruijn et al., 2016
Lysobacter enzymogenes B25	5.21	5,186	MTAY00000000	Hernández and Fernàndez, 2017
Lysobacter enzymogenes M497-1	6.09	4,891	AP014940	Takami et al., 2017
Lysobacter gummosus 3.2.11	6.06	5,322	CP011131	de Bruijn et al., 2016
Lysobacter maris HZ9B	4.02	3,466	CP029843	Unpublished
Lysobacter silvestris AM20-91^T	2.85	2,599	NPZB00000000	Unpublished
Lysobacter soli DCY21^T	3.95	3,622	QTJR00000000	Unpublished
Lysobacter spongiicola KMM 329^T	3.10	2,856	FUXP00000000	Unpublished
Lysobacter tolerans UM1^T	2.54	2,387	FTLW00000000	Unpublished

* Genome sizes are expressed in Mb

** CDS: Coding DNA Sequences

Table 2 Isolation of *Lysobacter* spp. type strains and list of growth media used

Species	Origin	Growth medium	Reference
Lysobacter agri HG-SKA3^T	Soil sample collected from a field	R2A[a] Agar	Singh et al., 2015b
Lysobacter antibioticus DSM 2044^T	Soil sample collected from a field	Yeast Cell Agar	Christensen and Cook, 1978
Lysobacter capsici DSM 19286^T	Pepper rhizosphere	2% Tryptic Soy Agar	Park et al., 2008
Lysobacter daejeonensis GH1-9^T	Greenhouse soil	R2A Agar	Weon et al., 2006
Lysobacter enzymogenes DSM 2043^T	Soil sample collected from a field	Yeast Cell Agar	Christensen and Cook, 1978
Lysobacter erysipheiresistens RS-LYSO-3^T	Soil cultivate with tobacco	Modified LB Agar[b]	Xie et al., 2016
Lysobacter fragariae THG-DN8.7^T	Strawberry rhizosphere	R2A Agar	Singh et al., 2015a
Lysobacter ginsengisoli Gsoil 357^T	Soil cultivated with ginseng	Diluted R2A Agar	Jung et al., 2008
Lysobacter gummosus DSM 6980^T	Soil sample collected from a field	Yeast Cell Agar	Christensen and Cook, 1978
Lysobacter koreensis Dae16^T	Soil cultivated with ginseng	R2A Agar	Lee et al., 2006a
Lysobacter lycopersici CC-Bw-6^T	Tomato stem	R2A Agar	Lin et al., 2015
Lysobacter niabensis GH34-4^T	Greenhouse soil cultivated with cucumber	R2A Agar	Weon et al., 2007
Lysobacter niastensis GH41-7^T	Greenhouse soil cultivated with cucumber	R2A Agar	Weon et al., 2007
Lysobacter oryzae YC6269^T	Rice rhizosphere	Diluted R2A Agar	Aslam et al. ,2009
Lysobacter panacisoli CJ29^T	Soil cultivated with ginseng	R2A Agar	Choi et al., 2014
Lysobacter rhizophilus THG-YS3.6^T	Mugunghwa flower rhizosphere	Nutrient Agar	Yan et al., 2016
Lysobacter rhizosphaerae THG-DN8.3^T	Strawberry rhizosphere	R2A Agar	Singh et al., 2015a
Lysobacter solanacearum T20R-70^T	Tomato rhizosphere	R2A Agar	Kim et al., 2017
Lysobacter soli DCY21^T	Soil cultivated with ginseng	R2A Agar	Srinivasan et al., 2010
Lysobacter terricola 5GH18-14^T	Greenhouse soil	R2A Agar	Kim et al., 2016
Lysobacter yangpyeongensis GH19-3^T	Greenhouse soil cultivated with lettuce	R2A Agar	Weon et al., 2006

*R2A: Reasoner's 2A

**Modified LB Agar: 20 g LB broth, 1 L of tobacco root exudates

Table 3 Evaluation of *Lysobacte*r spp. resistance to antibiotics

Antibiotics	Disc content (µg)	*Lysobacter antibioticus*	*Lysobacter capsici*	*Lysobacter enzymogenes*	*Lysobacter gummosus*	*Bacillus velezensis*	*Pseudomonas protegens*
Ampicillin	20	34.67 ± 0.72*	28.67 ± 0.27	0.00 ± 0.00	0.00 ± 0.00	20.67 ± 0.72	0.00 ± 0.00
Chloramphenicol	30	22.00 ± 0.47	37.67 ± 0.72	31.67 ± 0.72	22.33 ± 30.67	30.67 ± 0.67	0.00 ± 0.00
Erythromycin	30	0.00 ± 0.00	25.33 ± 0.72	0.00 ± 0.00	11.67 ± 0.72	29.33 ± 0.72	0.00 ± 0.00
Gentamicin	30	23.00 ± 0.47	17.33 ± 0.27	22.33 ± 0.27	20.67 ± 0.72	28.33 ± 0.54	16.67 ± 0.72
Kanamycin	30	7.00 ± 0.00	0.00 ± 0.00	0.00 ± 0.00	0.00 ± 0.00	26.67 ± 0.27	21.33 ± 0.27
Streptomycin	25	0.00 ± 0.00	0.00 ± 0.00	0.00 ± 0.00	0.00 ± 0.00	27.00 ± 0.47	9.33 ± 0.27
Tetracycline	30	0.00 ± 0.00	13.33 ± 0.27	0.00 ± 0.00	0.00 ± 0.00	36.33 ± 1.19	0.00 ± 0.00
Tobramycin	10	0.00 ± 0.00	0.00 ± 0.00	0.00 ± 0.00	0.00 ± 0.00	22.67 ± 0.54	13.33 ± 0.27
Trimethoprim	5	0.00 ± 0.00	13.33 ± 0.27	0.00 ± 0.00	0.00 ± 0.00	36.33 ± 1.19	0.00 ± 0.00
Vancomycin	30	26.33 ± 0.54	21.33 ± 0.27	21.33 ± 0.27	15.33 ± 0.54	20.33 ± 0.72	0.00 ± 0.00

*Mean diameters inhibition zone ± standard errors of pooled data for a repeated experiment with three replicates of each antibiotic for each experiment. The diameters of inhibition zone were determined using a calliper

Table 4 List of *Lysobacter* biocontrol strains and their mode of action.

Bacterial strains	Mode of action	Bioactive compounds	Activities	References
Lysobacter enzymogenes C3	Direct antagonism, induced resistance, release of antibiotics and lytic enzymes	Chitinases; β-1,3-glucanases; Heat Stable Antifungal Factor (HSAF)	Antifungal; antioomycete; nematicidal	Zhang and Yuen, 2000ab; Palumbo et al. 2003, 2005; Yu et al. 2007; Giesler and Yuen 1998; Zhang et al. 2001; Kilic-Ekici and Yuen 2003, 2004; Kobayashi et al. 2005; Kobayashi and Yuen 2005; Yuen et al. 2001, 2003; Jochum et al. 2006; Chen et al. 2006
Lysobacter capsici YS1215	Release of antibiotics and lytic enzymes in the medium	Chitinases; β-1,4-glucanases; Metallopeptidase; Lactic acid	Nematicidal	Lee et al. 2013ab, 2014ab, 2015
Lysobacter capsici SB-K88	Direct antagonism and release of antibiotics	Xanthobaccins A, B and C	Antifungal; antioomycete	Nakayama et al. 1999; Islam et al. 2005; Islam, 2008
Lysobacter antibioticus HS124	Production of antibiotics and lytic enzymes	4-hydroxyphenylacetic acid	Antioomycete	Ko et al. 2009
Lysobacter capsici AZ78	Production of antibiotics and lytic enzymes	Cyclo(L-Pro-L-Tyr)	Antioomycete	Puopolo et al. 2014b
Lysobacter antibioticus 13-1	Direct antagonism and release of antibiotics		Antibacterial	Ji et al. 2088
Lysobacter antibioticus MAD009	Production of antibiotics and lytic enzymes		Antifungal; antioomycete	Rondon et al. 1999
Lysobacter antibioticus YFY 02 and HY	Direct antagonism in soil		Antioomycete	Zhou et al. 2014
Lysobacter enzymogenes N4-7	Production of lytic enzymes	β-1,3-glucanase	Antifungal; antioomycete	Palumbo et al., 2003

Lysobacter capsici ZST1-2	Production of antibiotics and lytic enzymes		Antioomycete	Fu et al. 2018
Lysobacter enzymogenes OH11	Production of antibiotics and lytic enzymes	β-1,3-glucanase; WAP-8294A; HSAF	Antifungal; antioomycete; antibacterial	Zhang et al. 2011; Zhu et al. 2008; Tang et al. 2018ab
Lysobacter capsici PG4	Production of antibiotics and lytic enzymes	Chitinases; proteases	Antifungal	Puopolo et al. 2010
Lysobacter enzymogenes 3.1T8	Production of antibiotics, biosurfactants and lytic enzymes	Proteases; lipases	Antioomycete	Folman et al. 2003, 2004; Postma et al. 2009
Lysobacter enzymogenes ISE13	VOCs-mediated antagonism	2,4-di-tert-butylphenol	Antifungal; antioomycete	Sang et al. 2011
Lysobacter antibioticus DSM 2044^T	VOCs-mediated antagonism	2,5-dimethil pyrazine;	Antioomycete	Lazazzara et al., 2017
Lysobacter capsici DSM 19286^T		2-methoxy-3-methyl pyrazine;		
Lysobacter enzymogenes DSM 2043^T		Decanal;		
Lysobacter gummosus DSM 6980^T		Pyrrole;		

Figure 1.1

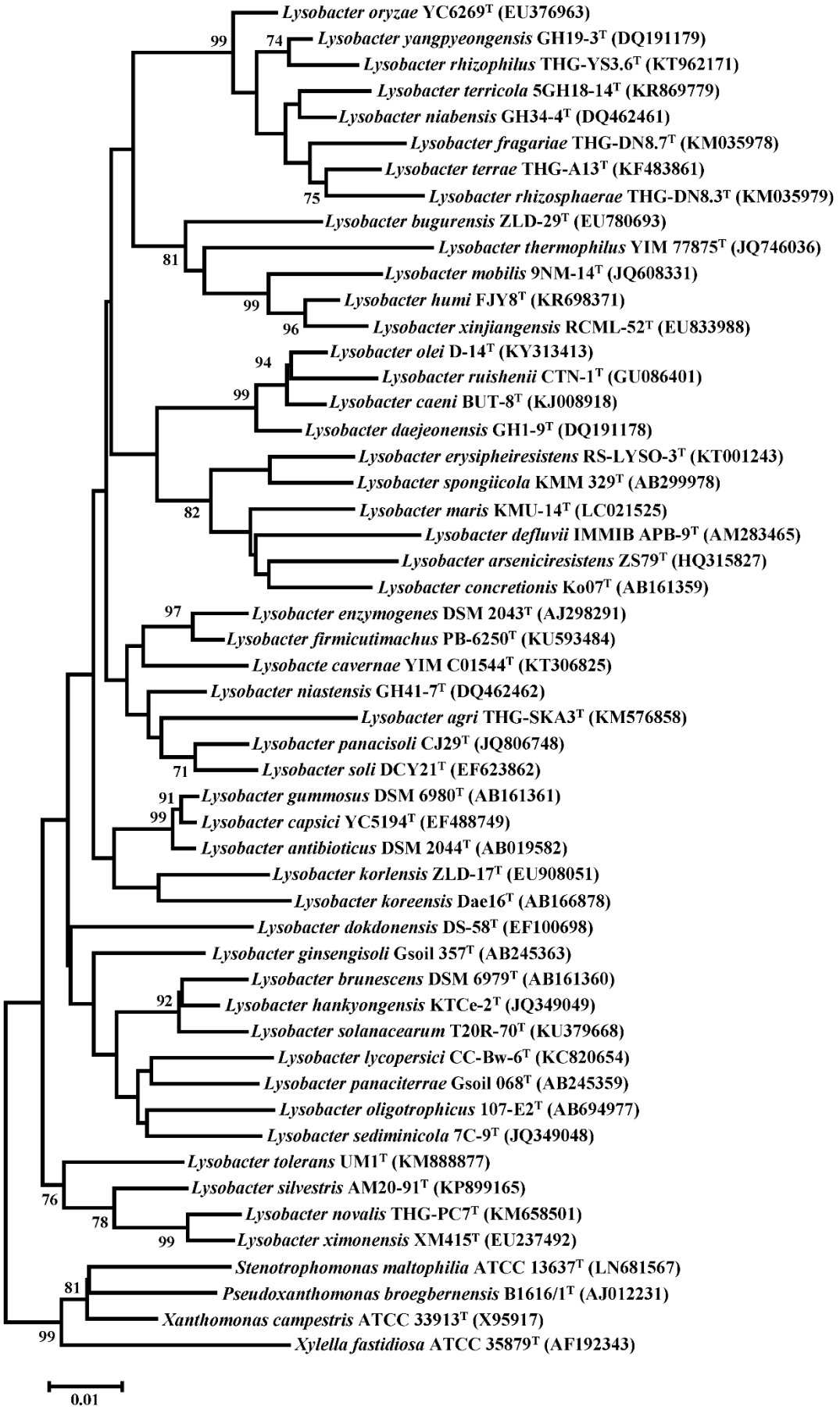
Lysobacter oryzae YC6269T (EU376963)
99
74
Lysobacter yangpyeongensis GH19-3T (DQ191179)
Lysobacter rhizophilus THG-YS3.6T (KT962171)
Lysobacter terricola 5GH18-14T (KR869779)
Lysobacter niabensis GH34-4T (DQ462461)
Lysobacter fragariae THG-DN8.7T (KM035978)
Lysobacter terrae THG-A13T (KF483861)
75
Lysobacter rhizosphaerae THG-DN8.3T (KM035979)
Lysobacter bugurensis ZLD-29T (EU780693)
Lysobacter thermophilus YIM 77875T (JQ746036)
81
Lysobacter mobilis 9NM-14T (JQ608331)
99
Lysobacter humi FJY8T (KR698371)
96
Lysobacter xinjiangensis RCML-52T (EU833988)
Lysobacter olei D-14T (KY313413)
94
Lysobacter ruishenii CTN-1T (GU086401)
99
Lysobacter caeni BUT-8T (KJ008918)
Lysobacter daejeonensis GH1-9T (DQ191178)
Lysobacter erysipheiresistens RS-LYSO-3T (KT001243)
Lysobacter spongiicola KMM 329T (AB299978)
82
Lysobacter maris KMU-14T (LC021525)
Lysobacter defluvii IMMIB APB-9T (AM283465)
Lysobacter arseniciresistens ZS79T (HQ315827)
Lysobacter concretionis Ko07T (AB161359)
97
Lysobacter enzymogenes DSM 2043T (AJ298291)
Lysobacter firmicutimachus PB-6250T (KU593484)
Lysobacte cavernae YIM C01544T (KT306825)
Lysobacter niastensis GH41-7T (DQ462462)
Lysobacter agri THG-SKA3T (KM576858)
Lysobacter panacisoli CJ29T (JQ806748)
71
Lysobacter soli DCY21T (EF623862)
91
Lysobacter gummosus DSM 6980T (AB161361)
99
Lysobacter capsici YC5194T (EF488749)
Lysobacter antibioticus DSM 2044T (AB019582)
Lysobacter korlensis ZLD-17T (EU908051)
Lysobacter koreensis Dae16T (AB166878)
Lysobacter dokdonensis DS-58T (EF100698)
Lysobacter ginsengisoli Gsoil 357T (AB245363)
Lysobacter brunescens DSM 6979T (AB161360)
92
Lysobacter hankyongensis KTCe-2T (JQ349049)
Lysobacter solanacearum T20R-70T (KU379668)
Lysobacter lycopersici CC-Bw-6T (KC820654)
Lysobacter panaciterrae Gsoil 068T (AB245359)
Lysobacter oligotrophicus 107-E2T (AB694977)
Lysobacter sediminicola 7C-9T (JQ349048)
Lysobacter tolerans UM1T (KM888877)
Lysobacter silvestris AM20-91T (KP899165)
76
78
Lysobacter novalis THG-PC7T (KM658501)
99
Lysobacter ximonensis XM415T (EU237492)
Stenotrophomonas maltophilia ATCC 13637T (LN681567)
81
Pseudoxanthomonas broegbernensis B1616/1T (AJ012231)
Xanthomonas campestris ATCC 33913T (X95917)
99
Xylella fastidiosa ATCC 35879T (AF192343)
0.01

Figure 1.2

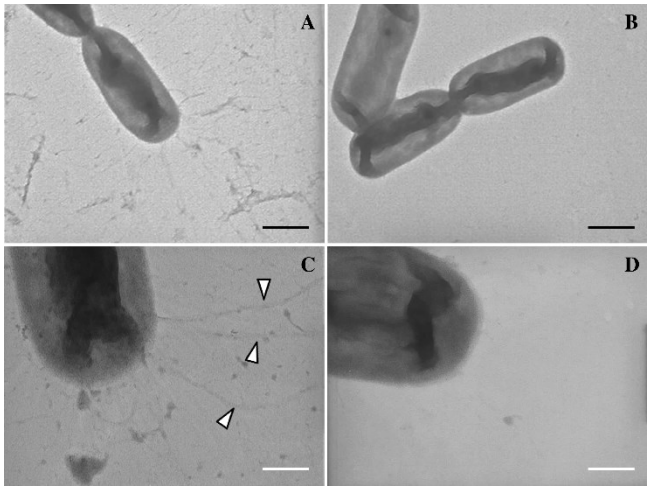

Figure 3.1

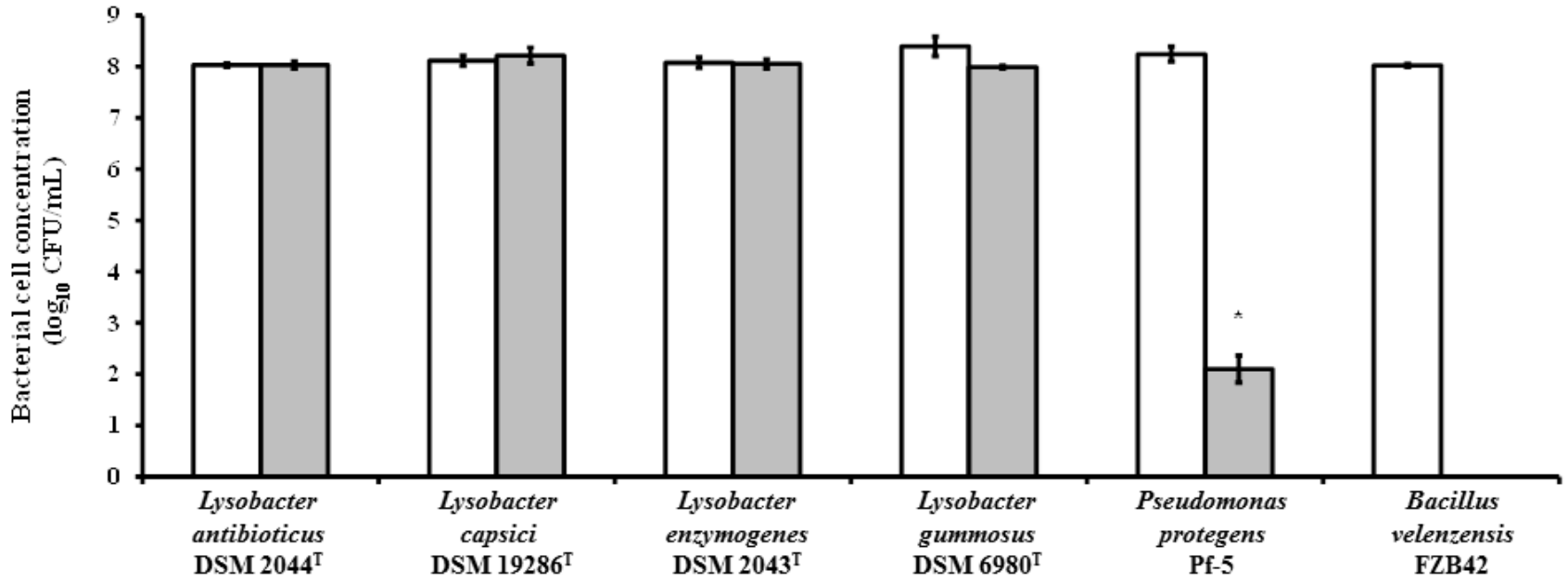
Bacterial cell concentration (log_{10} CFU/mL)
9
8
7
6
5
4
3
2
1
0
*
Lysobacter antibioticus DSM 2044^T
Lysobacter capsici DSM 19286^T
Lysobacter enzymogenes DSM 2043^T
Lysobacter gummosus DSM 6980^T
Pseudomonas protegens Pf-5
Bacillus velenzensis FZB42

Figure 4.1

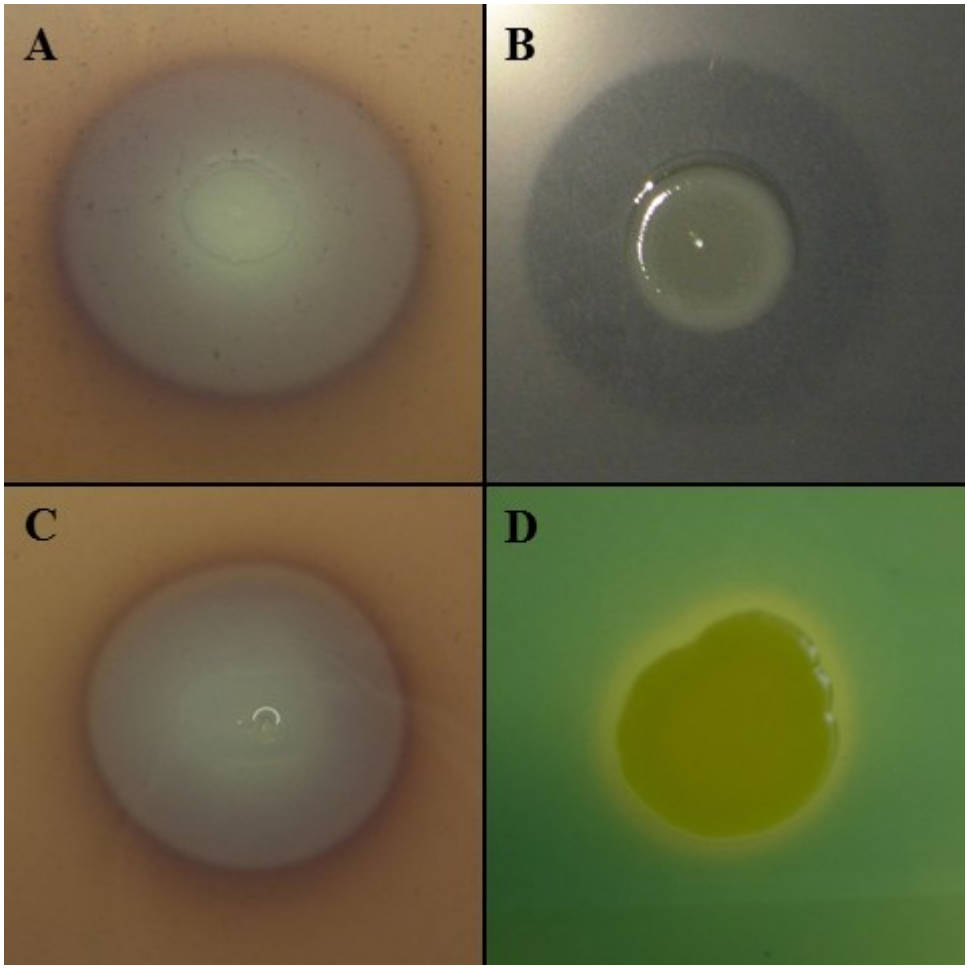

Figure 4.1

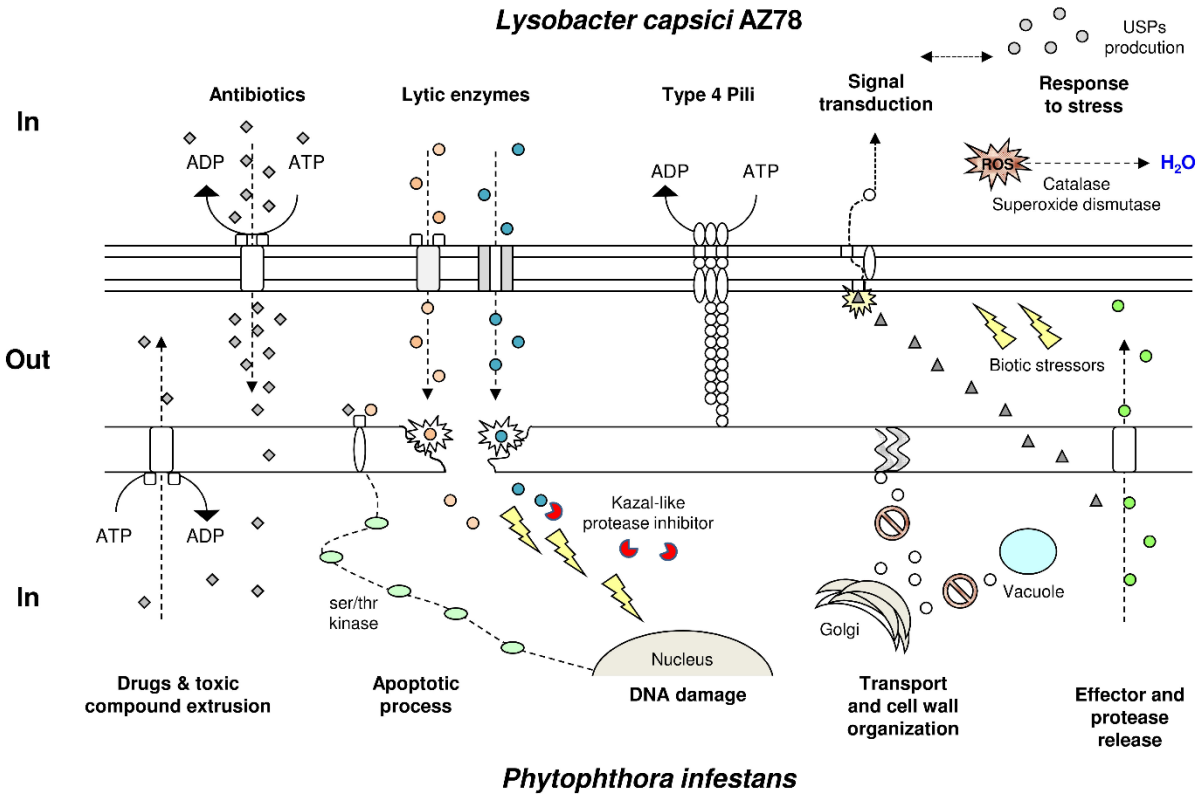
Lysobacter capsici AZ78
USPs
prodcution
Antibiotics
Lytic enzymes
Type 4 Pili
Signal
transduction
Response
to stress
In
ADP
ATP
ADP
ATP
ROS
H2O
Catalase
Superoxide dismutase
Out
Biotic stressors
Kazal-like
protease inhibitor
ATP
ADP
In
ser/thr
kinase
Vacuole
Golgi
Nucleus
Drugs & toxic
compound extrusion
Apoptotic
process
DNA damage
Transport
and cell wall
organization
Effector and
protease
release
Phytophthora infestans

Figure 4.3

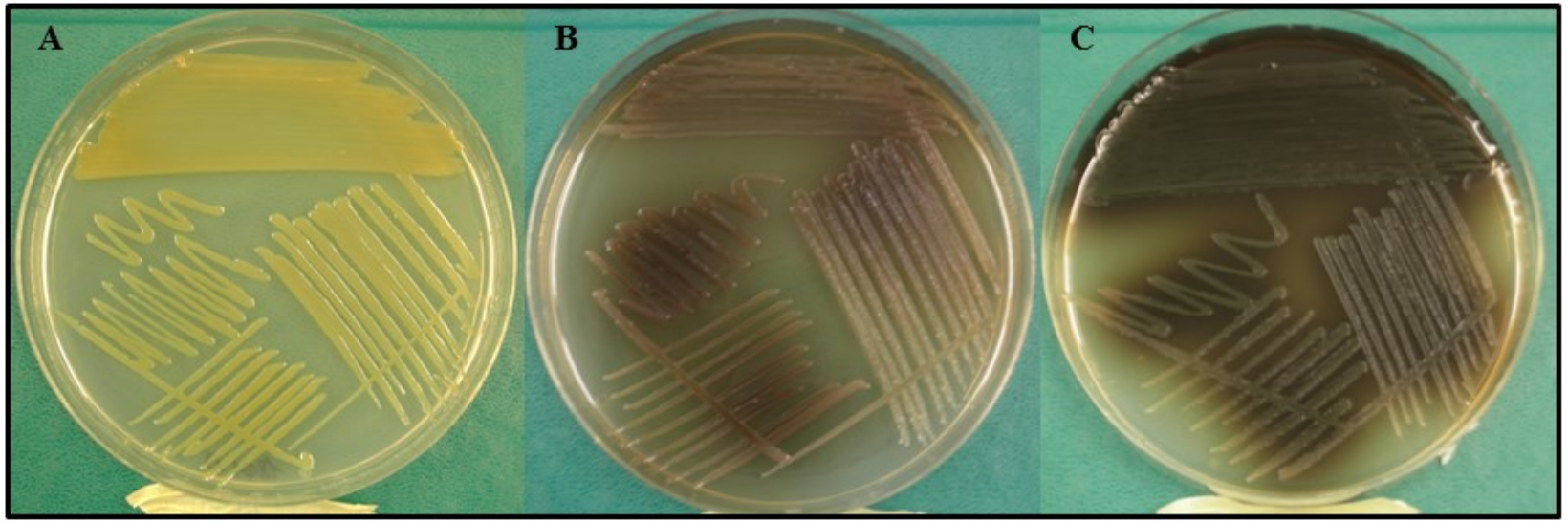

Aim of the study

Since the proposal of the genus, *Lysobacter* spp. attracted the attention for their potential application in biotechnological processes due to their ability to release a large number of lytic enzymes and toxic secondary metabolites. These physiological traits and the ability to induce resistance mechanisms in plants prompted also the selection and characterisation of *Lysobacter* spp. strains as biocontrol agents of plant pathogenic (micro)organisms.

Despite the *Lysobacter*'s activity in controlling plant diseases is well documented, the knowledge on their ecology and the physiology is still understudied compared to *Bacillus* and *Pseudomonas*, bacterial genera encompassing species able to effectively control plant pathogenic microorganisms.

Particularly, no information are available on the role played by macro- and micronutrients available in the rhizosphere on the physiological traits associated to rhizosphere competence in biocontrol *Lysobacter* spp. strains. Similarly, little is known on how *Lysobacter* spp. might face competition with other microorganisms residing in the ecological niches (e.g. rhizosphere, phyllosphere) offered by plants and how these interactions might affect *Lysobacter*'s physiological traits.

To shed a light on these aspects, the impact of the rhizosphere nutrients and bacteria inhabiting plant rhizosphere and phyllosphere on the physiological traits of the biocontrol bacterium *L. capsici* AZ78 was investigated in this study.

To have a picture on how *L. capsici* AZ78 cells might behave in the rhizosphere of crop plants, a growth medium containing components present in the plant rhizosphere was created and used to determine which physiological traits may be modulated in *L. capsici*

AZ78 cells residing in the rhizosphere. The *L. capsici* AZ78 cell ability to move, form biofilm and release bioactive secondary metabolites was investigated via a multitechnique approach including microbiology tests, microscopy, metabolomics and transcriptional analysis.

A similar multitechnique approach was used to have a comprehensive overview of the impact of *Bacillus amyloliquefaciens* S499 and *Pseudomonas protegens* Pf-5, two rhizosphere associated bacterial strains, on the physiological traits of *L. capsici* AZ78. Moreover, the influence of bacterial strains isolated from grapevine leaves on the antagonism activity of *L. capsici* AZ78 against plant pathogenic oomycetes was also investigated during this study to have a complete overview on the effect of bacterial populations on the biocontrol activity of *Lysobacter* members.

It is undeniable that acquiring this information might be relevant to understand better the ecological role of *Lysobacter* spp., particularly about the *L. capsici* species, in the agroecosystem. Results achieved in this study may also pave the way to future activities aimed at unravelling the role played by microbial interactions in soil fertility and the protection of crop plants. Furthermore, from a practical point of view, the selection of bacterial strains able to improve the antagonism efficacy of *L. capsici* AZ78 may represent the basis for the development of novel microbial consortia as biopesticides for the control of plant pathogenic microorganisms.

Chapter 2

The rhizosphere signature on the cell motility, biofilm formation and secondary metabolite production of a plant-associated *Lysobacter* strain

Francesca Brescia[ab], Martina Marchetti-Deschmann[c], Rita Musetti[d], Michele Perazzolli[ae], Ilaria Pertot[ae], Gerardo Puopolo[ae]*

[a]Department of Sustainable Agro-ecosystems and Bioresources, Research and Innovation Centre, Fondazione Edmund Mach, Via E. Mach 1, 38010 San Michele all'Adige, Italy

[b]PhD school in Agricultural Science and Biotechnology, Department of Agricultural, Food, Environmental and Animal Sciences, University of Udine, Udine, Italy

[c]Institute of Chemical Technologies and Analytics, TU Wien (Vienna University of Technology), Vienna, 1060, Austria

[d]Department of Agricultural, Food, Environmental and Animal Sciences, University of Udine, Udine, 33100, Italy

[e]Center Agriculture Food Environment (C3A), University of Trento, Via E. Mach 1, 38010 San Michele all'Adige, Italy

Abstract

Lysobacter spp. are common bacterial inhabitants of the rhizosphere of diverse plant species. However, the impact of the rhizosphere conditions on their physiology is still relatively understudied. To provide clues on the behaviour of *Lysobacter* spp. in this ecological niche, we investigated the physiology of *L. capsici* AZ78 (AZ78), a biocontrol strain isolated from tobacco rhizosphere, on a common synthetic growth medium (LBA) and on a growth medium containing components of the plant rhizosphere (RMA). The presence of a halo surrounding the AZ78 colony on RMA was a first visible effect related to differences in growth medium composition and it

corresponded to the formation of a large outer ring. The lower quantity of nutrients available in RMA as compared with LBA was associated to a higher expression of a gene encoding cAMP-receptor-like protein (Clp), responsible for cell motility and biofilm formation regulation. AZ78 cells on RMA were motile, equipped with cell surface appendages and organised in small groups embedded in a dense layer of fibrils. Metabolic profiling by mass spectrometry imaging revealed increased diversity of analytes produced by AZ78 on RMA as compared with LBA. In particular, putative cyclic lipodepsipeptides, polycyclic tetramate macrolactams, cyclic macrolactams and other putative secondary metabolites with antibiotic activity were identified. Overall, the results obtained in this study shed a light on AZ78 potential to thrive in the rhizosphere by its ability to move, form biofilm and release secondary metabolites.

Keywords

Rhizosphere, *Lysobacter*, biofilm, cell motility, secondary metabolites, mass spectrometric imaging

1. Introduction

In the rhizosphere, plant roots release organic matter, including root exudates, in an important and metabolically expensive process called rhizodeposition (Walker et al., 2003). It was estimated that young plants can invest in root exudates about 30-40% of their fixed carbon (Lynch and Whipps, 1990). Root exudates mainly encompass carbon-based compounds, such as amino acids, organic acids, sugars, secondary metabolites and high-molecular weight compounds like mucilage and proteins (Uren, 2007). The dialogue between plants and microbial community based on rhizodeposition is continuous and microbial communities change during plant development according to the chemical composition of root exudates (Zhalnina et al., 2018). As these compounds

are an easily available carbon source for soil microbes (van Hees et al., 2005), plants may improve their own fitness by actively selecting beneficial bacteria through rhizodeposition (Doornbos et al., 2012; Kobayashi et al., 2013). The capacity of plants to modify the microflora inhabiting the rhizosphere was demonstrated by adding root exudates or synthetic root exudates to solidified media or to formulated synthetic soils (Baudoin et al., 2003; Downie et al., 2012; Grayston et al., 1998), indicating that structural manipulation of rhizobacterial communities can be mediated by root exudates. The same approach was followed also to determine how the rhizosphere conditions may impact the behaviour of plant beneficial bacteria. In this way, it was shown that compounds exuded in the rhizosphere may actively modulate bacterial physiological traits such as formation of biofilm and biosynthesis of secondary metabolites (Debois et al., 2015; Kamilova et al., 2006; Nihorimbere et al., 2012). Therefore, a complex molecular crosstalk takes place at the soil-root interface. For instance, when beneficial bacteria sense the presence of the plant, they induce the systemic resistance of the plant starting the production of secondary metabolites (Debois et al., 2015).

Among the common inhabitants of plant rhizosphere, it was recently shown that *Lysobacter* spp. was part of the core microbiome of the rhizosphere of switchgrass (*Panicum virgatum* L.) plants collected from different soils and environments (Rodrigues et al., 2018). Regarding crop plants, type strains of *Lysobacter* spp. were isolated from the rhizosphere of pepper (*Capsicum annuum* L.), rice (*Oryza sativa* L.) and tomato (*Solanum lycopersicum* L.) plants, providing another proof of *Lysobacter* spp. as common inhabitants of plant rhizospheres (Aslam et al., 2009; Kim et al., 2017; Park et al., 2008). Notably, the presence of *Lysobacter* members in agricultural soils was often found in correlation with the suppressiveness of these soils against plant

pathogenic microorganisms such as *Ralstonia solanacearum*, *Rhizoctonia solani* and *Streptomyces* spp. (Postma et al., 2010; Rosenzweig et al., 2012; Wang et al., 2017).

The involvement of *Lysobacter* spp. in the active control of plant pathogens is sustained by their capacity to prey upon other microorganisms through a wolf-pack behaviour (Seccareccia et al., 2015) and to produce a vast array of lytic enzymes and bioactive secondary metabolites (Puopolo et al., 2018). *Lysobacter* biocontrol strains are characterised by the ability to produce toxic compounds belonging to the polycyclic tetramate macrolactams family against *Peronosporomycetes,* as in the case of Xanthobaccins A, B and C produced by *L. capsici* SB-K88 (Islam et al., 2005; Nakayama et al., 1999; Puopolo et al., 2018). Remaining in this family of bioactive secondary metabolites, particular interest was given to the dihydromalthophilin, also called heat stable antifungal factor (HSAF) produced by the biocontrol strain *L. enzymogenes* C3 (Yu et al., 2007), since it was involved in the control of plant pathogenic fungi and nematodes (Li et al., 2008; Yuen et al., 2018). The toxicity of dihydromalthophilin/HSAF was related to its ability to trigger the production of reactive oxygen species and its negative impact on the sphingolipid biosynthesis and tricarboxylic acid cycle (Amin et al., 2015; Ding et al., 2016; He et al., 2018; Li et al., 2009). Interestingly, the same bacterial strain was also able to produce other three polycyclic tetramate macrolactams, namely alteramide A, lysobacteramide A and B that, besides antifungal activity, showed activity against human carcinoma also (Xu et al., 2015). Other bioactive secondary metabolites produced by *Lysobacter* biocontrol strains received particular attention from sectors other than agriculture as in the case of the cyclic lipodepsipeptides WAP-8294A produced by *L. enzymogenes* OH11 toxic against human pathogenic Gram-positive bacteria (Zhang et al., 2011). Many of these bioactive secondary metabolites are encoded by polyketide synthase (PKS) gene

clusters (Xie et al., 2012). Polyketides are natural products structurally diverse as, once produced, they undergo post-PKS modifications (Pfeifer and Khosla, 2001). However, little is known on how rhizosphere conditions might influence the physiological traits of *Lysobacter* plant beneficial strains and the biosynthesis of secondary metabolites. To shed a light on aspects of rhizosphere colonization and secondary metabolite production, we formulated a culture medium containing components present in the plant rhizosphere and we evaluated its impact on the physiological traits of *L. capsici* AZ78 (AZ78), a biocontrol agent isolated from tobacco rhizosphere (Puopolo et al., 2014a). Particular attention was given to the capacity of this strain to move on solid surfaces, form biofilm and to release bioactive secondary metabolites. The AZ78 metabolic profile was investigated using Matrix Assisted Laser Desorption Ionisation Time of Flight Mass Spectrometric Imaging (MALDI-TOF-MSI), while Transmission Electron Microscope (TEM) and phase-contrast microscope were used to visualise motility appendages and the AZ78 macrocolony structure.

2. Materials and methods

2.1 Maintenance and preparation of Lysobacter capsici *AZ78 cell suspension*

AZ78 was stored at length in glycerol 40% at -80°C and routinely grown at 27°C on Luria–Bertani Agar [LBA; LB broth (Sigma Chemical-St.Louis, MO,USA, Tryptone 10 g/l, Yeast Extract 5 g/l, NaCl 10 g/l), Agar Technical No.2 16 g/l (Oxoid-Columbia, MD, USA)] in Petri dishes (90 mm diameter). To prepare cell suspension, AZ78 cells were picked from LBA dishes after 48 h incubation at 27°C using sterile 10 μl loops and suspended in 1 ml sterile saline solution (0.85% NaCl w/v) contained into sterile 2 ml microcentrifuge tubes. The AZ78 cell suspension was centrifuged (13,000 rpm, 1

min), supernatant was discarded and the pellet was suspended in 1 ml sterile saline solution. These steps were repeated twice to remove any trace of nutrients from LBA and secondary metabolites released during AZ78 growth. Finally, AZ78 pelleted cells were suspended into sterile saline solution, adjusted to a final concentration of 1×10^9 colony forming units per volume unit (cfu/ml) and used in all experiments.

2.2 Rhizosphere-Mimicking growth medium

The growth medium named Rhizosphere-Mimicking Agar (RMA) was prepared simulating the amount of carbon released by plants in the rhizosphere soil in one day according to Chen et al. (2006) and Jones et al. (2009). The ingredients included synthetic root exudates, recalcitrant organic carbon sources and salts (Table 1; Baudoin et al., 2003). RMA ingredient concentrations were estimated taking into account that plant tissue residues in soil are related to their decomposition rate (Chen et al., 2001). The pH was adjusted to 6.5 and Agar Technical No. 2 (Oxoid) was added (16 g/l). To avoid caramelization, sugars were filter-sterilised (0.2 μm Sartorius, Goettingen, Germany) and added after autoclaving.

2.3 Cell growth

Five μl of AZ78 cell suspension were spot-inoculated on LBA and RMA Petri dishes (50 mm diameter) and incubated at 25°C. The growth of AZ78 on LBA and RMA was monitored at 12, 24 and 36 h by capturing digital images of AZ78 macrocolonies using Bio-Rad Quantity One software implemented in a Bio-Rad Geldoc system (Bio-Rad Laboratories, Inc., Hercules, California, U.S.A.). Subsequently, the AZ78 macrocolony

area was measured using Fiji software (ImageJ1.50i; Schneider et al., 2012). To determine the quantity of AZ78 viable cells residing in the macrocolony area, plugs (5 mm diameter) were sampled from each macrocolony and transferred into sterile 2 ml microcentrifuge tubes containing 1 ml of sterile saline solution amended with Tween 20 (0.1% v/v). A sonication step was used to dissolve cell aggregates using three cycles of gentle sonication: 15 s at 15% of the power of the device [Branson sonifier 250-450 (Ultrasonics Corporation, Danbury, Connecticut, USA)] alternated to 10 s of pause. The resulting solution was serially diluted and plated on Tryptic Soy Agar 1/10 [TS broth (Sigma); Agar Technical No.2 (Oxoid) 16 g/l (w/v)], cfu were counted 48 h after incubation at 25°C and the cell concentration was expressed as the $\log_{10}$ (cfu)/macrocolony. Three replicates (Petri dishes) for each time-point were used and the experiment was carried out twice.

2.4 Total RNA extraction and gene expression analysis

Five µl of AZ78 cell suspension were spot-inoculated on LBA and RMA (3 ml) contained in Petri dishes (50 mm diameter). RNA was extracted after 36 h incubation at 25°C from macrocolonies developed on LBA and RMA according to the following procedure. Agar plugs (5 mm diameter) were collected in aluminium paper and instantly frozen in liquid nitrogen. The frozen plugs were placed in pre-frozen steel jars containing sterile beads and processed at 25 Hz for 1 min using a mixer mill disruptor (MM200, Retsch, Haan, Germany). The resulting powder was transferred into sterile 2 ml RNAse-free microcentrifuge tubes placing up to 100 mg of powder each. To lyse the AZ78 cell wall, 0.3 ml of lysis buffer (30 mM Tris, 30 mM EDTA, 10 mg/ml lysozyme, pH 6.2) were added to each microcentrifuge tube, vortexed vigorously and incubated at

37°C with constant shaking (1,000 rpm) for 30 min (Villa-Rodríguez et al., 2018). RNA was extracted using Spectrum™ Plant Total RNA Kit (Sigma-Aldrich) according to manufacturer's instructions. The extracted RNA was run in a 1% agarose gel to assess the integrity and quantified using Qubit® Fluorimetric Quantitation (Invitrogen, Life Technologies, Waltham, MA) with Qubit RNA BR assay (Invitrogen, Life Technologies). RNA was long term stored at -80°C. To process similar quantities of AZ78 cells, three replicates respectively made by five and 40 Petri dishes for LBA and RMA were used for each treatment and the experiments were carried out twice.

To carry out quantitative real-time PCR (qRT-PCR), first-strand cDNA was synthesised from 900 ng of purified total RNA with the SuperScript III Reverse Transcriptase RT kit (Thermo Fisher Scientific, Invitrogen, Waltham, Massachusetts, U.S.A.) with random hexamers, according to the manufacturer's instructions. qRT-PCR were carried out to monitor the expression level of the gene *AZ78_4111* encoding a cAMP-receptor-like protein (Clp), responsible for cell motility and biofilm formation, using previously designed primers (clpF: ACTCGGCCTATTCATCGAAA, clpR: GTCAGCAGCAGGTCGTACAG; Tomada et al., 2016).

The qRT-PCR reactions were carried out with LightCycler 480 (Roche Diagnostics, Mannheim, Germany) and Platinum SYBR Green qPCR SuperMix-UDG (Thermo Fisher Scientific, Invitrogen) and they consisted of 60 amplification cycles (95°C for 15 s and 60°C for 45 s) and melting curve analysis. LightCycler 480 SV1.5.0 software (Roche Diagnostics) was used to extract the cycle threshold (Ct) values using the second derivative calculation. LinRegPCR 11.1 software (Ruijter et al., 2009) was used to calculate the reaction efficiency. The relative quantities (RQ) were calculated according to the formula:

$RQ = Eff^{(Ct-Ct^*)}$

where Ct is the threshold cycle and Ct* is the average Ct of all the conditions analysed (Hellemans et al., 2007). To calculate the normalised relative quantities (NRQ) the RQ values of *AZ78_4111* were divided by the RQ of the housekeeping gene *AZ78_1089* encoding RecA using the previously designed primers (recAF: GAGCCAGATCGACAAGCAAT, recAR :GGACCGTAGATCTCGACCAC; Tomada et al., 2016). For each treatment, three replicates were used and qRT-PCR reactions were carried out for two independent experiments.

2.5 Cell motility

The impact of LBA and RMA on AZ78 cell motility was assessed according to Chen et al. (2018). Briefly, a sterilised glass slide was placed into a Petri dish (90 mm diameter) and 14 ml of LBA and/or RMA were poured on the top. Once solidified, the agar medium in excess was removed with a sterile scalpel and discarded. To create a thin inoculation line, the edge of a sterilised coverslip was dropped into an AZ78 cell suspension and then gently pressed onto the surface of each medium. After 36 h incubation at 25°C in a wet chamber, the glass slides were observed using a phase-contrast microscope (Nikon Eclipse 80i, Tokyo, Japan) under 20X and 100X magnification. Pictures were taken with a digital camera (Nikon DS-Fi1) connected to the microscope. Three replicates (glass slides) for each treatment were prepared and the experiment was carried out twice.

2.6 Transmission Electron Microscopy (TEM)

AZ78 was grown on LBA and RMA for 36 h at 25°C. To obtain a similar quantity of cells, AZ78 cells were collected with a sterile loop from the borders of the macrocolony developed on 40 RMA dishes (50 mm diameter) and on five LBA dishes (50 mm diameter) and suspended in 1 ml of sterile distilled water contained in sterile 2 ml microcentrifuge tubes. Drops (50 µl) of the cell suspension were adsorbed to TEM carbon-formvar coated nickel grids for 10 min, at room temperature. The bacterial cells were then stained 10 min with UAR-EMS (uranyl acetate replacement stain) (Electron Microscopy Sciences, Fort Washington, PA, USA), and observed under a PHILIPS CM 10 (FEI, Eindhoven, The Netherlands) TEM (Cowles and Gitai, 2010), operated at 80 kV, and equipped with a Megaview G3 CCD camera (EMSIS GmbH, Münster, Germany). Three replicates for each treatment were used and the experiment was carried out twice.

2.7 Biofilm production

AZ78 was evaluated for its ability to form biofilm on polystyrene microtiter plates according to Puopolo et al. (2014a). Briefly, 1.5 µl of AZ78 cell suspension was inoculated into 150 µl of sterile LB broth (LB) and Rhizosphere Mimicking broth (RM) contained in 96-well polystyrene plates. Wells containing uninoculated LB and RM were used as untreated samples. Plates were incubated for 36 h at 25°C without shaking and cell densities were determined by scoring the absorbance at optical density (OD) 600 nm ($A_{OD600nm}$). Unattached cells were removed by inverting the plate and tapping it vigorously onto absorbent paper. The AZ78 cells adhering to the wells were fixed for 20 min at 50°C and then stained for one min adding 150 µl of crystal violet solution (0.1% w/v in sterile distilled water) per well. Excess stain was removed by inverting the plate,

then washing it twice with distilled water (250 µl per well). Adherent cells were decolorised with an acetone/ethanol (20%/80%) solution (200 µl per well) for five min to release the dye into the solution. A volume of 100 µl was transferred from each well to another 96-well polystyrene plate and the amount of dye (proportional to the density of adherent cells) was quantified by scoring the absorbance at OD 540 nm ($A_{OD540nm}$). To determine the specific biofilm formation value (SBF) the following formula was applied:

$$SBF = (A_{OD540nm}X - A_{OD540nm}C) / (A_{OD600nm}X - A_{OD600nm}C)$$

where X indicated the treated samples whereas C indicated the untreated samples. For each treatment, ten replicates (wells) were used and the experiment was carried out twice.

2.8 Matrix-Assisted Laser Desorption/Ionisation Time of Flight Mass Spectrometric Imaging (MALDI-TOF-MSI)

AZ78 cells were spot-inoculated on 1 mm thick growth medium layer (LBA and/or RMA) poured onto sterile glass slides. To get reproducible conditions an even and smooth surface is of importance for MALDI-TOF-MSI. For this we further developed our recently published microassay (Holzlechner et al., 2016) and used two sterile glass slides which were hold in place in a distance of exactly 1 mm by sterile spacers. This construct was placed in a sterile Petri dish (90 mm diameter) and 13 ml of growth medium were poured in the Petri dish filling also the gap between the slides giving an area of 5.5 × 2.5 cm. Once solidified, the medium in excess was cut and discarded and the glass slide on the top and the spacers were gently removed. Lastly, five µl of AZ78

cell suspension were spot inoculated on the growth medium layer adhering to the glass slides. An area of 25 mm^2 of growth medium was kept apart from the inoculated medium in order to identify the mass spectrometric signals (*m/z* values) belonging to the growth medium (blank).

Once inoculated, the glass slides were incubated at 25°C for 36 h and, subsequently, samples were dried in a desiccator under vacuum overnight at room temperature. Afterwards, a photograph was taken using a glass slides scanner and 0.15-0.20 mg of a 1:1 mixture of 2,5-dihydroxybenzoic acid (2,5-DHB) and α-cyano-4-hydroxy-cinnamic acid (α-CHCA) were sublimed per cm^2 onto the sample using a home-built instrumentation. A subsequent recrystallisation step at 86°C for 1 min using 1% acetic acid in water ensured analyte incorporation (Yang and Caprioli, 2011). MALDI-TOF-MSI experiments were then immediately performed on a Synapt G2 HDMS (Waters, Milford, Massachusetts, United States) in positive linear mode, with 150 × 75 µm laser step, the laser energy was set to 250 a.u., 1000 Hz of firing rate, 1 scan per pixel and a mass range of 20–4000 Da. For accurate mass measurements the instrument was calibrated before each run using red phosphorous. Data of three biological replicates of the microassay per treatment (growth medium) were analysed using Datacube Explorer (Klinkert et al., 2014), MSiReader (Robichaud et al., 2013), and MassLynx (Waters). For tentative assignment of analytes to measure signals, accurate *m/z* values (± 0.002 Da) extracted from the profile mass spectra present at least in two biological replicates were submitted to "The Metabolomics Workbench" (http://www.metabolomicsworkbench.org/, 2019) and searched in literature. To carry out a presence/absence analysis, *m/z* values that were not present in the blank were searched in the centre core (CC), the outer ring (OR) of the AZ78 macrocolony and in a sector of growth medium adjacent to the OR of the AZ78 macrocolony (GM).

2.8 Genome mining

An antiSMASH 5.0.0 analysis (Blin et al., 2019; https://antismash.secondarymetabolites.org) was used to find gene clusters potentially involved in the biosynthesis of bioactive secondary metabolites in AZ78 genome (JAJA02000000.2; Puopolo et al., 2016). The detection strictness of the analysis was relaxed and the extra features KnownClusterBlast, ClusterBlast, ActiveSiteFinder, Cluster Pfam analysis and Pfam-based GO term annotation were selected.

2.10 Statistical analysis

The statistical analysis was performed using R package (https://www.r-project.org/). The repetitions of the experiments were tested for significant differences with a two-way analysis of variance (ANOVA). In absence of significant differences, the experiments were pooled and data were analysed using one-way ANOVA. Mean comparisons were carried out using Student's *T*-test (α=0.05).

3. Results

3.1 Growth medium modulates Lysobacter capsici *AZ78 cell growth and the expression of the master regulator* clp

The appearance of AZ78 macrocolony changed according to the growth medium. It was creamy and yellowish on LBA (Figure 1A), while it was whitish-transparent on RMA (Figure 1B). Moreover, the macrocolony was surrounded by a halo that reached the maximum area after 36 h growth exclusively on RMA (Figure 1B). The different

appearance of AZ78 macrocolony was associated to differences in the AZ78 cell growth. At each time point, the number of AZ78 viable cells residing in the macrocolony was two orders of magnitude lower on RMA than on LBA (Figure 1C). These differences were associated to a higher *clp* expression on RMA (3.11 ± 0.25; mean ± standard error) than LBA (0.46 ± 0.01; Figure S1).

3.2 Morphology of Lysobacter capsici *AZ78 macrocolonies and cell motility are affected by growth medium*

AZ78 macrocolonies developed on LBA showed a well-defined and compact growth front with cells tightly disposed on the surface of the medium (Figure 2A). On LBA, a centre core (CC) composed by multiple layers of cells and a mono-layer outer ring (OR) were identified (Figure 2B). A CC constituted by multiple cell layers was also observed on RMA (Figure 2C). However, the mono-layer OR observed on RMA was more extended compared to LBA and the AZ78 cells were disposed in small groups packed along the same axis (Figure 2D). Moreover, AZ78 cells moved on RMA surface, while no cell movement was observed on LBA surface.

TEM analysis revealed that many of the AZ78 cells grown on LBA were in division and were surrounded by heterogeneous biomaterials such as membrane vesicles, long fibrils and cellular detritus (Figure 3A, B, C). Compared to RMA, AZ78 cells grown on LBA were slightly bigger and their cytoplasm presented nucleoid-like areas with low electron density (Figure 3A, C). When grown on RMA, AZ78 cells were tightly packed along the same axis in small groups, surrounded by fibrils and by electron-dense granules, probably part of the extracellular polymeric substance (Figure 3D, E). Polar fimbriae were visible in some AZ78 cells grown on RMA only (Figure 3F).

These differences on the cell morphology due to the growth medium were also reflected in the different capacity of AZ78 cells to form biofilm in LB and RM (Figure S2). The SBF values reached by AZ78 in RM (0.55 ± 0.09) were five time higher than those reached in LB (0.11 ± 0.01).

3.3 The growth medium impacts Lysobacter capsici *AZ78 metabolic profile and analyte spatial distribution*

In general, the comparison of the metabolic profiles of AZ78 macrocolonies originated on the two growth media revealed a higher quantity number of biologically relevant signals on RMA compared to LBA (Figure 4A); whereas the ion intensities in RMA were lower than in LBA. Moreover, almost no spatial differiation was observed for CC and OR in LBA. In contrast, the OR was clearly distinguishable from the rest of the AZ78 macrocolony in MALDI-TOF-MSI images on RMA (Figure 4A, B). On RMA, no biologocaly relevant signals were found in the GM region, but 35 signals were detected inside the OR and CC regions. Among the latter, 31 *m/z* values were shared by OR and CC regions while four signals were found in the OR region only. In particular, *m/z* 498.973, tentatively assigned to be thiamine pyrophosphate based on accurate mass measurements, was exclusively found in the OR region of RMA and was not present in the three regions of AZ78 macrocolony on LBA (Figure 4A).

The high number of signals found in the CC and OR of AZ78 macrocolonies developed on RMA was characterised by a robust presence of analytes (*m/z* 523.455, 750.467, 762.459, 764.433, 778.430, 806.469, 1421.856, 1423.823) that might match compounds belonging to the classes of fatty acid lipids, glycerophospholipids, hopanoids, sphingolipids and sterol lipids. Moreover, these regions were also characterised by

signals at *m/z* 71.989, 811.410 and 825.401 tentatively assigned to be hydroxylamine, a triterpene saponin-like compound and a nucleoside-like compound, respectively. Finally, eight signals (i.e. the *m/z* 1419.956, 1421.856, 1447.818, 1461.858, 1606.755, 1622.825, 1636.829, 1650.838) detected in the CC and OR of AZ78 macrocolonies grown on RMA did not match with any compound in the database so far (Figure 4A).

AZ78 macrocolonies developed on LBA and RMA shared some signals with different distribution according to the growth medium. For instance, signals at *m/z* 96.077 and 112.051 that might match with amine derivatives were found only in the OR of AZ78 macrocolonies on RMA, while they were present in the CC and OR in the case of AZ78 macrocolonies on LBA. Similarly, the signal at *m/z* 156.042, tentatively assignd to be indole, was found in the CC, OR and GM on LBA, while only in the OR on RMA (Figure 4A, C). The signal at *m/z* 602.919 that might match with a pyrimidine nucleotide sugar was found in CC and OR on RMA and only in GM on LBA (Figure 4A). Other signals were specific for AZ78 macrocolonies developed on LBA, as in the case of the signals at *m/z* 74.097 and 257.149 possibly matching with amine derivatives and a cyclodipeptide respectively found in CC and OR on LBA and the signal at *m/z* 265.966 matching with a pyrrole derivative found in GM on LBA (Figure 4A, D).

The influence of the growth media on the production and release of antibiotics was determined by coupling genome mining and MALDI-TOF-MSI. Firstly, an antiSMASH analysis was carried out to identify genome regions putatively involved in the biosynthesis of secondary metabolites. This analysis revealed the presence of genome regions showing similarity with already known regions involved in the biosynthesis of antibiotics by *L. enzymogenes* strains (Table 2). In particular, the region 1.3 showed 100% of similarity with a genome region of *L. enzymogenes* C3 involved in the biosynthesis of the polycyclic tetramate lactam dihydromalthophilin/HSAF (Figure

S3A; Yu et al., 2007) whereas the region 1.1 showed 50% similarity with the genome region of *L. enzymogenes* OH11 involved in the biosynthesis of the cyclic lipodepsipeptide WAP-8294A2 (Figure S3B; Zhang et al., 2011). The region 1.2 and 1.9 showed 18 and 6% similarity respectively with genome regions responsible for the production of pyrrolopyrazines Le- pyrrolopyrazines A, B and C by *L. enzymogenes* OH11 (Li et al., 2017), and macrocyclic depsipeptide Lysobactin by *Lysobacter* sp. ATCC 53042 (Hou et al., 2011). Other regions did not show similarity with any known cluster and included regions putatively responsible for the biosynthesis of bacteriocins (1.4, 1.6), lanthipeptides (1.5, 3.1) and polyketide-like compounds (2.1; Table 2).

Based on antiSMASH analysis outcome, signals at *m/z* values possibly matching with antibiotics synthesised by *L. enzymogenes* strains were searched in the AZ78 metabolic profiles obtained by MALDI-TOF-MSI analysis. Signals at *m/z* values of 535.495 and 549.437 possibly match these secondary metabolites, especially those belonging to the polycyclic tetramate macrolactams, such as dihydromalthophilin/HSAF, which was exclusively found in the CC and OR regions of AZ78 macrocolonies developed on RMA (Figure 4A, E). Similarly, signals that might match with polyketide-like compounds of the macrolide class were found at *m/z* 740.452, 754.445, 766.433, 780.424, 792.431, 794.455 in these regions of AZ78 macrocolonies grown on RMA (Figure 4A, F). Moreover, these regions on RMA were also characterised by the presence of signals at *m/z* 776.414 and 823.413 possibly matching with cyclic macrolactam compounds (Figure 4A). Looking at the LBA, the signals at *m/z* 1584.749, 1586.877 and 1598.824 were exclusively found in the CC, OR and GM regions of AZ78 macrocolonies originated on this medium and they might match with secondary metabolites belonging to the cyclic lipodepsipeptides such as WAP-8294A2 (Figure 4A, G). By today, no *m/z* value possibly matching with bacteriocins, lanthipeptides, le-

pyrrolopyrazines and lysobactin was found in CC, OR and GM regions of AZ78 grown on LBA and RMA (Table 2; Figure 4).

4. Discussion

Having a picture of how AZ78 might behave in the rhizosphere may provide useful insights on its ability to colonise this environment and to produce bioactive secondary metabolites. To take this picture, we formulated an agarised growth medium reproducing the nutrient conditions found in the rhizosphere considering the amount of organic carbon released on average in one day by plants (Jones et al., 2009). The resulting RMA contained root exudates, salts and recalcitrant substances that are found in the rhizosphere, such as cellulose, lignin and starch (Chen et al., 2006). Moreover, we decided to add also humic acids that play an important role in the biotic and abiotic interactions occurring in the rhizosphere (Guo Gao et al., 2015; Kulikova et al., 2016; Olaetxea et al., 2015). We are aware that RMA is a mere simplification of a natural environment, nonetheless, this medium allowed us to have a glimpse into what AZ78 cells might engage in their natural habitat.

Firstly, the appearance of AZ78 macrocolony on RMA was different compared to that originated on LBA and the main visible differences consisted in the colour and in the formation of a surrounding halo. In addition, the quantity of AZ78 viable cells present in the macrocolony on RMA was strongly reduced compared to LBA. Since laboratory growth media, as LBA, are richer in nutrients compared to the rhizosphere (Lugtenberg et al., 2017), it was presumable that AZ78 cells might face nutrient limitation during their growth on RMA. Bacteria respond to nutrient limitation through the activity of master regulators, such as the cAMP receptor protein (CRP) firstly described in

Escherichia coli (Emmer et al., 1970). In this bacterium, CRP is involved in the regulation of carbon metabolism and plays also a role in the formation of biofilms and cell surface appendages (Hardiman et al., 2007; Jackson et al., 2002; Müller et al., 2009; Zheng et al., 2004). Similarly, a cAMP-receptor-like protein (Clp) controls physiological and cellular processes, such as biofilm formation, cell motility and virulence in *Xanthomonas campestris* pv. *campestris* (Chin et al., 2010; He et al., 2007). Interestingly, a *L. enzymogenes* C3 mutant knocked out in *clp* showed different colony morphology compared to the wild type and it was impaired in cell motility (Kobayashi et al., 2005). Moreover, *clp* is crucial in the cell motility and biosynthesis of bioactive secondary metabolites in *L. enzymogenes* OH11 (Qian et al., 2013; Wang et al., 2014). Based on these evidences, we assessed *clp* involvement in the phenotypic changes observed in AZ78 by monitoring its expression, since AZ78 strain is not genetically tractable. The higher expression level of *clp* in AZ78 grown on RMA compared to LBA indicated that changes in AZ78 cell growth rate and macrocolony morphology are possibly associated with a modulation of *clp* expression.

The changes occurring in the AZ78 colony morphology were further explored through microscopy analysis. In the case of AZ78 macrocolony on LBA, cells disposed themselves on the agar surface in a circular colony composed by multi-layers of cells in the centre core and a mono-layer in the outer ring, acquiring morphology similar to other bacterial strains growing on LBA (Su et al., 2012). On this medium rich in protein content, AZ78 macrocolonies were characterised by the presence of many membrane vesicles probably containing proteolytic enzymes as in the case of *Lysobacter* sp. XL1 (Kudryakova et al., 2016). A different scenario was observed on RMA, where such membrane vesicles were not visible and AZ78 macrocolonies were characterised by an extended mono-layer outer ring including AZ78 cells heterogeneously distributed in

small groups. TEM observations indicated that the small AZ78 cell groups originated on RMA were embedded in a dense layer of fibrils that may be part of a biofilm (Jones et al., 1969). Accordingly, AZ78 cells produced a biofilm in RM broth and, on RMA; they were equipped by surface appendages that play a key role in biofilm formation and plant root colonisation in *Lysobacter* members (Islam, 2010; Islam et al., 2005; Xia et al., 2018). Biofilms are cosy niches where some bacterial cells may become metabolically less active, reducing the overall growth rate (Guilhen et al., 2016; Wan et al., 2018). Accordingly, we observed that the AZ78 growth was lower on RMA than LBA, where it was also possible to observe AZ78 cells in division. In the process of biofilm dispersal, it is well accepted that individual cells and multicellular aggregates are released from the biofilm to colonise new environments (Guilhen et al., 2017; Hunt et al., 2004). It is conceivable that AZ78 forms a biofilm on RMA that reaches a mature stage after 36 h and cells located in the mono-layer outer ring differentiate into a subpopulation to explore the surrounding areas. Indeed, microscope analysis revealed that the AZ78 cells located in this region were moving whereas they were immobile in the centre core.

The AZ78 cell motility may be related to the formation of cell surface appendages, that we previously showed to be dependent on the growth medium composition (Tomada et al., 2016), and to the release of amphipathic compounds (Mattingly et al., 2018). Indeed, many *m/z* signals putatively matching with lipids were found only in RMA and could be involved in the reduction of surface tension to facilitate cell motility and to disperse cells from biofilm (Glick et al., 2010; Kinsinger et al., 2003; Wang et al., 2013, 2011). Interestingly, a signal at *m/z* 156.042 that might match indole was found in the outer ring of AZ78 grown on RMA. Recently, indole was proven to improve nutrient absorption and regulate twitching motility in *L. enzymogenes* OH11 (Feng et al., 2019;

Wang et al., 2019). Therefore, it is conceivable that indole may serve to increase the nutrient uptake in single starved AZ78 cells once they move from the biofilm. Notably, the biofilm formation and the cell dispersal observed on RMA are strategies that AZ78 might implement also in the rhizosphere given the importance to reach nutrients before other competitors as well as to firmly occupy the most favourable ecological niches (Kamilova et al., 2005).

As nutrient conditions affect the production of secondary metabolites in *Lysobacter* spp. (Folman et al., 2004; Lazazzara et al., 2017; Wang et al., 2016), the different AZ78 phenotype on the two growth media was also associated to a substantial difference between the metabolic profiles retrieved from MALDI-TOF-MSI. Particularly, the RMA nutrient conditions increased the diversity of analytes produced by AZ78 compared to LBA. This latter growth medium was characterised by the specific presence of a signal at *m/z* 257.149 matching with a putative cyclodipeptide confirming the ability of AZ78 to produce compounds belonging to this family, such as cyclo-L-Pro-L-Tyr (Puopolo et al., 2014b). Similarly, AZ78 released in LBA an analyte with *m/z* 265.966 that matches pyrrole derivatives, not only confirming the ability of *Lysobacter* spp. to produce pyrrole, but also localising it when grown in protein rich growth media (Lazazzara et al., 2017). The putative cyclic lipodespipeptides WAP-8294A1/A2/A4 (respectively *m/z* 1586.877, 1584.749, 1598.824) were exclusively detected on LBA, confirming the presence of an AZ78 genome region showing similarity with a homologous region in *L. enzymogenes* OH11 involved in the biosynthesis of cyclic lipodespipeptides (Zhang et al., 2011). However, the comparison of the two genome regions revealed differences in the arrangement of the regions deputed to the biosynthesis of cyclic lipodespipeptides indicating that the AZ78 genome region may be

involved in the production of novel bioactive metabolites and this would deserve more attention in future studies.

Generally, higher ion intensities were visible in the outer ring of AZ78 macrocolony grown on RMA compared to the centre core. Consistently with previous studies (Yu et al., 2007), the putative dihydromalthophilin/HSAF signal (*m/z* 535.495) was found in nutrient-limited conditions, namely on RMA, and was not detected on LBA. The presence of this substance confirmed the high similarity level found between the AZ78 genome region and the genome region of *L. enzymogenes* C3 deputed to the biosynthesis of the dihydromalthophilin/HSAF (Yu et al., 2007). Another proof of the production of this metabolite relied on the presence of the signal at *m/z* 549.437 that might match with other polycyclic tetramate macrolactams such as alteramide B (*m/z* 549.37 $[M+K]^+$), catacandins A/B (*m/z* 549.37 $[M+K]^+$), and malthophilin (*m/z* 549.39 $[M+K]^+$). Indeed, alteramide B and malthophilin are compounds very close to dihydromalthophilin/HSAF and probably they are intermediate in the synthesis of this compound (Lou et al., 2011). Within the signals exclusively found on RMA, the tentative assigned compounds match with other bioactive secondary metabolites belonging to the family of cyclodepsipeptides (*m/z* 742.397, 748.365), cyclic macrolactams (*m/z* 776.414 and 823.413) and macrolides (*m/z* 740.452, 754.445, 766.433, 780.424, 792.431, 794.455) and it would be interesting to assess the genome region involved in the production of these metabolites in future studies.

Overall, the use of a growth medium mimicking the rhizosphere highlighted how nutrient conditions stimulated processes as cell motility, biofilm formation and biosynthesis of bioactive secondary metabolites in AZ78. All these processes were also associated with a positive modulation of the master regulator *clp*, which role is highly conserved in the members of the *Xanthomonadaceae* family and also in *L. enzymogenes*

(Qian et al., 2013; Wang et al., 2014). AZ78 showed physiological traits fundamental to survive in the rhizosphere, such as attachment to surfaces and biofilm formation, as well as quick movement and colonisation of new niches, producing a variety of secondary metabolites to antagonise competitors. However, more work is needed to characterise AZ78 secondary metabolites and to investigate the role of other components of the microbial community on the physiological traits associated to its rhizosphere competency.

5. References

Amin, S.A., Hmelo, L.R., van Tol, H.M., Durham, B.P., Carlson, L.T., Heal, K.R., Morales, R.L., Berthiaume, C.T., Parker, M.S., Djunaedi, B., Ingalls, A.E., Parsek, M.R., Moran, M.A., Armbrust, E.V., 2015. Interaction and signalling between a cosmopolitan phytoplankton and associated bacteria. Nature 522, 98–101. doi:10.1038/nature14488

Aslam, Z., Yasir, M., Jeon, C.O., Chung, Y.R., 2009. *Lysobacter oryzae* sp. nov., isolated from the rhizosphere of rice (*Oryza sativa* L.). International Journal of Systematic and Evolutionary Microbiology 59, 675–680. doi:10.1099/ijs.0.000588-0

Baudoin, E., Benizri, E., Guckert, A., 2003. Impact of artificial root exudates on the bacterial community structure in bulk soil and maize rhizosphere. Soil Biology and Biochemistry 35, 1183–1192. doi:10.1016/S0038-0717(03)00179-2

Blin, K., Shaw, S., Steinke, K., Villebro, R., Ziemert, N., Lee, S.Y., Medema, M.H., Weber, T., 2019. antiSMASH 5.0: updates to the secondary metabolite genome mining pipeline. Nucleic Acids Research. doi:10.1093/nar/gkz310

Chen, J., Shen, D., Odhiambo, B.O., Xu, D., Han, S., Chou, S.-H., Qian, G., 2018. Two direct gene targets contribute to Clp-dependent regulation of type IV pilus-mediated twitching motility in *Lysobacter enzymogenes* OH11. Applied Microbiology and Biotechnology 102, 7509–7519. doi:10.1007/s00253-018-9196-x

Chen, M.-C., Wang, M.-K., Chiu, C.-Y., Huang, P.-M., King, H.-B., 2001. Determination of low molecular weight dicarboxylic acids and organic functional

groups in rhizosphere and bulk soils of Tsuga and Yushania in a temperate rain forest. Plant and Soil 231, 37–44. doi:10.1023/A:1010347421351

Chen, Y.M., Wang, M.K., Zhuang, S.Y., Chiang, P.N., 2006. Chemical and physical properties of rhizosphere and bulk soils of three tea plants cultivated in Ultisols. Geoderma 136, 378–387. doi:10.1016/J.GEODERMA.2006.04.003

Chin, K.-H., Lee, Y.-C., Tu, Z.-L., Chen, C.-H., Tseng, Y.-H., Yang, J.-M., Ryan, R.P., McCarthy, Y., Dow, J.M., Wang, A.H.-J., Chou, S.-H., 2010. The cAMP Receptor-Like Protein CLP Is a Novel c-di-GMP Receptor Linking Cell–Cell Signaling to Virulence Gene Expression in *Xanthomonas campestris*. Journal of Molecular Biology 396, 646–662. doi:10.1016/j.jmb.2009.11.076

Cowles, K.N., Gitai, Z., 2010. Surface association and the MreB cytoskeleton regulate pilus production, localization and function in *Pseudomonas aeruginosa*. Molecular Microbiology 76, 1411–1426. doi:10.1111/j.1365-2958.2010.07132.x

Debois, D., Fernandez, O., Franzil, L., Jourdan, E., de Brogniez, A., Willems, L., Clément, C., Dorey, S., De Pauw, E., Ongena, M., 2015. Plant polysaccharides initiate underground crosstalk with bacilli by inducing synthesis of the immunogenic lipopeptide surfactin. Environmental Microbiology Reports 7, 570–582. doi:10.1111/1758-2229.12286

Ding, Y., Li, Z., Li, Y., Lu, C., Wang, H., Shen, Y., Du, L., 2016. HSAF-induced antifungal effects in *Candida albicans* through ROS-mediated apoptosis. RSC Advances 6, 30895–30904. doi:10.1039/C5RA26092B

Doornbos, R.F., van Loon, L.C., Bakker, P.A.H.M., 2012. Impact of root exudates and plant defense signaling on bacterial communities in the rhizosphere. A review.

Agronomy for Sustainable Development 32, 227–243. doi:10.1007/s13593-011-0028-y

Downie, H., Holden, N., Otten, W., Spiers, A.J., Valentine, T.A., Dupuy, L.X., 2012. Transparent Soil for imaging the rhizosphere. PLoS ONE 7, e44276. doi:10.1371/journal.pone.0044276

Emmer, M., deCrombrugghe, B., Pastan, I., Perlman, R., 1970. Cyclic AMP receptor protein of *E. coli*: its role in the synthesis of inducible enzymes. Proceedings of the National Academy of Sciences 66, 480–487. doi:10.1073/pnas.66.2.480

Feng,T., Han, Y., Li, B., Li, Z., Yu, Y., Sun, Q., Li, X., Du, L., Zhang, X-H., Wang Y., 2019. Interspecies and intraspecies signals synergistically regulate the twitching motility in *Lysobacter enzymogenes*. Applied and Environmental Microbiology doi:10.1128/AEM.01742-19

Folman, L., De Klein, M.J.E., Postma, J., van Veen, J., 2004. Production of antifungal compounds by *Lysobacter enzymogenes* isolate 3.1T8 under different conditions in relation to its efficacy as a biocontrol agent of *Pythium aphanidermatum* in cucumber. Biological Control 31, 145–154. doi:10.1016/j.biocontrol.2004.03.008

Glick, R., Gilmour, C., Tremblay, J., Satanower, S., Avidan, O., Deziel, E., Greenberg, E.P., Poole, K., Banin, E., 2010. Increase in rhamnolipid synthesis under iron-limiting conditions influences surface motility and biofilm formation in *Pseudomonas aeruginosa*. Journal of Bacteriology 192, 2973–2980. doi:10.1128/JB.01601-09

Goel, A.K., Rajagopal, L., Nagesh, N., Sonti, R.V., 2002. Genetic locus encoding functions involved in biosynthesis and outer membrane localization of

xanthomonadin in *Xanthomonas oryzae* pv. *oryzae*. Journal of Bacteriology 184, 3539–3548. doi:10.1128/jb.184.13.3539-3548.2002

Grayston, S.J., Wang, S., Campbell, C.D., Edwards, A.C., 1998. Selective influence of plant species on microbial diversity in the rhizosphere. Soil Biology and Biochemistry 30, 369–378. doi:10.1016/S0038-0717(97)00124-7

Guilhen, C., Charbonnel, N., Parisot, N., Gueguen, N., Iltis, A., Forestier, C., Balestrino, D., 2016. Transcriptional profiling of *Klebsiella pneumoniae* defines signatures for planktonic, sessile and biofilm-dispersed cells. BMC Genomics 17, 237. doi:10.1186/s12864-016-2557-x

Guilhen, C., Forestier, C., Balestrino, D., 2017. Biofilm dispersal: multiple elaborate strategies for dissemination of bacteria with unique properties. Molecular Microbiology 105, 188–210. doi:10.1111/mmi.13698

Guo Gao, T., Yuan Xu, Y., Jiang, F., Zhen Li, B., Shui Yang, J., Tao Wang, E., Li Yuan, H., 2015. Nodulation characterization and proteomic profiling of *Bradyrhizobium liaoningense* CCBAU05525 in response to water-soluble humic materials. Scientific Reports 5, 10836. doi:10.1038/srep10836

Hardiman, T., Lemuth, K., Keller, M.A., Reuss, M., Siemann-Herzberg, M., 2007. Topology of the global regulatory network of carbon limitation in *Escherichia coli*. Journal of Biotechnology 132, 359–374. doi:10.1016/j.jbiotec.2007.08.029

He, F., Li, B., Ai, G., Kange, A., Zhao, Y., Zhang, X., Jia, Y., Dou, D., Liu, F., Cao, H., 2018. Transcriptomics analysis of the chinese pear pathotype of *Alternaria alternata* gives insights into novel mechanisms of HSAF antifungal activities. International Journal of Molecular Sciences 19, 1841. doi:10.3390/ijms19071841

He, Y.-W., Ng, A.Y.-J., Xu, M., Lin, K., Wang, L.-H., Dong, Y.-H., Zhang, L.-H., 2007. *Xanthomonas campestris* cell-cell communication involves a putative nucleotide receptor protein Clp and a hierarchical signalling network. Molecular Microbiology 64, 281–292. doi:10.1111/j.1365-2958.2007.05670.x

Hellemans, J., Mortier, G., De Paepe, A., Speleman, F., Vandesompele, J., 2007. qBase relative quantification framework and software for management and automated analysis of real-time quantitative PCR data. Genome Biology 8, R19. doi:10.1186/gb-2007-8-2-r19

Holzlechner, M. , Reitschmidt, S. , Gruber, S. , Zeilinger, S., Marchetti-Deschmann, M., 2016. Visualizing fungal metabolites during mycoparasitic interaction by MALDI mass spectrometry imaging. Proteomics, 16, 1742-1746. doi:10.1002/pmic.201500510

Hou, J., Robbel, L., Marahiel, M.A., 2011. Identification and characterization of the Lysobactin biosynthetic gene cluster reveals mechanistic insights into an unusual termination module architecture. Chemistry & Biology 18, 655–664. doi:10.1016/j.chembiol.2011.02.012

Hunt, S.M., Werner, E.M., Huang, B., Hamilton, M.A., Stewart, P.S., 2004. Hypothesis for the role of nutrient starvation in biofilm detachment. Applied and Environmental Microbiology 70, 7418–7425. doi:10.1128/AEM.70.12.7418-7425.2004

Islam, M.T., 2010. Mode of antagonism of a biocontrol bacterium Lysobacter sp. SB-K88 toward a damping-off pathogen *Aphanomyces cochlioides*. World Journal of Microbiology and Biotechnology 26, 629–637. doi:10.1007/s11274-009-0216-y

Islam, M.T., Hashidoko, Y., Deora, A., Ito, T., Tahara, S., 2005. Suppression of damping-off disease in host plants by the rhizoplane bacterium *Lysobacter* sp. strain SB-K88 is linked to plant colonization and antibiosis against soilborne Peronosporomycetes. Applied and Environmental Microbiology 71, 3786–96. doi:10.1128/AEM.71.7.3786-3796.2005

Jackson, D.W., Simecka, J.W., Romeo, T., 2002. Catabolite repression of *Escherichia coli* biofilm formation. Journal of Bacteriology 184, 3406–10. doi:10.1128/jb.184.12.3406-3410.2002

Jones, D.L., Nguyen, C., Finlay, R.D., 2009. Carbon flow in the rhizosphere: carbon trading at the soil-root interface. Plant and Soil 321, 5–33. doi:10.1007/s11104-009-9925-0

Jones, H.C., Roth, I.L., Sanders, W.M., 1969. Electron microscopic study of a slime layer. Journal of Bacteriology 99, 316–25.

Kamilova, F., Kravchenko, L. V., Shaposhnikov, A.I., Azarova, T., Makarova, N., Lugtenberg, B., 2006. Organic acids, sugars, and l -tryptophane in exudates of vegetables growing on stonewool and their effects on activities of rhizosphere bacteria. Molecular Plant-Microbe Interactions 19, 250–256. doi:10.1094/MPMI-19-0250

Kamilova, F., Validov, S., Azarova, T., Mulders, I., Lugtenberg, B., 2005. Enrichment for enhanced competitive plant root tip colonizers selects for a new class of biocontrol bacteria. Environmental Microbiology 7, 1809–1817. doi:10.1111/j.1462-2920.2005.00889.x

Kim, S.-J., Ahn, J.-H., Weon, H.-Y., Joa, J.-H., Hong, S.-B., Seok, S.-J., Kim, J.-S.,

Kwon, S.-W., 2017. *Lysobacter solanacearum* sp. nov., isolated from rhizosphere of tomato. International Journal of Systematic and Evolutionary Microbiology 67, 1102–1106. doi:10.1099/ijsem.0.001729

Kinsinger, R.F., Shirk, M.C., Fall, R., 2003. Rapid surface motility in *Bacillus subtilis* is dependent on extracellular surfactin and potassium ion. Journal of Bacteriology 185, 5627–31. doi:10.1128/jb.185.18.5627-5631.2003

Klinkert, I., Chughtai, K., Ellis, S.R., Heeren, R.M.A., 2014. Methods for full resolution data exploration and visualization for large 2D and 3D mass spectrometry imaging datasets. International Journal of Mass Spectrometry 362, 40–47. doi:10.1016/J.IJMS.2013.12.012

Kobayashi, D.Y., Reedy, R.M., Palumbo, J.D., Zhou, J.-M., Yuen, G.Y., 2005. A *clp* gene homologue belonging to the Crp gene family globally regulates lytic enzyme production, antimicrobial activity, and biological control activity expressed by *Lysobacter enzymogenes* strain C3. Applied and Environmental Microbiology 71, 261–269. doi:10.1128/AEM.71.1.261-269.2005

Kobayashi, Yasufumi, Lakshmanan, V., Kobayashi, Yuriko, Asai, M., Iuchi, S., Kobayashi, M., Bais, H.P., Koyama, H., 2013. Overexpression of AtALMT1 in the *Arabidopsis thaliana* ecotype Columbia results in enhanced Al-activated malate excretion and beneficial bacterium recruitment. Plant Signaling & Behaviour 8. doi:10.4161/psb.25565

Kudryakova, I. V., Shishkova, N.A., Vasilyeva, N. V., 2016. Outer membrane vesicles of *Lysobacter* sp. XL1: biogenesis, functions, and applied prospects. Applied Microbiology and Biotechnology 100, 4791–4801. doi:10.1007/s00253-016-7524-6

Kulikova, N.A., Abroskin, D.P., Badun, G.A., Chernysheva, M.G., Korobkov, V.I., Beer, A.S., Tsvetkova, E.A., Senik, S. V, Klein, O.I., Perminova, I. V, 2016. Label distribution in tissues of wheat seedlings cultivated with tritium-labeled Leonardite humic acid. Scientific Reports 6, 28869. doi:10.1038/srep28869

Lazazzara, V., Perazzolli, M., Pertot, I., Biasioli, F., Puopolo, G., Cappellin, L., 2017. Growth media affect the volatilome and antimicrobial activity against *Phytophthora infestans* in four *Lysobacter* type strains. Microbiological Research 201, 52–62. doi:10.1016/J.MICRES.2017.04.015

Li, S., Calvo, A.M., Yuen, G.Y., Du, L., Harris, S.D., 2009. Induction of cell wall thickening by the antifungal compound dihydromaltophilin disrupts fungal growth and is mediated by sphingolipid biosynthesis. The Journal of Eukaryotic Microbiology 56, 182–7.

Li, S., Jochum, C.C., Yu, F., Zaleta-Rivera, K., Du, L., Harris, S.D., Yuen, G.Y., 2008. An antibiotic complex from *Lysobacter enzymogenes* strain C3: antimicrobial activity and role in plant disease control. Phytopathology 98, 695–701. doi:10.1094/PHYTO-98-6-0695

Li, S., Wu, X., Zhang, L., Shen, Y., Du, L., 2017. Activation of a cryptic gene cluster in *Lysobacter enzymogenes* reveals a module/domain portable mechanism of nonribosomal peptide synthetases in the biosynthesis of pyrrolopyrazines. Organic Letters 19, 5010–5013. doi:10.1021/acs.orglett.7b01611

Lou, L., Qian, G., Xie, Y., Hang, J., Chen, H., Zaleta-Rivera, K., Li, Y., Shen, Y., Dussault, P.H., Liu, F., Du, L., 2011. Biosynthesis of HSAF, a tetramic acid-containing macrolactam from *Lysobacter enzymogenes*. Journal of the American Chemical Society 133, 643–645. doi:10.1021/ja105732c

Lugtenberg, B., Rozen, D.E., Kamilova, F., 2017. Wars between microbes on roots and fruits. F1000Research 6, 343. doi:10.12688/F1000RESEARCH.10696.1

Lynch, J.M., Whipps, J.M., 1990. Substrate flow in the rhizosphere. Plant and Soil 129, 1. https://doi.org/10.1007/BF00011685

Mattingly, A.E., Weaver, A.A., Dimkovikj, A., Shrout, J.D., 2018. Assessing travel conditions: environmental and host influences on bacterial surface motility. Journal of Bacteriology 200, e00014-18. doi: 10.1128/JB.00014-18.

Müller, C.M., Åberg, A., Straseviçiene, J., Emődy, L., Uhlin, B.E., Balsalobre, C., 2009. Type 1 fimbriae, a colonization factor of uropathogenic *Escherichia coli*, are controlled by the metabolic sensor CRP-cAMP. PLoS Pathogens 5, e1000303. doi:10.1371/journal.ppat.1000303

Nakayama, T., Homma, Y., Hashidoko, Y., Mizutani, J., Tahara, S., 1999. Possible role of xanthobaccins produced by *Stenotrophomonas* sp. strain SB-K88 in suppression of sugar beet damping-off disease. Applied and Environmental Microbiology 65, 4334–9.

Nihorimbere, V., Cawoy, H., Seyer, A., Brunelle, A., Thonart, P., Ongena, M., 2012. Impact of rhizosphere factors on cyclic lipopeptide signature from the plant beneficial strain *Bacillus amyloliquefaciens* S499. FEMS Microbiology Ecology 79, 176–191. doi:10.1111/j.1574-6941.2011.01208.x

Olaetxea, M., Mora, V., Bacaicoa, E., Baigorri, R., Garnica, M., Fuentes, M., Casanova, E., Zamarreño, A.M., Iriarte, J.C., Etayo, D., Ederra, I., Gonzalo, R., Garcia-Mina, J.M., 2015. ABA-regulation of root hydraulic conductivity and aquaporin gene-expression is crucial to the plant shoot rise caused by rhizosphere humic acids.

Plant Physiology 169, pp.00596.2015. doi:10.1104/pp.15.00596

Park, J.H., Kim, R., Aslam, Z., Jeon, C.O., Chung, Y.R., 2008. *Lysobacter capsici* sp. nov., with antimicrobial activity, isolated from the rhizosphere of pepper, and emended description of the genus *Lysobacter*. International Journal of Systematic and Evolutionary Microbiology 58, 387–392. doi:10.1099/ijs.0.65290-0

Pfeifer, B.A., Khosla, C., 2001. Biosynthesis of polyketides in heterologous hosts. Microbiology and Molecular Biology Reviews 65, 106–118. doi:10.1128/MMBR.65.1.106-118.2001

Postma, J., Scheper, R.W.A., Schilder, M.T., 2010. Effect of successive cauliflower plantings and *Rhizoctonia solani* AG 2-1 inoculations on disease suppressiveness of a suppressive and a conducive soil. Soil Biology and Biochemistry 42, 804–812. doi:10.1016/J.SOILBIO.2010.01.017

Puopolo, G., Cimmino, A., Palmieri, M.C., Giovannini, O., Evidente, A., Pertot, I., 2014b. *Lysobacter capsici* AZ78 produces cyclo(L-Pro-L-Tyr), a 2,5-diketopiperazine with toxic activity against sporangia of *Phytophthora infestans* and *Plasmopara viticola*. Journal of Applied Microbiology 117, 1168–1180. doi:10.1111/jam.12611

Puopolo, G., Giovannini, O., Pertot, I., 2014a. *Lysobacter capsici* AZ78 can be combined with copper to effectively control *Plasmopara viticola* on grapevine. Microbiological Research 169, 633–642. doi:10.1016/j.micres.2013.09.013

Puopolo, G., Tomada, S., Pertot, I., 2018. The impact of the omics era on the knowledge and use of *Lysobacter* species to control phytopathogenic micro-organisms. Journal of Applied Microbiology 124, 15–27. doi:10.1111/jam.13607

Puopolo, G., Tomada, S., Sonego, P., Moretto, M., Engelen, K., Perazzolli, M., Pertot, I., 2016. The *Lysobacter capsici* AZ78 genome has a gene pool enabling it to interact successfully with phytopathogenic microorganisms and environmental factors. Frontiers in Microbiology 7, 1–14. doi:10.3389/fmicb.2016.00096

Qian, G., Wang, Y., Liu, Y., Xu, F., He, Y.-W., Du, L., Venturi, V., Fan, J., Hu, B., Liu, F., 2013. *Lysobacter enzymogenes* uses two distinct cell-cell signaling systems for differential regulation of secondary-metabolite biosynthesis and colony morphology. Applied and Environmental Microbiology 79, 6604–16. doi:10.1128/AEM.01841-13

Robichaud, G., Garrard, K.P., Barry, J.A., Muddiman, D.C., 2013. MSiReader: An Open-Source Interface to View and Analyze High Resolving Power MS Imaging Files on Matlab Platform. Journal of The American Society for Mass Spectrometry 24, 718–721. doi:10.1007/s13361-013-0607-z

Rodrigues, R.R., Rodgers, N.C., Wu, X., Williams, M.A., 2018. COREMIC: a web-tool to search for a niche associated CORE MICrobiome. PeerJ 6, e4395. doi:10.7717/peerj.4395

Rosenzweig, N., Tiedje, J.M., Quensen, J.F., Meng, Q., Hao, J.J., 2012. Microbial communities associated with potato common scab-suppressive soil determined by pyrosequencing analyses. Plant Disease 96, 718–725. doi:10.1094/PDIS-07-11-0571

Ruijter, J.M., Ramakers, C., Hoogaars, W.M.H., Karlen, Y., Bakker, O., van den Hoff, M.J.B., Moorman, A.F.M., 2009. Amplification efficiency: linking baseline and bias in the analysis of quantitative PCR data. Nucleic Acids Research 37, e45–e45. doi:10.1093/nar/gkp045

Schneider, C.A., Rasband, W.S., Eliceiri, K.W., 2012. NIH Image to ImageJ: 25 years of image analysis. Nature Methods 9, 671–5.

Seccareccia, I., Kost, C., Nett, M., 2015. Quantitative analysis of *Lysobacter* predation. Applied and Environmental Microbiology 81, 7098–105. doi:10.1128/AEM.01781-15

Su, P.-T., Liao, C.-T., Roan, J.-R., Wang, S.-H., Chiou, A., Syu, W.-J., 2012. Bacterial colony from two-dimensional division to three-dimensional development. PLoS ONE 7, e48098. doi:10.1371/journal.pone.0048098

Tomada, S., Puopolo, G., Perazzolli, M., Musetti, R., Loi, N., Pertot, I., 2016. Pea broth enhances the biocontrol efficacy of *Lysobacter capsici* AZ78 by triggering cell motility associated with biogenesis of type IV pilus. Frontiers in Microbiology 7, 1–14. doi:10.3389/fmicb.2016.01136

Uren, N., 2007. Types, amounts, and possible functions of compounds released into the rhizosphere by soil-grown plants. In: Pinton, R., Varanini, Z., Nannipieri, P. (Eds.), The Rhizosphere. CRC Press, Boca Raton, pp. 1-21. doi:10.1201/9781420005585.ch1

van Hees, P.A.W., Jones, D.L., Finlay, R., Godbold, D.L., Lundström, U.S., 2005. The carbon we do not see—the impact of low molecular weight compounds on carbon dynamics and respiration in forest soils: a review. Soil Biology and Biochemistry 37, 1–13. doi:10.1016/J.SOILBIO.2004.06.010

Villa-Rodríguez, E., Ibarra-Gámez, C., de los Santos-Villalobos, S., 2018. Extraction of high-quality RNA from *Bacillus subtilis* with a lysozyme pre-treatment followed by the Trizol method. Journal of Microbiological Methods 147, 14–16.

doi:10.1016/J.MIMET.2018.02.011

Villadsen, N.L., Jacobsen, K.M., Keiding, U.B., Weibel, E.T., Christiansen, B., Vosegaard, T., Bjerring, M., Jensen, F., Johannsen, M., Tørring, T., Poulsen, T.B., 2017. Synthesis of ent-BE-43547A1 reveals a potent hypoxia-selective anticancer agent and uncovers the biosynthetic origin of the APD-CLD natural products. Nature Chemistry 9, 264–272. doi:10.1038/nchem.2657

Walker, T.S., Bais, H.P., Grotewold, E., Vivanco, J.M., 2003. Root exudation and rhizosphere biology. Plant Physiology 132, 44–51. doi:10.1104/pp.102.019661

Wan, N., Wang, H., Ng, C.K., Mukherjee, M., Ren, D., Cao, B., Tang, Y.J., 2018. Bacterial metabolism during biofilm growth investigated by 13C tracing. Frontiers in Microbiology 9, 2657. doi:10.3389/fmicb.2018.02657

Wang, J., Yu, B., Tian, D., Ni, M., 2013. Rhamnolipid but not motility is associated with the initiation of biofilm seeding dispersal of *Pseudomonas aeruginosa* strain PA17. Journal of Biosciences 38, 149–56.

Wang, R., Khan, B.A., Cheung, G.Y.C., Bach, T.-H.L., Jameson-Lee, M., Kong, K.-F., Queck, S.Y., Otto, M., 2011. *Staphylococcus epidermidis* surfactant peptides promote biofilm maturation and dissemination of biofilm-associated infection in mice. Journal of Clinical Investigation 121, 238–248. doi:10.1172/JCI42520

Wang, R., Xu, H., Du, L., Chou, S.-H., Liu, H., Liu, Y., Liu, F., Qian, G., 2016. A TonB-dependent receptor regulates antifungal HSAF biosynthesis in *Lysobacter*. Scientific Reports 6, 26881. doi:10.1038/srep26881

Wang, R., Zhang, H., Sun, L., Qi, G., Chen, S., Zhao, X., 2017. Microbial community composition is related to soil biological and chemical properties and bacterial wilt

outbreak. Scientific Reports 7, 343. doi:10.1038/s41598-017-00472-6

Wang, Y., Tian, T., Zhang, J., Jin, X., Yue, H., Zhang, X.-H., Du, L., Bai, F., 2019. Indole reverses intrinsic antibiotic resistance by activating a novel dual-function importer. MBio 10, e00676-19. doi:10.1128/mBio.00676-19

Wang, Y., Zhao, Yuxin, Zhang, J., Zhao, Yangyang, Shen, Y., Su, Z., Xu, G., Du, L., Huffman, J.M., Venturi, V., Qian, G., Liu, F., 2014. Transcriptomic analysis reveals new regulatory roles of Clp signaling in secondary metabolite biosynthesis and surface motility in *Lysobacter enzymogenes* OH11. Applied Microbiology and Biotechnology 98, 9009–9020. doi:10.1007/s00253-014-6072-1

Xia, J., Chen, J., Chen, Y., Qian, G., Liu, F., 2018. Type IV pilus biogenesis genes and their roles in biofilm formation in the biological control agent *Lysobacter enzymogenes* OH11. Applied Microbiology and Biotechnology 102, 833–846. doi:10.1007/s00253-017-8619-4

Xie, Y., Wright, S., Shen, Y., Du, L., 2012. Bioactive natural products from *Lysobacter*. Natural Product Reports 29, 1277. doi:10.1039/c2np20064c

Xu, L., Wu, P., Wright, S.J., Du, L., Wei, X., 2015. Bioactive polycyclic tetramate macrolactams from *Lysobacter enzymogenes* and their absolute configurations by theoretical ECD calculations. Journal of Natural Products 78, 1841–1847. doi:10.1021/acs.jnatprod.5b00099

Yang, J., Caprioli, R.M., 2011. Matrix sublimation/recrystallization for imaging proteins by mass spectrometry at high spatial resolution. Analytical Chemistry 83, 5728–5734. doi:10.1021/ac200998a

Yu, F., Zaleta-Rivera, K., Zhu, X., Huffman, J., Millet, J.C., Harris, S.D., Yuen, G., Li,

X.-C., Du, L., 2007. Structure and biosynthesis of Heat-Stable Antifungal Factor (HSAF), a broad-spectrum antimycotic with a novel mode of action. Antimicrobial Agents and Chemotherapy 51, 64–72. doi:10.1128/AAC.00931-06

Yuen, G.Y., Broderick, K.C., Jochum, C.C., Chen, C.J., Caswell-Chen, E.P., 2018. Control of cyst nematodes by *Lysobacter enzymogenes* strain C3 and the role of the antibiotic HSAF in the biological control activity. Biological Control 117, 158–163. doi:10.1016/J.BIOCONTROL.2017.11.007

Zhalnina, K., Louie, K.B., Hao, Z., Mansoori, N., da Rocha, U.N., Shi, S., Cho, H., Karaoz, U., Loqué, D., Bowen, B.P., Firestone, M.K., Northen, T.R., Brodie, E.L., 2018. Dynamic root exudate chemistry and microbial substrate preferences drive patterns in rhizosphere microbial community assembly. Nature Microbiology 3, 470–480. doi:10.1038/s41564-018-0129-3

Zhang, W., Li, Y., Qian, G., Wang, Y., Chen, H., Li, Y.-Z., Liu, F., Shen, Y., Du, L., 2011. Identification and characterization of the anti-methicillin-resistant *Staphylococcus aureus* WAP-8294A2 biosynthetic gene cluster from *Lysobacter enzymogenes* OH11. Antimicrobial Agents and Chemotherapy 55, 5581–5589. doi:10.1128/AAC.05370-11

Zheng, D., Constantinidou, C., Hobman, J.L., Minchin, S.D., 2004. Identification of the CRP regulon using *in vitro* and *in vivo* transcriptional profiling. Nucleic Acids Research 32, 5874–5893. doi:10.1093/nar/gkh908

Figure legends

Figure 1. *Lysobacter capsici* AZ78 macrocolony morphology and growth on the two growth media. AZ78 cell suspension was spot inoculated on Luria–Bertani Agar (LBA; A) and Rhizosphere-Mimicking Agar (RMA; B) and incubated at 25°C for 36 h. The arrow indicates a halo surrounding AZ78 macrocolony (B). The viable cells of AZ78 were monitored at 12, 24, 36 hours post-inoculation on LBA and RMA (C). A Two-way ANOVA revealed no significant differences between two independent experiments ($P = 0.43$) and data were pooled. The mean cell concentration ± standard error values of 18 replicates (Petri dishes) from two experiments are reported. For each time point, asterisk indicate values that differ significantly according to Student's t-test ($\alpha = 0.05$).

Figure 2. Visualization of the growth front of *Lysobacter capsici* AZ78 macrocolony. AZ78 cell suspension was spot inoculated on a thin layer of on Luria–Bertani Agar (A, B) or Rhizosphere-Mimicking Agar (C, D) on glass slides and incubated at 25°C for 36 h. AZ78 was observed with a phase-contrast microscope at magnification 20× (A, C) and 100× (B, D). The white bar corresponds to 1 mm and the black bar corresponds to 10 μm.

Figure 3. Visualization of *Lysobacter capsici* AZ78 cellular morphology. AZ78 cell suspensions were spot inoculated on Luria–Bertani Agar (LBA; A, B, C) and Rhizosphere-Mimicking Agar (RMA; D, E, F) dishes and incubated at 25°C for 36 h and analysed by transmission electron microscopy. On LBA nucleoid-like less electron-dense areas in the cytoplasm (n), long fibrils (lf), membrane vesicles (v) and cellular

detritus (d) were visible. On RMA, fibrils (f), electron-dense granules (g), polar fimbriae (pf) were visible. The white bar corresponds to 1 μm, the black bar corresponds to 500 nm.

Figure 4. Mass spectrometric imaging of *Lysobacter capsici* AZ78 grown in the two growth media. Some signals of interest identified in the MALDI-TOF-MSI analysis were selected and reported in the presence/absence analysis (A). AZ78 macrocolony was divided in three regions of interest (RoI): the centre core of the macrocolony (CC), the outer ring of the macrocolony (OR), and the growth medium adjacent to the outer ring (GM) (B). Grey colour indicates the presence of the ion in the corresponding RoI (A). The optical images of the AZ78 macrocolony grown on Luria–Bertani Agar (LBA; left) and Rhizosphere-Mimicking Agar (RMA; right) were acquired just before matrix application. MALDI-TOF-MSI images were recorded at a lateral resolution of 150 x 75 μm and represent TIC (total ion count) normalised data corresponding to *m/z* 156.042, 257.149, 535.495, 740.452 and 1584.749 ± 0.1 Th (respectively C, D, E, F, G), the colour bar shows the intensity values.

Figure S1. Expression analysis of *clp* in *Lysobacter capsici* AZ78 grown in the two media. The normalised relative quantity (NRQ) for the *clp* expression in AZ78 grown on Luria–Bertani Agar (LBA) and Rhizosphere-Mimicking Agar (RMA) at 25°C for 36 h was calculated. A two-way ANOVA revealed no significant difference between two independent experiments ($P = 0.27$) and data were pooled. Columns represent mean NRQ ± standard errors of three replicates for each treatment. Asterisk indicates values that differ significantly according to Student's t-test ($\alpha = 0.05$).

Figure S2. Biofilm formation by *Lysobacter capsici* AZ78 grown in the two liquid media. The specific biofilm formation (SBF) values were calculated for AZ78 grown in and Luria–Bertani broth (LB) and Rhizosphere-Mimicking broth (RM). A two-way ANOVA revealed no significant difference between two independent experiments ($P = 0.24$) and data were pooled. Columns represent mean specific biofilm formation ± standard errors of ten replicates. Asterisk indicates values that differ significantly according to Student's t-test ($\alpha = 0.05$).

Figure S3. Dihydromalthophilin and WAP-8294A gene organization in the *Lysobacter capsici* AZ78, *L. enzymogenes* C3 and *L. enzymogenes* OH11 genome. Putative genes encoding dihydromalthophilin/HSAF in the AZ78 genome are compared to the homologue putative genes in the *L. enzymogenes* C3 (A). Putative genes encoding involved in the biosynthesis of the cyclic lipodepsipeptide WAP-8294A in the AZ78 genome are compared to the homologue putative genes in the *L. enzymogenes* OH11 genome (B). The corresponding accession number is given under each gene.

Table 1. Composition of Rhizosphere Mimicking Agar.

Type	Ingredients[a]	Concentration (g/l)
Synthetic root exudates	Citric acid	0.010
	Fructose[b]	0.039
	Glucose	0.039
	Glutamic acid	0.019
	L-Alanine	0.019
	L-Serine	0.023
	Lactic acid	0.001
	Succinic acid	0.010
	Sucrose	0.037
Recalcitrant organic carbon sources	Cellulose	0.079
	Humic acids	0.033
	Lignin	0.065
	Starch	0.017
Salts	$CuSO_4$ $5H_2O$	0.005
	KCl	0.499
	KH_2PO_4	0.680
	$Fe_2(SO_4)_3$	0.031
	$MgSO_4$ $7H_2O$	0.493
	$MnSO_4$	0.001
	Na_2MoO_4 $2H_2O$	0.008
	$(NH_4)_2SO_4$	0.002

[a]The pH was adjusted to 6.5 and agar was added in a concentration of 1.6 % (w/v)

[b]Fructose, glucose and sucrose were added after autoclaving

Table 2. Regions of *Lysobacter capsici* AZ78 genome potentially involved in the biosynthesis of bioactive secondary metabolites.

Region[a]	From (bp)	To (bp)	Type[b]	Potential product[c]	Similar cluster[d]	Similarity[e]	*m/z*[f]	Reference
1.1[g]	460,280	648,277	NRPS, Type I PKS	Cyclic depsipeptide	WAP-8294A2	50%	1562.83	Zhang et al. (2011)
1.2	1,093,882	1,113,823	Lanthipeptide cluster	Lanthipeptide	Le-pyrrolopyrazines	18%	193.13	Li et al. (2017)
1.3	1,347,924	1,397,412	Type I PKS, NRPS	Polycyclic tetramate lactam	Dihydromalthophilin/HSAF	100%	513.30	Yu et al. (2007)
1.4	1,468,724	1,478,439	Bacteriocin	Bacteriocin	Unknown	_	_	_
1.5	2,928,156	2,928,156	Lanthipeptide cluster	Lanthipeptide	Unknown	_	_	_
1.6	3,764,006	3,764,006	Bacteriocin	Bacteriocin	Unknown	_	_	_
1.7	4,143,953	4,185,179	Aryl polyene cluster	Arylpolyene	Xanthomonadin	57%	552.00	Goel et al. (2002)
1.8	4,245,240	4,329,436	NRPS	Cyclic depsipeptide	BE-43547 A1-C2	13%	_	Villadsen et al. (2017)
1.9	4,447,365	4,470,235	Lanthipeptide cluster	Lanthipeptide	Lysobactin	6%	1276.73	Hou et al. (2011)
2.1	182,279	223,271	PKS-like	Polyketide-like	Unknown	_	_	_
3.1	4,629	27,295	Lanthipeptide cluster	Lanthipeptide	Unknown	_	_	_

[a]Regions of *Lysobacter capsici* AZ78 genome (JAJA02000000.2) indentified through antiSMASH 5.0.0 analysis using default settings and extra features such as KnownClusterBlast, ClusterBlast, ActiveSiteFinder, Cluster Pfam analysis and Pfam-based GO term annotation.

[b]Class of genes cluster according to antiSMASH 5.0.0

[c]Family of probable syntethised bioactive metabolites based on the region of *L. capsici* AZ78 genome

[d]Most similar cluster based on antiSMASH 5.0.0 analysis

[e]Percentage of similar genes located in closest similar cluster

[f]Mass-to-charge ratios $[M+H]^+$

[g]Regions 1.1-1.9, 2.1 and 3.1 are respectively located in the contigs JAJA02000001.1, JAJA02000002.1 and JAJA02000003.1

Figure 1

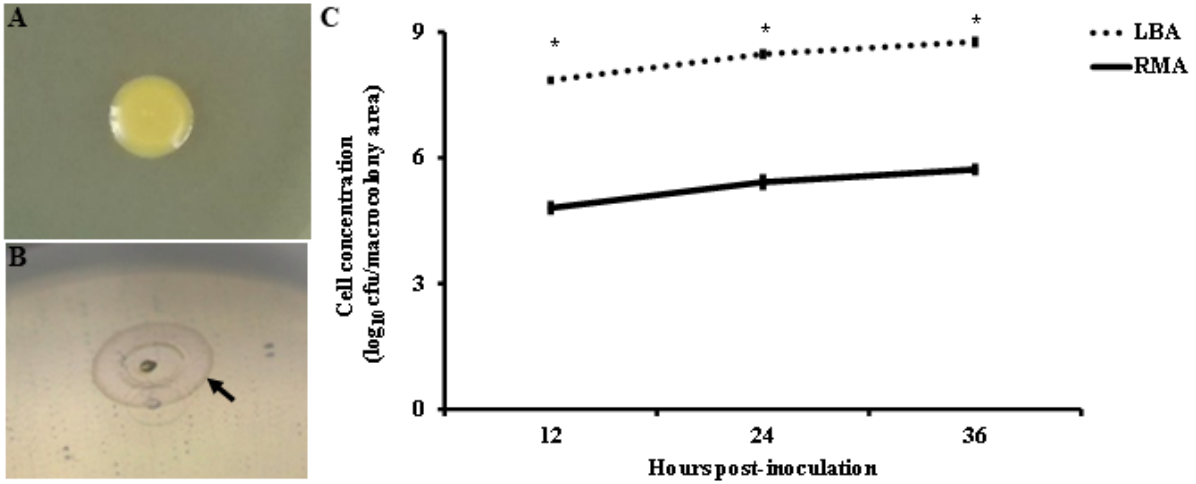
A
B
C
9
6
3
0
12
24
36
Hours post-inoculation
Cell concentration
(log10 cfu/macrocolony area)
LBA
RMA
*
*
*

Figure 2

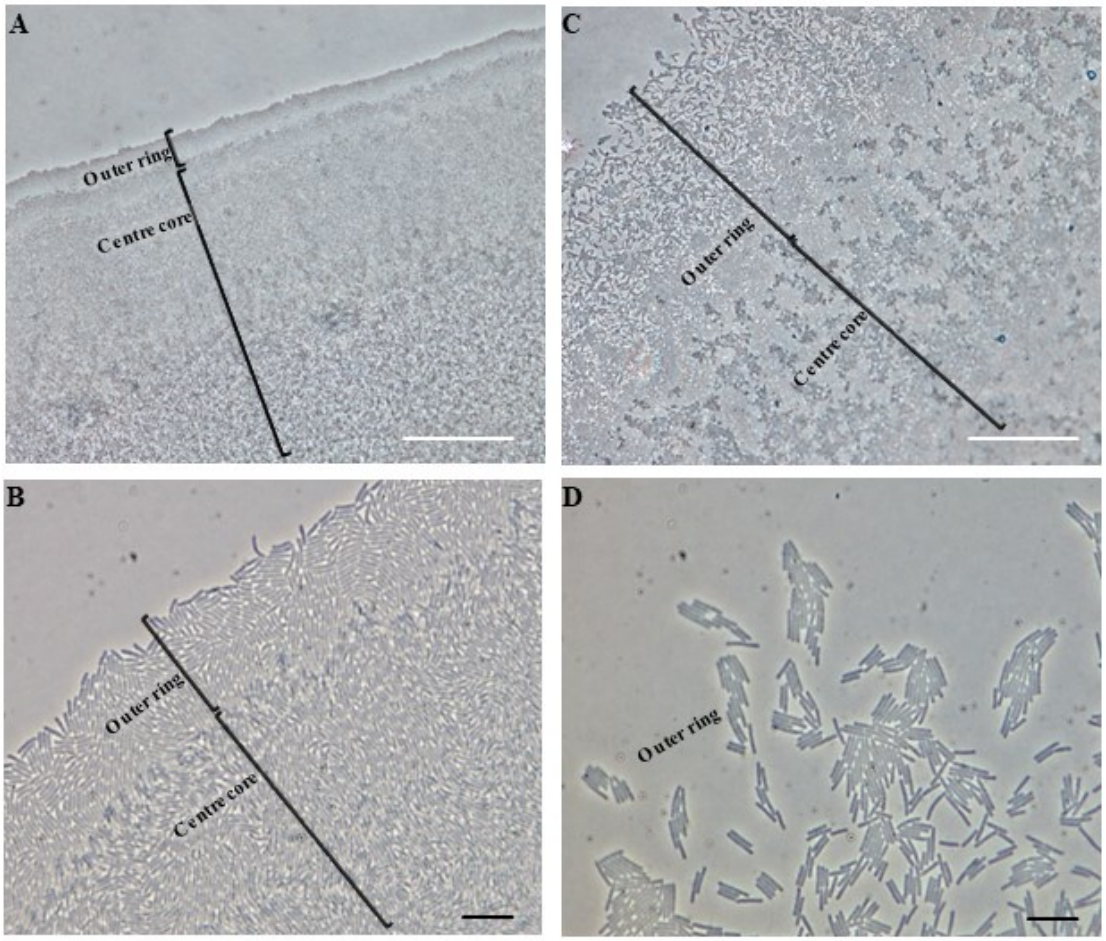
A
Outer ring
Centre core
C
Outer ring
Centre core
B
Outer ring
Centre core
D
Outer ring

Figure 3

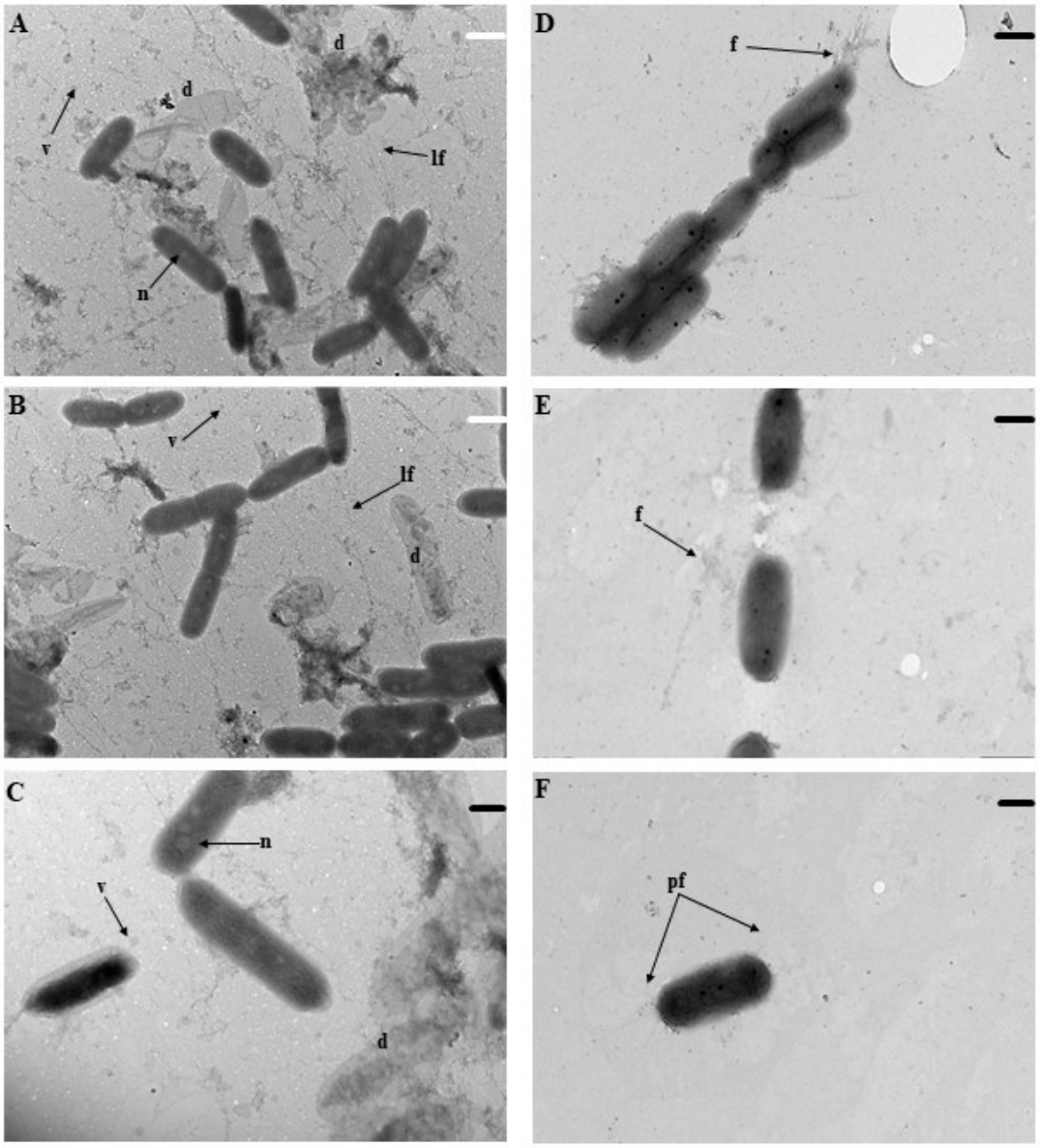

Figure 4

A

m/z	LBA			RMA		
	CC	OR	GM	CC	OR	GM
71.989				■	■	
74.097	■	■				
96.077	■	■			■	
112.051	■	■			■	
156.042	■	■	■		■	
257.149	■	■				
265.966			■			
498.973					■	
523.455				■	■	
535.495				■	■	
549.437				■	■	
602.920			■	■	■	
740.452				■	■	
742.397				■	■	
748.365				■	■	
750.467				■	■	
754.446				■	■	
762.459				■	■	
764.433				■	■	
766.433				■	■	
776.414				■	■	
778.430				■	■	
780.424				■	■	
792.431				■	■	
794.455				■	■	
806.470				■	■	
811.470				■	■	
823.413				■	■	
825.401				■	■	
1,419.956				■	■	
1,421.856				■	■	
1,423.823				■	■	
1,447.818				■	■	
1,461.859				■	■	
1,584.749	■	■	■			
1,586.877	■	■	■			
1,598.824	■	■	■			
1,606.755				■	■	
1,622.825				■	■	
1,636.829				■	■	
1,650.838				■	■	

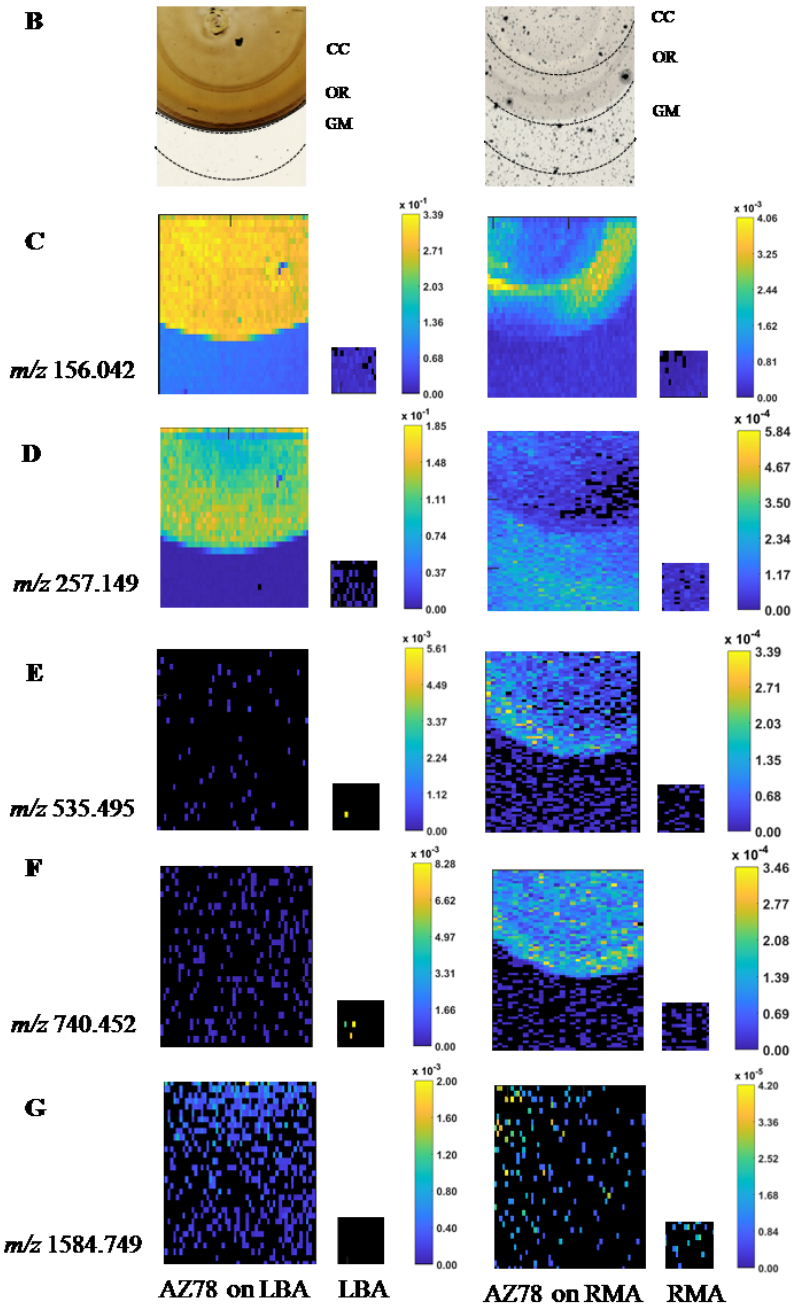

Figure S1

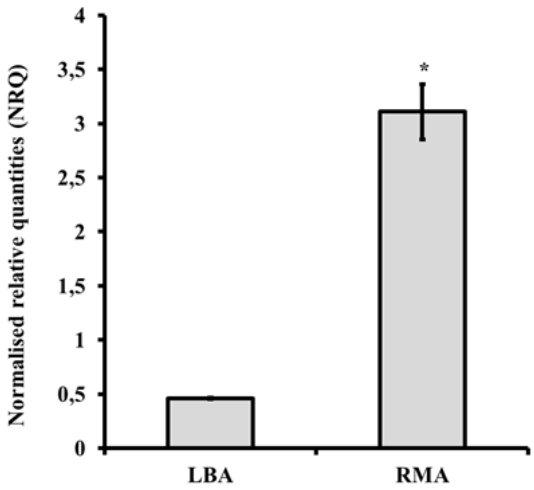
Normalised relative quantities (NRQ)
4
3,5
3
2,5
2
1,5
1
0,5
0
*
LBA
RMA

Figure S2

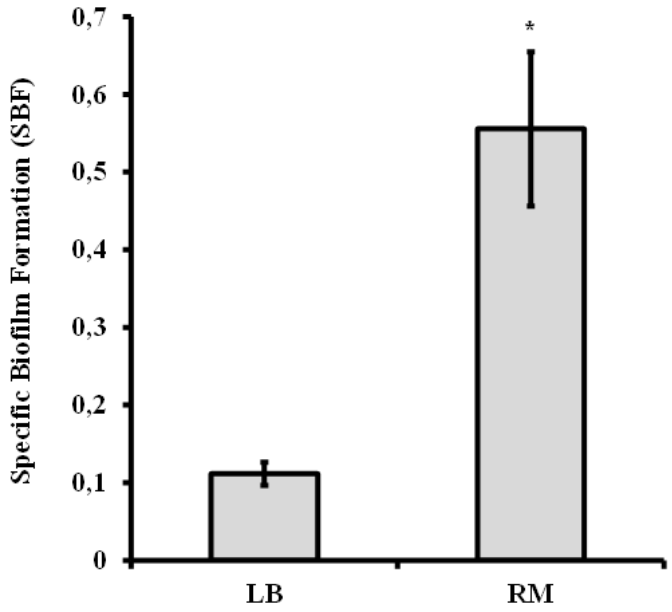

Figure S3

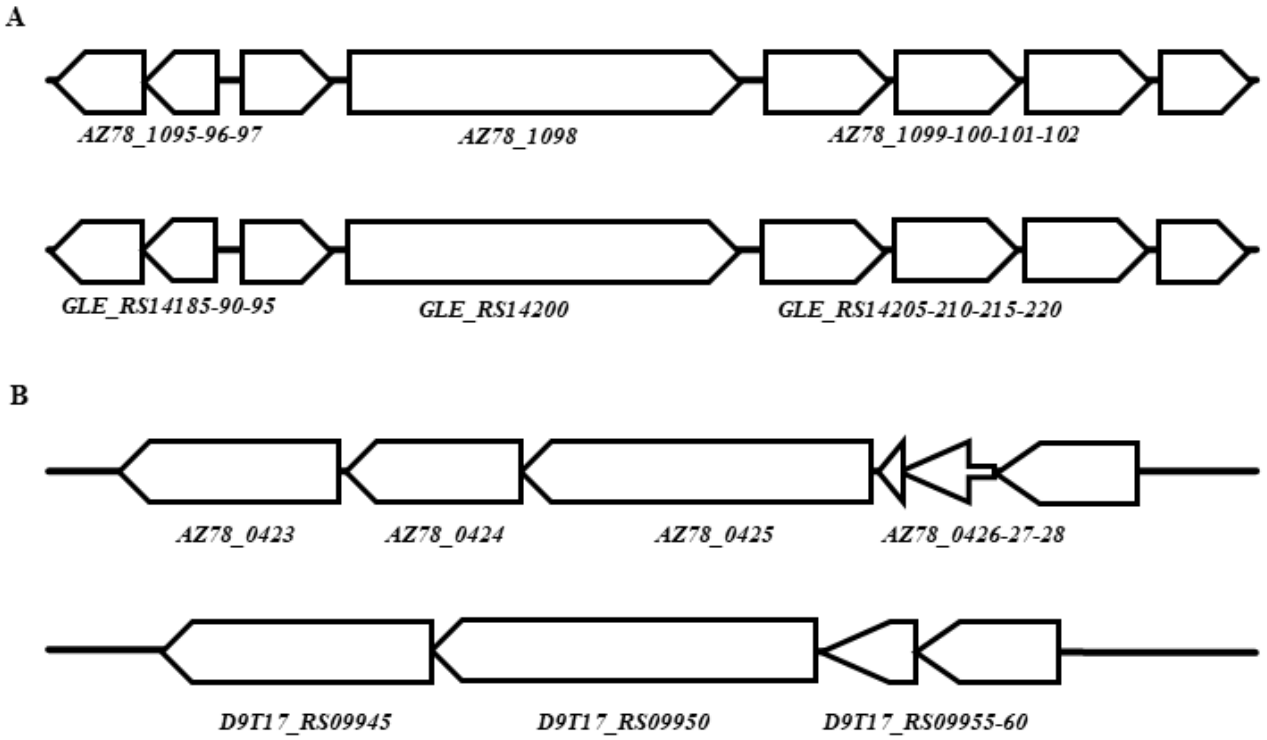
A
AZ78_1095-96-97
AZ78_1098
AZ78_1099-100-101-102
GLE_RS14185-90-95
GLE_RS14200
GLE_RS14205-210-215-220
B
AZ78_0423
AZ78_0424
AZ78_0425
AZ78_0426-27-28
D9T17_RS09945
D9T17_RS09950
D9T17_RS09955-60

Chapter 3

Underground wars: microbial interactions in the rhizosphere modulate *Lysobacter capsici* AZ78 motility and antagonism

Francesca Brescia[abd], Martina Marchetti-Deschmann[c], Marco Moretto[e], Michele Perazzolli[af], Ilaria Pertot[af], Gerardo Puopolo[af]

[a]Department of Sustainable Agro-ecosystems and Bioresources, Research and Innovation Centre, Fondazione Edmund Mach, Via E. Mach 1, 38010 San Michele all'Adige, Italy

[b]PhD school in Agricultural Science and Biotechnology, Department of Agricultural, Food, Environmental and Animal Sciences, University of Udine, Udine, Italy

[c]Institute of Chemical Technologies and Analytics, TU Wien (Vienna University of Technology), Vienna, 1060, Austria

[d]Department of Agricultural, Food, Environmental and Animal Sciences, University of Udine, Udine, 33100, Italy

[e]Department of Computational Biology, Research and Innovation Centre, Fondazione Edmund Mach (FEM), San Michele all'Adige, Italy

[f]Center Agriculture Food Environment (C3A), University of Trento, Via E. Mach 1, 38010 San Michele all'Adige, Italy

Abstract

Lysobacter spp. are common bacterial inhabitants of the rhizosphere of diverse plant species. However, the study of their ability to colonise and persist in this ecological niche is still in its infancy. To assess the impact of rhizosphere inhabitants on the establishment of *Lysobacter* spp., two and three-way interactions between *L. capsici* AZ78 (AZ78), *Bacillus amyloliquefaciens* subsp. *plantarum* S499 (S499) and *Pseudomonas protegens* Pf-5 (Pf-5) were studied on a growth medium mimicking the plant rhizosphere environment. The AZ78 cell viability was not affected by S499 and

by the three-way interaction, whereas it was negatively affected during the interaction with Pf-5. The presence of Pf-5 affected also AZ78 macrocolony morphology, impairing the motility of AZ78 cells located in the macrocolony outer ring. A drastic effect was encountered in the interaction with S499, where AZ78 macrocolony outer ring was reduced and cells were transparent. S499 negatively modulated also AZ78 inhibitory activity against the phytopathogenic oomycete *Pythium ultimum*. In contrast, Pf-5 increased AZ78 inhibitory activity and reduced the negative effect of S499 in the three-way interaction. Given the negative effect of S499, *Bacillus velezensis* FZB42 and its mutants were used to identify which S499 metabolites were responsible for the negative effects on AZ78. Difficidin and Bacilysin were the main metabolites responsible for the negative effects on AZ78 inhibitory activity and macrocolony morphology. The negative effect of S499 was associated to a decrease in the number of secondary metabolites released by AZ78 during the interactions. In contrast, the presence of Pf-5 induced the majority of the changes in AZ78 metabolic profile, such as the production of the antifungal compound pyrrole and WAP-8294A, an antibiotic against Gram-positive bacteria. On the other hand, AZ78 transcriptome was strongly modulated by the presence of S499. During the interactions AZ78 up-regulated genes involved in the response to oxydative stress and in the detoxyfication from antibiotics produced by the interacting strains. Overall, the results obtained in this study gave a first hint on the impact that competitive interactions occurring in the rhizosphere might have on the *Lysobacter* establishment.

Keywords

Lysobacter, rhizosphere, microbial interactions, cell motility, secondary metabolites, mass spectrometric imaging

1. Introduction

Rhizosphere represents a hotspot for several bacterial species due to the release of exudates from plant roots (Hartmann et al., 2009). Hence, the establishment of a bacterial strain in this ecological niche relies on its ability to build connections with other rhizosphere microbial inhabitants (Baran et al., 2015; Shi et al., 2016). It is now widely accepted that the outcome of microbe-microbe interactions represents one of the major drivers of the rhizosphere microbiota assembly and, as a consequence, the plant health (Durán et al., 2018; Mendes et al., 2011). *Proteobacteria* and *Firmicutes* are among the most represented *phyla* of the rhizosphere microbiome (Mendes et al., 2011; Roesch et al., 2007; Weinert et al., 2011). Inside these phyla, *Pseudomonas* and *Bacillus* spp. inhabiting the rhizosphere received particular attention for their capacity to promote plant growth and inhibit plant pathogenic microorganisms (Haas and Défago, 2005; Ongena and Jacques, 2008).

Lysobacter spp. are common inhabitants of the rhizosphere of different crop plants (Kim et al., 2017; Park et al., 2008; Xiao et al., 2019) and their establishment is due to specific traits as lytic activity, secondary metabolites production and predatory behaviour (Puopolo et al., 2018; Seccareccia et al., 2015; Xie et al., 2012). Similarly to *Bacillus* and *Pseudomonas* spp., the genus *Lysobacter* encompasses several biocontrol agents that can effectively control plant pathogens by diverse modes of action, as the production of bioactive secondary metabolites. Among these, the polycyclic tetramate macrolactam dihydromalthophilin, or Heat Stable Antifungal Factor (HSAF), is produced by the biocontrol strain *L. enzymogenes* C3 (Yu et al., 2007) and it is a broad-spectrum antifungal compound that impairs the sphingolipid production, the cell-wall synthesis and the tricarboxylic acid cycle and induces reactive oxygen species accumulation (Ding et al., 2016; He et al., 2018; Li et al., 2009). In addition, the

presence of the genus *Lysobacter* in agricultural soils was correlated to disease-suppressiveness against different plant pathogens, such as *Ralstonia solanacearum*, *Rhizoctonia solani* and *Streptomyces* spp. (Postma et al., 2010; Rosenzweig et al., 2012; Wang et al., 2017). In spite of this correlations, studies have recently shown that *Lysobacter* spp. isolated from disease-suppressive soils were not able to effectively colonise plant roots and, as a consequence, control *R. solani* when not sterile soils were used in the experiments (Expósito et al., 2015; Postma and Schilder, 2015). These results might be the outcome of the competitive interactions between microorganisms residing in the plant rhizosphere that can modulate the expression of genes and release of secondary metabolites (De Boer et al., 2007; Schulz-Bohm et al., 2015; Tyc et al., 2015).

Starting from these information, we aimed at understanding how the presence of other rhizosphere associated bacteria might affect *Lysobacter* spp. survival and secondary metabolite production in the rhizosphere. To do that, we investigated the two- and three-way interactions between *Lysobacter capsici* AZ78 (AZ78, Puopolo et al., 2014ab), *Bacillus amyloliquefaciens* subsp. *plantarum* S499 and *Pseudomonas protegens* Pf-5 (Pf-5), two well studied biocontrol agents of plant pathogenic microorganisms (Molinatto et al. 2016; Paulsen et al. 2016). Matrix-Assisted Laser Desorption/Ionisation Time Of Flight Mass Spectrometric Imaging (MALDI-TOF-MSI) with phase-contrast microscopy where combined to visualise the changes in the AZ78 metabolic profiles and macrocolony structure during the interactions.

2. Materials and methods

2.1 Maintainance of microorganisms and preparation of cell suspensions

The bacterial strains used in this study were stored at lenght in glycerol 40 % at −80°C and routinely grown at 27°C on Nutrient Agar (NA, Oxoid, United Kingdom) amended with antibiotics when necessary (Table 1). The plant pathogenic oomycete *Pythium ultimum* was routinely grown at 25°C on Potato Dextrose Agar (PDA, Oxoid).

To prepare cell suspensions, bacterial cells were collected from NA dishes after 48 h incubation at 27°C using sterile 10 µl loops and suspended in 1 ml sterile saline solution (0.85% NaCl w/v) contained into sterile 2 ml microcentrifuge tubes. The cell suspensions were centrifuged (13,000 rpm, 1 min), supernatants were discarded and the cells suspended in 1 ml sterile saline solution. These steps were repeated twice to remove any trace of nutrients from NA, secondary metabolites released during bacterial cell growth and antibiotics included in the growth media. Finally, pelleted cells were suspended into sterile saline solution, adjusted to a final concentration of 1×10^9 colony forming units (cfu)/ml and used in all experiments.

2.2 Experimental design to investigate two- and three-way interactions

All the possible two- and three-way interactions between *L. capsici* AZ78 (AZ78) and the bacterial strains included in this study were compared to the stand-alone treatments (Table S1). All the experiments were carried out on Rhizosphere-Mimicking Agar (RMA, Table S2) contained into sterile Petri dishes (50 mm ∅) and/or poured on sterile glass slides. The same procedure to establish the interactions between bacterial macrocolonies was followed in all the experiments. Briefly, drops (5µl) of bacterial cell suspensions were spot-inoculated on RMA at 1 cm of distance from each other according to the schemes reported in Figure S1. The impact of the interactions on the behaviour of AZ78 was evaluated after 36 h incubation at 25°C in all the experiments.

2.3 Interaction impact on Lysobacter capsici *AZ78 cell viability*

The AZ78 cell viability grown alone or in two- and three-way interactions with Pf-5 and S499 (Figure S1, Table S1) was monitored by capturing digital images of the AZ78 macrocolonies using Bio-Rad Quantity One software implemented in a Bio-Rad Geldoc system (Bio-Rad Laboratories, Inc., Hercules, California, U.S.A.). Subsequently, the macrocolony areas were measured using Fiji software (ImageJ1.50i; Schneider et al., 2012). To determine the quantity of viable cells residing in the AZ78 macrocolonies, plugs (5 mm ∅) were sampled from each macrocolony and transferred into sterile 2 ml microcentrifuge tubes containing 1 ml sterile saline solution amended with Tween 20 (0.1% v/v). A sonication step was used to dissolve cell aggregates. It consisted in three cycles of gentle sonication: 15 s at 15% of the power of the device [Branson sonifier 250-450 (Ultrasonics Corporation, Danbury, Connecticut, USA)] were alternated to 10 s of pause. The resulting solution was serially diluted and plated on NA. Colony forming units were determined after 48 h incubation at 25°C and the cell concentration was expressed as the $\log_{10}$ (cfu)/macrocolony. Subsequently, the Modulation of Cell Viability (MCV) was calculated as follows:

$$-[(A - I)/A] \times 100$$

where A is the $\log_{10}$ (cfu)/macrocolony value of AZ78 grown alone and I is the $\log_{10}$ (cfu)/macrocolony value of the AZ78 grown in two- and three-way interactions (modified from Mesanza et al., 2016). Three replicates (Petri dishes) for each treatment (interaction) were prepared and the experiment was carried out twice.

2.4 Impact of the interactions on Lysobacter capsici *AZ78 macrocolony structure and cell motility*

The experiments were carried out according to Chen et al. (2018) with a slight modification. Briefly, a sterilised glass slide was placed into a Petri dish (90 mm ∅) and 14 ml of RMA were poured on the top. Once solidified, the agar medium in excess was removed with a sterile scalpel and discarded. Drops of bacterial cell suspensions were spot-inoculated in interaction (Table S1) on the glass slides according to the scheme reported in Figure S1 A and dried under a laminar flow. Subsequently, a sterilized coverslip was gently placed on the top. After 36 h incubation at 25°C in a wet chamber, the glass slides were observed using a phase-contrast microscope (Nikon Eclipse 80i, Tokyo, Japan) under 100X magnification. Pictures were taken with a digital camera (Nikon DS-Fi1) connected to the microscope. Three replicates (glass slides) for each treatment were prepared and the experiment was carried out twice.

2.5 Influence of two- and three-way interactions on in vitro *inhibitory activity of* Lysobacter capsici *AZ78*

Drops of bacterial cell suspensions were spot-inoculated on RMA contained in Petri dishes (50 mm ∅) at 1 cm of distance from each other (Figure S1 B). After 36 h incubation at 25°C, a mycelial plug (5 mm) taken from the external margin of an actively growing *P. ultimum* colony was placed 3 cm far from AZ78 macrocolony. After 48 h incubation at 25°C, the inhibition of *P. ultimum* growth was assessed by capturing digital images as reported above and *P. ultimum* growth area was measured using Fiji software. The modulation of inhibitory activity was calculated as follows:

$[(A_c - A_i)/A_c] \times 100$

where A_c is *P. ultimum* growth area in presence of AZ78 grown alone and A_i is *P. ultimum* growth area in presence of AZ78 grown in two- and three-way interactions (modified from Mesanza et al., 2016). Five replicates (Petri dishes) for each treatment were used and the experiment was carried out twice.

2.6 Matrix-Assisted Laser Desorption/Ionisation Time of Flight Mass Spectrometric Imaging (MALDI-TOF-MSI)

Drops of AZ78, Pf-5 and S499 cells suspensions were spot-inoculated in two- and three-way interaction on 1 mm thick growth medium layer poured onto sterile glass slides (Figure S1). An even and smooth surface is of importance for MALDI-TOF-MSI. For this we further developed our recently published microassay (Holzlechner et al., 2016) and used two sterile glass slides which were hold in place in a distance of exactly 1 mm by sterile spacers. This construct was placed in a sterile Petri dish (90 mm diameter) and 13 ml of growth medium were poured in the Petri dish filling also the gap between the slides giving an area of 5.5 × 2.5 cm. Once solidified, the medium in excess was cut and discarded and the glass slide on the top and the spacers were gently removed. An area of 25 mm^2 of growth medium was kept apart from the inoculated medium in order to identify the mass spectrometric signals (*m/z* values) belonging to the growth medium (blank).

Once inoculated, the glass slides were incubated at 25°C for 36 h and, subsequently, samples were dried in a desiccator under vacuum overnight at room temperature. Afterwards, a photograph was taken using a glass slides scanner and 0.15-0.20 mg of a

1:1 mixture of 2,5-dihydroxybenzoic acid (2,5-DHB) and α-cyano-4-hydroxy-cinnamic acid (α-CHCA) were sublimed per cm^2 onto the sample using a home-built instrumentation. A subsequent recrystallisation step at 86°C for 1 min using 1% acetic acid in water ensured analyte incorporation (Yang and Caprioli, 2011). MALDI-TOF-MSI experiments were then immediately performed on a Synapt G2 HDMS (Waters, Milford, Massachusetts, United States) in positive linear mode, with 150 × 75 µm laser step intervals, the laser energy was set to 250 a.u., 1000 Hz of firing rate, 1 scan per pixel and a mass range of 20–4000 Da. For accurate mass measurements the instrument was calibrated before each run using red phosphorous. Data of three biological replicates of the microassay per treatment (bacterial interaction) were analysed using Datacube Explorer (Klinkert et al., 2014), MSiReader (Robichaud et al., 2013), and MassLynx (Waters). For tentative assignment of analytes to measure signals, accurate *m/z* values (± 0.002 Da) extracted from the profile mass spectra present at least in two biological replicates were submitted to "The Metabolomics Workbench" (http://www.metabolomicsworkbench.org/, 2019) and searched in literature.

To carry out a presence/absence analysis, *m/z* values that were not present in the blank (RMA without any bacterial strain) were manually-selected in the MALDI-TOF-MSI profiles and distributed in five functional classes (Table S3). Moreover, the distribution of ions in AZ78 macrocolony center core, outer ring and a sector of growth medium adjacent to the outer ring of the macrocolony was also taken into consideration for the analysis.

2.7 Total RNA extraction

Five µl of bacterial cell suspensions were spot-inoculated on RMA (3 ml) contained in Petri dishes (50 mm ∅) (Figure S1). RNA was extracted after 36 h incubation at 25°C

from the developed macrocolonies according to the following procedure. Agar plugs (5 mm ∅) were collected in aluminum paper and instantly frozen in liquid nitrogen. To process similar quantities of bacterial cells, three replicates respectively made by 40 RMA Petri dishes for each treatment were made.

The frozen plugs were placed in pre-frozen steel jars containing sterile beads and processed at 25 Hz for 1 min using a mixer mill disruptor (MM200, Retsch, Haan, Germany). The resulting powder was transferred into sterile 2 ml RNAse-free microcentrifuge tubes placing up to 100 mg of powder each. To lyse the cell wall, 0.3 ml of lysis buffer (30 mM Tris, 30 mM EDTA, 10 mg/ml lysozyme, pH 6.2) were added to each microcentrifuge tube, vortexed vigorously and incubated at 37°C with constant shaking (1,000 rpm) for 30 min (Villa-Rodríguez et al., 2018). RNA was extracted using Spectrum™ Plant Total RNA Kit (Sigma-Aldrich, St. Louis, MO, USA) according to manufacturer's instructions. The integrity and concentration of extracted RNA were assessed using TapeStation System 4200 (Agilent Technologies®) and Qubit® Fluorimetric Quantitation (Invitrogen, Life Technologies, Waltham, MA) with Qubit RNA BR assay (Invitrogen, Life Technologies). RNA was long term stored at -80°C.

2.8 Illumina sequencing and mapping to reference genome

Library construction and Illumina Sequencing were carried out at IGA Technology Services (Udine, Italy). Each sample of total purified RNA was diluted with RNase-free water to a final concentration of 50 ng/µl. rRNA depletion was performed using the Universal Prokaryotic RNA-Seq (NuGEN Technologies, Redwood City, CA ,

U.S.A.). mRNA-Seq libraries were multiplexed (two libraries per lane) and sequenced with Illumina HiSeq High Output (HO) Version 4 – paired reads (Illumina, San- Diego,

CA), according to the manufacturer's instructions. Complementary DNA (cDNA) libraries were synthesized using TruSeq RNA Sample Preparation Kit v2 (Illumina) and the process was carried out according to standard protocol mRNA stranded sample preparation (Illumina). Paired-end reads of 125 nucleotides were obtained using an Illumina HiSeq 2500.

Illumina HiSeq data were assessed for quality using FastQC (http://www.bioinformatics.babraham.ac.uk/projects/fastqc/). Illumina paired-end (2 × 125 bp) reads for each sample were merged to increase overall read length using Illumina PEAR (Paired-End reAd mergeR version 0.9.8) software (Zhang et al., 2014). The resulting merged reads were aligned separately to the AZ78 genome (version JAJA00000000.2 deposited at DDBJ/EMBL/GenBank) (Puopolo et al., 2016) using the Subread aligner with default parameters (Liao et al., 2013). Read counts were extracted from Subread alignments using the featureCounts read summarization program (Liao et al., 2014).

2.9 Identification of differentially expressed genes and functional annotation

The raw data were pre-processed by removing genes with zero counts in all samples (unexpressed genes) and normalizing across samples using the trimmed mean of M-values method. Differentaially expressed gens (DEGs) were selected using the voom method (Law et al., 2014), which estimates the mean–variance relationship of log counts, generating a precision weight for each observation that is fed into the limma empirical Bayes analysis pipeline (Smyth, 2004).

A Volcano Plot generated using the ShinyVolcanoPlot Web App (https://github.com/onertipaday/ShinyVolcanoPlot) was used to select sets of DEGs for

each comparison, based on both P-value and expression fold change. A $\log_2FC \geq 1$ and a P-value ≤ 0.05 were imposed to identify DEGs through pairwise comparison.

The protein sequences of all predicted genes (Puopolo et al., 2016) were functionally annotated using the Blast2GO program (Conesa et al., 2005; http://www.blast2go.org). Default settings were applied and a minimum E-value of 1×10^{-5} was imposed as cut-off. The DEGs were further annotated on the basis of the NCBI gene description and Blast2GO description, imposing a minimum E-value of 1×10^{-5}.

2.9 Statistical analysis

The statistical analysis was performed using R package version 3.5.3 (https://www.r-project.org/). The Venn diagrams were generated within the Bioconductor Project with the R package "limma". The repetitions of the experiments were tested for significant differences with a two-way ANOVA. In absence of significant differences, the experiments were pooled and data were analysed using one-way ANOVA and mean comparisons were performed using Tukey's test ($\alpha = 0.05$) as post-hoc test.

3. Results

3.1 Lysobacter capsici AZ78 *cell viability changed depending on the interaction*

Differences in the quantity of viable cells residing in AZ78 macrocolonies developed during the interactions compared to the stand-alone treatments were observed.

The viability of AZ78 cells was negatively affected during the interaction with Pf-5 (mean MCV ± standard error, − 10.31 ± 3.71 %) whereas a slight increase of viable

cells (+ 1.97 ± 1.05 %) residing in AZ78 macrocolony was registered in the two-way interaction with S499. The negative effect of Pf-5 registered in the two-way interaction was reduced in the three-way interaction (− 4.38 ± 2.16 %).

3.2 Morphology of Lysobacter capsici AZ78 *bacterial macrocolonies and cell motility were affected by the presence of interacting strains*

AZ78 macrocolony grown alone was characterised by the presence of groups of motile cells in the outer ring (Figure 1 A). Although groups of AZ78 cells were still visible in the outer ring, a loss in their motility in the two- and three-way interactions was observed. No differences in the AZ78 outer ring were observed in the two-way interaction with Pf-5 and it was extended with well visible groups of cells when facing Pf-5 in the three-way interaction (Figure 1 B, C). In contrast, AZ78 outer ring was strongly reduced and cells were transparent during the two-way interaction with S499 and in the region facing S499 in the three-way interaction (Figure 1 D, E).

3.3 Bacillus amyloliquefaciens *subsp.* plantarum *S499 negatively influenced the inhibitory activity of* Lysobacter capsici *AZ78 against* Pythium ultimum

When grown alone on RMA, *P. ultimum* covered the entire surface area of Petri dishes. AZ78 grown alone was able to reduce consistently the *P. ultimum* mycelium growth. Interestingly, the presence of S499 significantly impaired AZ78 inhibitory activity (average MI ± standard error, − 7.61% ± 0.99) in the two-way interaction.

In contrast, the interaction with Pf-5 significantly contributed to an increase of AZ78 inhibitory activity (+ 8.49% ± 0.68). The positive effect of Pf-5 on AZ78 inhibitory

activity allowed to counteract the negative effect of S499 in the three-way interaction (+ 13.44% ± 2.01; Figure 2).

3.4 Difficidin and Bacilysin are the main secondary metabolites produced by Bacillus amyloliquefaciens *subsp.* plantarum *S499 modulating the behaviour of* Lysobacter capsici *AZ78*

Bacillus velezensis FZB42 and its mutants AK1, AK2, CH01, CH06, CH07 and CH39 showed a negative impact on AZ78 inhibitory activity (Figure 3). In contrast, the mutant CH08, unable to produce difficidin, had a lower negative impact on AZ78 inhibitory activity (− 5.66% ± 0.71, average MI ± standard error), as well as RS06 (− 3.76% ± 2.01), unable to produce lipopeptides, polyketides and bacilysin (Figure 3).

Similarly, both CH08 and RS06 did not show the negative impact of FZB42 and S499 on AZ78 macrocolony structure and motility. Indeed, both mutants did not affect the outer ring of AZ78 macrocolony. Moreover, AZ78 cells interacting with CH08 were not transparent and were longer compared to AZ78 grown alone and in the two-way interaction with FZB42 and S499 (Figure 4 D, E).

3.5 Interactions modulated the metabolic profile of Lysobacter capsici *AZ78*

AZ78 metabolic profile was characterised by 141 biologically relevant signals found in AZ78 macrocolony regions taken into consideration (Figure 5; Supplementary Tables S1, S2). The signals for which a possible match was found were mainly assigned to cell structure-related metabolites (29.08 %) and antagonism metabolites (24.82 %).

The production of 44 analytes was not influenced by the presence of an interacting strain and they were found in the AZ78 macrocolony regions taken into considerations.

Most of the signals (47.73 %) were tentatively assigned to be metabolites related to cell structure while the minority (2.27 %) were tentatively assigned to be cell signals, such as a putative indole (*m/z* 156.043 $[M+K]^+$; Figure 6 A). The 27.27 % of these 44 analytes were putatively matching with antagonism analytes produced by AZ78, such as the macrocyclic lactam HSAF, *m/z* 535.490 $[M+Na]^+$ (Figure 6 B), that was found in the whole macrocolony in all the treatments, as well as the cephem antibiotics Cephabacin H2 (*m/z* 716.482 $[M+H]^+$, 738.486 $[M+Na]^+$, 754.464 $[M+K]^+$) and Cephabacin H3 (*m/z* 825.427 $[M+K]^+$). A 6.82 % of the analytes was possibly matching with primary metabolites and the 4.54 % of the analytes was possibly matching with lipids. For the 11.36 % of the analytes, a possible match was not found.

Nine analytes were found in the region of AZ78 macrocolony in all the two- and three-way interactions. These analytes were specifically produced when AZ78 was grown in the presence of at least one interacting strain. The 44.44 % of these analytes were tentatively assigned to be cell structure-related metabolites, while the 22.22 % of the analytes were putatively matching with cell signals, such as N-hydroxybenzoic acid, *m/z* 197.075 $[M+K]^+$, or 2,3-butanediol, *m/z* 129.043 $[M+K]^+$. The latter was found only in the outer ring region of AZ78 macrocolony in the three-way interaction, while it was present in the whole macrocolony when AZ78 was grown in the two-way interactions. The 11.11 % of the analytes were matching possibly with primary metabolites. For the other 22.22 %, a possible match was not found.

Nineteen signals were found in AZ78 macrocolony when Pf-5 was present in two- and three-way interactions. A possible match was not found for the 57.89 % of these. The 21.05% was tentatively assigned to be antagonism metabolites such as a pyrrole derivative, *m/z* 130.050 $[M+H]^+$. The 15.79 % of these analytes was possibly matching

with cell structure-related metabolites and the 5.26% was possibly matching with primary metabolites.

Four analytes were found only when AZ78 was grown in a two-way interaction with Pf-5. The 50.00% of them was tentatively assigned to be antagonism metabolites, such as Tripropeptin Z, *m/z* 1134.525 $[M+Na]^+$ that was found only the centre core of AZ78 macrocolony. For the remaining 50% of the analytes, a possible match was not found.

Twenty-nine signals were specifically found in AZ78 macrocolony when it was grown in a three-way interaction. The 37.93 % of these might match with antagonism metabolites produced by AZ78, such as WAP-8294A2 (*m/z* 1584.852 $[M+Na]^+$, Figure 6 C), WAP-8294A1 (*m/z* 1586.877 $[M+K]^+$), WAP-8294A4 (*m/z* 1615.021 $[M+Na]^+$). The 20.69 % of the analytes might match with metabolites related to cell-structure, such as *m/z* 1216.392 $[M+Na]^+$ that was found only in the EXT region of AZ78 macrocolony and was tentatively assigned to be a peptidoglycan-related metabolite. The 10.34 % of the analytes might be related to AZ78 primary metabolism. For the 31.03 % of the analytes a possible match was not found.

Fifteen signals were found in all the treatments except when AZ78 was grown with S499 in a two-way interaction. Of these, the 26.67% was matching possibly with antagonism metabolites, as well as 26.67% of analytes matching with metabolites related to cell-structure. The 13.33% of the analytes was possibly matching with primary metabolites. For the 33.33% of the analytes, a possible match was not found.

Five signals were found in all the treatments except when AZ78 was grown with Pf-5 in a two-way interaction. Of these, the 40% was possibly matching with metabolites related to cell structure and the 20% was matching with primary metabolites. For the 40% of the analytes, a possible match was not found.

Sixteen signals were found in AZ78 macrocolony when it was grown alone and in a three-way interaction. The 6.25 % of these analytes was possibly matching with metabolites related to cell structure, such as the *m/z* 1172.408 $[M+Na]^+$ that was tentatively assigned to be a peptidoglycan component. For the other 93.75 % of the analytes, a possible match was not found.

3.6 Interactions modulated Lysobacter capsici *AZ78 transcriptome*

AZ78 transcriptome was analysed after 36 h growth in the presence of the interacting strains S499 and Pf-5 (Table S1). To assess the changes in the total transcriptome of AZ78, the data for the interactions were compared to the AZ78 stand-alone treatment.

The total number of raw read pairs (sum of reads for two sequencing technical replicates), ranged between approximately 910,725 and 3,580,721.

The AZ78 two-way interaction with S499 resulted in 1,473 DEGs (27.60 % of AZ78 total genes) as compared with AZ78 grown alone. Of these DEGs, 787 were down-regulated and 686 were up-regulated (Table 2, Figure 7 A).

The AZ78 two-way interaction with Pf-5 resulted in 298 (5.58% of total genes) DEGs as compared with AZ78 grown alone. Of the DEGs, 46 were down-regulated and 252 were up-regulated (Table 2, Figure 7 A).

The AZ78 three-way interaction with S499 and Pf-5 resulted in 1,408 (26.39% of total genes) DEGs as compared with AZ78 grown alone. Of the DEGs, 625 were down-regulated and 783 were up-regulated (Table 2, Figure 7 A).

The DEGs were divided into two clusters (up and down-regulated genes) and these were compared according to each treatment in order to identify the differences (Figure 7 B).

Among the down-regulated genes, only 20 DEGs were shared by all the treatments.

These genes were mainly associated with functional categories of antagonism activity, defense, metabolism (aminoacid and lipid), signal transduction (Figure 8).

Among the up-regulated genes, 126 DEGs were shared by all the treatments.

These genes were mainly associated with functional categories of antagonism activity, defense, metabolism (aminoacid, carbohydrate, DNA, energy, lipid), signal transduction, cell structure and transport (Figure 8). In particular, among AZ78 DEGs related to cell structures biosynthetic processes there was AZ78_1246 encoding a transglycosylase family protein involved in the peptidoglycan biosynthesis and AZ78_2165 encoding a 3-deoxy-D-manno-octulosonic acid transferase, involved in the lipopolysaccharide core region biosynthetic process. Moreover, among AZ78 genes involved in the defense form oxidative stress and from antibiotics, there were genes encoding transcriptional regulators of the ArsR family (AZ78_4719), MarR family (AZ78_4679) and TetR/AcrR family (AZ78_0327 and AZ78_4696), a serine hydrolase with β-lactamase activity (AZ78_3781) and a metallo-β-lactamase (AZ78_3218). Among AZ78 genes related to transport there was AZ78_0033 encoding a transcriptional regulator belonging to the family of transcriptional regulator Rrf2 and AZ78_3117 encoding a TonB-dependent receptor. Some of AZ78 DEGs related to antagonism were encoding transcriptional regulators of the LysR family (AZ78_0624, AZ78_3531, AZ78_3805).

4. Discussion

Recently, we showed that AZ78 has the physiological traits useful to establish itself on plant rhizosphere and its transcriptome is modulated during an intimate interaction with *Phytophthora infestans* (Brescia et al., 2019, submitted; Tomada et al., 2017). In this study, we questioned ourselves on how the interaction with bacterial strains belonging

to *Pseudomonas* and *Bacillus*, two of the most represented bacterial genera in plant rhizosphere, (Duineveld et al., 2001; Felske et al., 1998; Garbeva et al., 2003), might impact its behaviour and, as a consequence, its establishment in the rhizosphere.

Differently from the interaction between the Gram-negative bacterial strain *Burkholderia* sp. AD24 and the Gram-positive bacterial strain *Paenibacillus* sp. AD87 (Tyc et al., 2017), no negative impact on AZ78 cell viability was registered when grown with S499. A slight decrease of AZ78 cell viability was registered, contrarily, when interacting with the Gram-negative bacterial strain Pf-5. Interestingly, in the three-way interaction both Pf-5 and S499 nullified this negative effect, giving a first hint on how the outcome of the interactions may change depending on the number of the players involved.

Changes occurred in the phenotype of AZ78 macrocolonies gave more clues on the impact of Pf-5 and S499 on AZ78 cell behaviour. As recently reported, AZ78 macrocolony originated on RMA was characterised by a cell multilayer centre core and an extended cell monolayer outer ring encompassing motile cells heterogeneously distributed in small groups (Brescia et al., 2019, submitted). When grown in a two-way interaction with Pf-5, AZ78 outer ring appearance remained the same whereas an impairment of AZ78 cell motility was observed. A more drastic change in AZ78 macrocolony structure occurred during the interaction with S499. In this case, AZ78 cells residing in the outer ring were transparent and not motile and the dimension of the outer ring was strongly reduced. Noteworthy, AZ78 macrocolonies originated during the three-way interactions conserved the characteristics observed in the two-way interactions. In more details, the AZ78 macrocolony regions facing Pf-5 were characterised by an extended outer ring whereas this feature was missing in the regions facing S499.

Changes occurring in the morphology of bacterial macrocolonies and cell motility are the outcome of the growth strategies adopted by bacterial strains to face abiotic and biotic factors (Hall-Stoodley et al., 2004; Hibbing et al., 2010). For instance, the shape of the macrocolony of *B. subtilis* OG-01, as well as its motility, depended on the environmental pH (Tasaki et al., 2017) while cell motility played a key role in the two-way interaction between *Agrobacterium tumefaciens* C58 and *P. aeruginosa* PAO1 (An et al., 2006).

It is reasonable that the drastic changes observed in AZ78 behaviour when facing S499 might be linked to its ability to release a vast array of secondary metabolites (Cawoy et al., 2015; Ongena et al., 2005). Recently, the sequencing and mining of S499 genome allowed determining the arsenal that this bacterial strain might use in its warfare against other microbes (Molinatto et al., 2016). However, S499 is not genetically tractable making difficult to determine which secondary metabolite might be involved in the modulation of AZ78 behaviour. Given the close similarity at genomic level between S499 and *B. velezensis* (ex. *amyloliquefaciens* subsp. *plantarum)* FZB42 (Molinatto et al., 2017), we evaluated this strain and its mutants unable to produce several secondary metabolites (Fan et al., 2018) in two-way interactions with AZ78. In these two-way interactions, the AZ78 outer ring remained similar to the stand-alone treatment when AZ78 was interacting with the *B. velezensis* FZB42 (FZB42) mutants CH08 and RS06 respectively unable to produce difficidin and all the lipopeptides, polyketides and bacilysin (Chen et al., 2006). This outcome was in agreement with the reported toxic activity of bacilysin and difficidin against *Xanthomonas oryzae* pv. *oryzae* PXO99 and *Xanthomonas oryzae* pv. *oryzicola* RS105 (Wu et al., 2015). Bacilysin and difficidin respectively impair bacterial peptidoglycan and cell wall synthesis (Kenig and Abraham, 1976; Zweerink and Edison, 1987), thus the transparent AZ78 cells observed

in the outer-ring of macrocolonies grown with S499 and FZB42 may be a sign of the effect of these metabolites on their cell structures. These secondary metabolites explained also the negative impact of FZB42 and S499 on the inhibitory activity of AZ78 against *P. ultimum* that was restored during the interactions with CH08 and RS06.

In contrast to FZB42 and S499, AZ78 inhibitory activity was increased during the two- and three-way interactions including Pf-5, thus we hypothesised that the presence of the interacting strains might have induced in AZ78 a change in the secondary metabolites released by AZ78. MALDI-TOF-MSI allowed identifying the AZ78 analytes and their spatial location in the macrocolony centre core and outer ring in the mm range. This technique has been used to study microbial interactions often between two species (Boya et al., 2017; Michelsen et al., 2015; Traxler et al., 2013) and, at the best of our knowledge, this is the first time that MALDI-TOF-MSI was used to dissect the the metabolic profiles of a bacterial three-way interaction.

The majority of the signals found in the AZ78 metabolic profile were present in both the stand-alone treatment and in the interactions. For instance, the presence of putative cephem antibiotics Cephabacin H2 and Cephabacin H3, active against the peptidoglycan synthesis (Nozaki et al., 1984) was not affected by the presence of the interacting strain. Similarly, the signal tentatively assigned to be dihydromalthophilin/HSAF, usually produced in nutrient-limited conditions (Yu et al., 2007), was constantly present in the centre core of AZ78 macrocolony in all the treatments. However higher intensity values in the AZ78 macrocolony outer ring in the stand-alone treatment and in the three-way interaction, suggested a difference in AZ78 cell metabolism during the two- and three-way interactions.

The presence of Pf-5 had a strong influence on the metabolic profile of AZ78; indeed many analytes were found when AZ78 was grown in two- and three-way interactions with this strain. Among the secondary metabolites related to the presence of Pf-5, there was a putative pyrrole derivative. Pyrrole, a broad spectrum antifungal compound, was recently found to be emitted by *L. capsici* DSM 19286^{T} and was toxic against the plant pathogenic oomycete *Phytophthora infestans* (Lazazzara et al., 2017). Thus, the production of pyrrole derivatives might partly explain the increase in AZ78 inhibitory activity during the interaction with Pf-5.

Interestingly, a putative tripropeptin Z, an antibiotic active against Gram-positive bacteria (Hashizume et al., 2001), was produced by AZ78 in the two-way interaction with Pf-5, whereas it was not produced when S499 was present in the three-way interaction. However, this interaction was characterised by the presence of putative WAP-8294A1/A2/A4, cyclic lipodepsipeptides toxic against Gram-positive bacteria, disrupting their cell membrane (Itoh et al., 2018; Zhang et al., 2011). It is probable that the presence of Pf-5 might trigger in AZ78 a self-defence response against S499 and/or Pf-5 might induce a change in the metabolome of S499 relieving the negative impact on AZ78, giving it the chance to trigger a defence-response against S499.

The treatments analysed were also characterised by the presence of analytes involved in the bacterial cell-cell communication as putative 2,3-butanediol, indole and N-hydroxybenzoic acid (Venturi and Keel, 2016). In *L. enzymogenes* OH11, 3-hydroxybenzoic acid and 4-hydroxybenzoic acid are involved in the regulation of dihydromalthophilin/HSAF production (Qian et al., 2014). However, signals tentatively assigned to be dihydromalthophilin/HSAF were found in all the treatments while N-hydroxybenzoic acid was found only in the presence of two- and three-way interactions. Given the involvement of 3-hydroxybenzoic acid also in cell viability and antioxidant

activity in *Xanthomonas campestris* pv. *campestris* (He et al., 2011), it is possible that this compound may have a similar role, regulating the stress response also in AZ78.

The involvement of N-hydroxybenzoic acid in the cell protection is enforced also by the presence of 2,3-butanediol in AZ78 macrocolony region in all the interactions. Indeed, this bacterial cell signal is involved in the bacterial self-defence response triggered by the acidification of the environment (Ryu et al., 2003; Van Houdt et al., 2007).

Interestingly, putative indole was found only in the macrocolony outer ring of the stand-alone treatment in agreement with its involvement in the twitching motility of *L. enzymogenes* OH11 cells (Feng et al., 2019) and with the motility observed in AZ78 outer-ring cells. In contrast, indole was present in the macrocolony centre core when AZ78 was interacting with S499, when an impairment with AZ78 motility was observed.

We thus hypothesised that indole may play a role in the response of AZ78 to the presence of S499. One possibility might be the involvement of indole in the phenomenon of persistence in bacteria, during which a subpopulation of the bacterial strain resist to environmental stresses, such as the exposure to antibiotics (Vega et al., 2012). However, it is worth noting that the involvement of indole in the formation of "persister cells" is still debated (Kim and Wood, 2016), thus it is difficult to have a clear picture of the function played by indole in the interaction between AZ78 and S499.

In order to have a more complete understanding of the mechanisms underlying the interactions, AZ78 transcriptome was analysed, revealing a strong influence given by the presence of S499 both in the two- and in three-way interactions. We concentrated our attention on AZ78 DEGs shared by all the two- and three-way interactions that were mainly up-regulated. Among these, there were genes related to cell structures

biosynthetic processes, such as peptidoglycan and lipopolysaccharide (respectively AZ78_1246 and AZ78_2165). Lipopolysaccharides are constituents of the outer membrane of Gram-negative bacteria and protect the bacterial peptidoglycan cell wall from lysis (Begunova et al., 2004). The up-regulation of genes related to cell structure biosynthetic process may be a response after the exposure to Difficidin and Bacilysin, produced by S499, degrading AZ78 cell wall. In addition, during the interactions AZ78 was facing multiple stresses, for instance oxydative stress, since genes involved in cell detoxyfication were up-regulated. Indeed, AZ78 up-regulated ArsR (AZ78_4719), a transcriptional regulator of the family MarR that is involved in sensing and in regulating the response of oxidative stress (Lebreton et al., 2012). Also the family of transcriptional regulators Rrf2 (AZ78_0033) involved in stress response was upregulated. It includes iron/sulfur (FeS)-cluster redox sensors in response to nitric oxide (NsrR) (Crack et al., 2015; Yukl et al., 2008), IscR which senses the iron/sulfur status of the cell (Santos et al., 2015) and RirA that is involved in iron metabolism sensing iron limitation (Hibbing et al., 2011).

A transcriptional regulator of the MarR family (AZ78_4679) was also up-regulated during all the interactions. This family of transcriptional regulators is involved in the detoxification response to multiple antibiotics and toxic compounds (Alekshun and Levy, 1999; Cohen et al., 1993). This may indicate that AZ78 cells during the interactions were in presence of antibiotic compounds produced by competitors. Consistently, also two transcriptional regulators of the TetR/AcrR family (AZ78_0327 and AZ78_4696) were up-regulated during the interactions, regulating genes that encode transmembrane tetracycline efflux pumps (Ma et al., 1996; Su et al., 2007). A serine hydrolase with β-lactamase activity (AZ78_3781) and a metallo-β-lactamase (AZ78_3218) were up-regulated during the interactions, confirming the defense strategy

of AZ78 against antibiotic compounds produced by competitors. Indeed, β-lactamases provide resistance through inactivation by hydrolysis of β-lactam antibiotics, such as penicillin and cephalosporin (Bonnet, 2004).

An increased competition for nutrients and public goods may have played an important role in the interactions, since a TonB-dependent receptor was up-regulated (AZ78_3117). In fact, TonB is involved in large substrate uptake, such as siderophores, namely iron-chelating molecules, vitamin B12 and even large aromatic compound uptake in Gram-negative bacteria (Fujita et al., 2019). Therefore, AZ78 cells might have increased their ability to exploit public goods, also produced by competitors, during the interactions with S499 and Pf-5.

In addition, AZ78 cells were up-regulating three transcriptional regulators of the LysR family (AZ78_0624, AZ78_3531, AZ78_3805) in the presence of the interacting strains. In *Lysobacter enzymogenes,* LysR, together with the global regulator Clp, has been linked to the regulation of HSAF biosynthesis (Han et al., 2020; Su et al., 2017, Su et al., 2018). Thus, the presence of interacting strains was not negatively affecting in AZ78 the production of this secondary metabolite, very useful for the biocontrol of fungal pathogens (He et al., 2018).

Taken together, our results may indicate that both Pf-5 and S499 had a negative impact on AZ78 rhizosphere colonisation ability, impairing its motility, fundamental to colonize new ecological niches, and modifying its metabolic profile and inhibitory activity even if with different outcomes. The presence of S499 and Pf-5 triggered in AZ78 the overexpression of genes related to defense from oxydative stress and antibiotic detoxyfication, and at the same time, the overexpression of genes involved in the uptake of public goods, suggesting that an intense competition was occurring in this

simplified model system. These data and are in agreement with the well accepted hypothesis that the majority of microbial interactions in nature are competitive (Foster and Bell, 2012).

It is undeniable that microbial interactions in nature are far more complex than the one analysed, but we are convinced that our results put the basis to better understand the ecological role of *L. capsici* members within the competitive interactions occurring among rhizosphere microorganisms.

5. References

Alekshun, M.N., Levy, S.B. 1999. The mar regulon: multiple resistance to antibiotics and other toxic chemicals. Trends in Microbiology 7,410–413. doi:10.1016/S0966-842X(99)01589-9.

An, D., Danhorn, T., Fuqua, C., Parsek, M.R., 2006. Quorum sensing and motility mediate interactions between *Pseudomonas aeruginosa* and *Agrobacterium tumefaciens* in biofilm cocultures. Proceedings of the National Academy of Sciences U S A. 2006 Mar 7;103(10):3828-33. doi: 10.1073/pnas.0511323103

Baran, R., Brodie, E.L., Mayberry-Lewis, J., Hummel, E., Da Rocha, U.N., Chakraborty, R., Bowen, B.P., Karaoz, U., Cadillo-Quiroz, H., Garcia-Pichel, F., Northen, T.R., 2015. Exometabolite niche partitioning among sympatric soil bacteria. Nature Communications 6, 8289. doi:10.1038/ncomms9289

Begunova, E.A., Stepnaya, O.A., Tsfasman, I.M. et al. 2004. The Effect of the Extracellular Bacteriolytic Enzymes of *Lysobacte*r sp. on Gram-Negative Bacteria. Microbiology 73, 267. https://doi.org/10.1023/B:MICI.0000032235.06143.5e

Bonnet, R. 2004. Growing group of extended-spectrum beta-lactamases: the CTX-M enzymes. Antimicrobial Agents and Chemotherapy 48(1), 1–14.

Boya, C.A., Fernández-Marín, H., Mejiá, L.C., Spadafora, C., Dorrestein, P.C., Gutiérrez, M., 2017. Imaging mass spectrometry and MS/MS molecular networking reveals chemical interactions among cuticular bacteria and pathogenic fungi associated with fungus-growing ants. Scientific Reports 7. doi:10.1038/s41598-017-05515-6

Brescia, F., Marchetti-Deschmann, M., Musetti, R., Perazzolli, M., Pertot, I., Puopolo, G., 2019. The rhizosphere signature on the cell motility, biofilm formation and secondary metabolite production of a plant-associated *Lysobacter* strain. Soil Biology and Biochemistry, submitted.

Cawoy, H., Debois, D., Franzil, L., De Pauw, E., Thonart, P., Ongena, M., 2015. Lipopeptides as main ingredients for inhibition of fungal phytopathogens by *Bacillus subtilis*/*amyloliquefaciens*. Microbial Biotechnology 8, 281–295. doi: 10.1111/1751-7915.12238.

Chen, J., Shen, D., Odhiambo, B.O., Xu, D., Han, S., Chou, S.-H., Qian, G., 2018. Two direct gene targets contribute to Clp-dependent regulation of type IV pilus-mediated twitching motility in *Lysobacter enzymogenes* OH11. Applied Microbiology and Biotechnology 102, 7509–7519. doi:10.1007/s00253-018-9196-x

Chen, X.-H., Vater, J., Piel, J., Franke, P., Scholz, R., Schneider, K., Koumoutsi, A., Hitzeroth, G., Grammel, N., Strittmatter, A.W., Gottschalk, G., Süssmuth, R.D., Borriss, R., 2006. Structural and functional characterization of three polyketide synthase gene clusters in *Bacillus amyloliquefaciens* FZB 42. Journal of Bacteriology 188, 4024–36. doi:10.1128/JB.00052-06

Cohen, S.P., Levy, S.B., Foulds, J., Rosner, J.L. 1993. Salicylate induction of antibiotic resistance in *Escherichia coli*: activation of the *mar* operon and a *mar*-independent pathway. Journal of Bacteriology 175, 7856–7862. doi:10.1128/jb.175.24.7856-7862.

Conesa, A., Götz, S., García-Gómez, J.M., Terol, J., Talón, M., and Robles, M. 2005. Blast2GO: a universal tool for annotation, visualization and analysis in functional genomics research. Bioinformatics 21, 3674–3676.

Crack, J.C., Munnoch, J., Dodd, E.L., Knowles, F., Al Bassam, M.M., Kamali, S., Holland, A.A., Cramer, S.P., Hamilton, C.J., Johnson, M.K., Thomson, A.J., Hutchings, M.I., Le Brun, N.E. 2015. NsrR from *Streptomyces coelicolor* is a nitric oxide-sensing [4Fe-4S] cluster protein with a specialized regulatory function. Journal of Biological Chemistry 290, 12689–12704.

De Boer, W., Wagenaar, A.M., Klein Gunnewiek, P.J.A., Van Veen, J.A., 2007. *In vitro* suppression of fungi caused by combinations of apparently non-antagonistic soil bacteria. FEMS Microbiology Ecology 59, 177–185. doi:10.1111/j.1574-6941.2006.00197.x

Ding, Y., Li, Z., Li, Y., Lu, C., Wang, H., Shen, Y., Du, L., 2016. HSAF-induced antifungal effects in *Candida albicans* through ROS-mediated apoptosis. RSC Advances 6, 30895–30904. doi:10.1039/C5RA26092B

Duineveld, B.M., Kowalchuk, G.A., Keijzer, A., Van Elsas, J.D., Van Veen, J.A., 2001. Analysis of bacterial communities in the rhizosphere of chrysanthemum via denaturing gradient gel electrophoresis of PCR-amplified 16S rRNA as well as DNA fragments coding for 16S rRNA. Applied and Environmental Microbiology 67, 172–178. doi:10.1128/AEM.67.1.172-178.2001

Durán, P., Thiergart, T., Garrido-Oter, R., Agler, M., Kemen, E., Schulze-Lefert, P., Hacquard, S., 2018. Microbial Interkingdom Interactions in Roots Promote Arabidopsis Survival. Cell 175, 973-983.e14. doi:10.1016/j.cell.2018.10.020

Expósito, R.G., Postma, J., Raaijmakers, J.M., De Bruijn, I., 2015. Diversity and

activity of Lysobacter species from disease suppressive soils. Frontiers in Microbiology 6, 1–12. doi:10.3389/fmicb.2015.01243

Fan, B., Wang, C., Song, X., Ding, X., Wu, L., Wu, H., Gao, X., Borriss, R., 2018. *Bacillus velezensis* FZB42 in 2018: The Gram-positive model strain for plant growth promotion and biocontrol. Frontiers in Microbiology 9, 2491. doi: 10.3389/fmicb.2018.02491

Felske, A., Wolterink, A., Van Lis, R., Akkermans, A.D.L., 1998. Phylogeny of the main bacterial 16S rRNA sequences in drentse A grassland soils (The Netherlands). Applied and Environmental Microbiology 64, 871–879.

Feng, T., Han, Y., Li, B., Li, Z., Yu, Y., Sun, Q., Li, X., Du, L., Zhang, X.-H., Wang, Y., 2019. Interspecies and Intraspecies Signals Synergistically Regulate the Twitching Motility in *Lysobacter enzymogenes*. Applied and Environmental Microbiology. doi:10.1128/aem.01742-19

Foster, K.R., Bell, T., 2012. Competition, not cooperation, dominates interactions among culturable microbial species. Current Biology 22, 1845–1850. doi:10.1016/j.cub.2012.08.005

Fujita, M., Mori, K., Hara, H. et al. 2019. A TonB-dependent receptor constitutes the outer membrane transport system for a lignin-derived aromatic compound. Communications Biology 2, 432. doi:10.1038/s42003-019-0676-z.

Garbeva, P., Van Veen, J.A., Van Elsas, J.D., Ecol, M., 2003. Predominant *Bacillus* spp. in Agricultural Soil under Different Management Regimes Detected via PCR-DGGE 45, 302–316. doi:10.1007/s00248-002-2034-8

Haas, D., Défago, G., 2005. Biological control of soil-borne pathogens by fluorescent

pseudomonads. Nature Review Microbiology 3, 307-19. doi: 10.1038/nrmicro1129

Hall-Stoodley, L., Costerton, J.W., Stoodley, P., 2004. Bacterial biofilms: from the natural environment to infectious diseases. Nature Review Microbiology 2, 96–108. doi: 10.1038/nrmicro821

Han, S., Shen, D., Wang, Y.C., Chou, S.H., Gomelsky, M., Gao, Y.G., Qian, G. 2020. A YajQ-LysR-like, cyclic di-GMP-dependent system regulating biosynthesis of an antifungal antibiotic in a crop-protecting bacterium, *Lysobacter enzymogenes*. Molecular Plant Pathology. doi:10.1111/mpp.12890

Hartmann, A., Schmid, M., van Tuinen, D., Berg, G., 2009. Plant-driven selection of microbes. Plant and Soil. doi:10.1007/s11104-008-9814-y

Hashizume, H., Igarashi, M., Hattori, S., Hori, M., Hamada, M., Takeuchi, T., 2001. Tripropeptins, Novel Antimicrobial Agents Produced by *Lysobacter* sp. I. Taxonomy, Isolation and Biological Activities. The Journal of Antibiotics 54, 1054–1059. doi:10.7164/antibiotics.54.1054

He, F., Li, B., Ai, G., Kange, A.M., Zhao, Y., Zhang, X., et al. 2018. Transcriptomics analysis of the chinese pear pathotype of *Alternaria alternata* gives insights into novel mechanisms of HSAF antifungal activities. International Journal of Molecular Sciences 19, pii: E1841.

He, Y.,W., Wu, J., Zhou, L., Yang, F., He, Y.,Q., Jiang, B.,L., Bai, L., Xu, Y., Deng, Z., Tang, J.,L., Zhang, L.,H., 2011. *Xanthomonas campestris* Diffusible Factor Is 3-Hydroxybenzoic Acid and Is Associated with Xanthomonadin Biosynthesis, Cell Viability, Antioxidant Activity, and Systemic Invasion. Molecular Plant-Microbe Interactions 24, 948–957. doi:10.1094/MPMI-02-11-0031

Hibbing, M.E., Fuqua, C. 2011. Antiparallel and interlinked control of cellular iron levels by the Irr and RirA regulators of *Agrobacterium tumefaciens*. Journal of Bacteriology 193, 3461–3472.

Hibbing, M.E., Fuqua, C., Parsek, M.R., Peterson, S.B., 2010. Bacterial competition: surviving and thriving in the microbial jungle. Nature Review Microbiology 8, 15–25. doi: 10.1038/nrmicro2259

Holzlechner, M., Reitschmidt, S., Gruber, S., Zeilinger, S., Marchetti-Deschmann, M., 2016. Visualizing fungal metabolites during mycoparasitic interaction by MALDI mass spectrometry imaging. Proteomics, 16, 1742-1746. doi:10.1002/pmic.201500510

Itoh, H., Tokumoto, K., Kaji, T., Paudel, A., Panthee, S., Hamamoto, H., Sekimizu, K., Inoue, M., 2018. Total Synthesis and Biological Mode of Action of WAP-8294A2: A Menaquinone-Targeting Antibiotic. The Journal of Organic Chemistry 83, 6924–6935. doi:10.1021/acs.joc.7b02318

Kenig, M., Abraham, E.P., 1976. Antimicrobial activities and antagonists of bacilysin and anticapsin. Journal of General Microbiology 94, 37–45. doi: 10.1099/00221287-94-1-37

Kim, J.,S., Wood, T.K., 2016. Persistent persister misperceptions. Frontiers in Microbiology 7,2134. doi: 10.3389/fmicb.2016.02134

Kim, S.,J., Ahn, J., H., Weon, H.,Y., Joa, J.,H., Hong, S.,B., Seok, S.,J., Kim, J.,S., Kwon, S.,W., 2017. *Lysobacter solanacearum* sp. nov., isolated from rhizosphere of tomato. International Journal of Systematic and Evolutionary Microbiology 67, 1102–1106. doi:10.1099/ijsem.0.001729

Klinkert, I., Chughtai, K., Ellis, S.R., Heeren, R.M.A., 2014. Methods for full resolution data exploration and visualization for large 2D and 3D mass spectrometry imaging datasets. International Journal of Mass Spectrometry 362, 40–47. doi:10.1016/J.IJMS.2013.12.012

Koumoutsi, A., Chen, X.-H., Henne, A., Liesegang, H., Hitzeroth, G., Franke, P., Vater, J., Borriss, R., 2004. Structural and functional characterization of gene clusters directing nonribosomal synthesis of bioactive cyclic lipopeptides in *Bacillus amyloliquefaciens* strain FZB42. Journal of Bacteriology 186, 1084–96. doi:10.1128/jb.186.4.1084-1096.2004

Lazazzara, V., Perazzolli, M., Pertot, I., Biasioli, F., Puopolo, G., Cappellin, L., 2017. Growth media affect the volatilome and antimicrobial activity against *Phytophthora infestans* in four *Lysobacter* type strains. Microbiological Research 201, 52–62. doi:10.1016/J.MICRES.2017.04.015

Lebreton, F., van Schaik, W., Sanguinetti, M., Posteraro, B., Torelli, R., Le Bras, F., et al. 2012. AsrR is an oxidative stress sensing regulator modulating *Enterococcus faecium* opportunistic traits, antimicrobial resistance, and pathogenicity. PLoS Pathogens 8(8), e1002834. https://doi.org/10.1371/journal.ppat.1002834.

Li, S., Calvo, A.M., Yuen, G.Y., Du, L., Harris, S.D., 2009. Induction of cell wall thickening by the antifungal compound dihydromaltophilin disrupts fungal growth and is mediated by sphingolipid biosynthesis. Journal of Eukaryotic Microbiology 56, 182–187. doi:10.1111/j.1550-7408.2008.00384.x

Liao, Y., Smyth, G.K, and Shi, W. 2014. FeatureCounts: an efficient general-purpose program for assigning sequence reads to genomic features. Bioinformatics 30**,** 923–930.

Liao, Y., Smyth, G.K., and Shi, W. 2013. The Subread aligner: fast, accurate and scalable read mapping by seed-and-vote**.** Nucleic Acids Research 41**,** e108.

Ma, D., Alberti, M., Lynch, C., Nikaido, H., Hearst, J.E. 1996. The local repressor AcrR plays a modulating role in the regulation of *acrAB* genes of *Escherichia coli* by global stress signals. Molecular Microbiology 19, 101–112.

Mendes, R., Kruijt, M., De Bruijn, I., Dekkers, E., Van Der Voort, M., Schneider, J.H.M., Piceno, Y.M., DeSantis, T.Z., Andersen, G.L., Bakker, P.A.H.M., Raaijmakers, J.M., 2011. Deciphering the rhizosphere microbiome for disease-suppressive bacteria. Science 332, 1097–1100. doi:10.1126/science.1203980

Mesanza, N., Iturritxa, E., Patten, C.L., 2016. Native rhizobacteria as biocontrol agents of *Heterobasidion annosum* s.s. and *Armillaria mellea* infection of *Pinus radiata*. Biological Control 101, 8–16. doi:10.1016/J.BIOCONTROL.2016.06.003

Michelsen, C.F., Mohammad, S., Khademi, H., Krogh Johansen, H., Ingmer, H., Dorrestein, P.C., Jelsbak, L., 2015. Evolution of metabolic divergence in *Pseudomonas aeruginosa* during long-term infection facilitates a proto-cooperative interspecies interaction. The ISME Journal 10, 1323–1336. doi:10.1038/ismej.2015.220

Molinatto, G., Franzil, L., Steels, S., Puopolo, G., Pertot I., Ongena, M., 2017. Key impact of an uncommon plasmid on *Bacillus amyloliquefaciens* subsp. *plantarum* S499 developmental traits and lipopeptide production. Frontiers in Microbiology 8, . doi: 10.3389/fmicb.2017.00017

Molinatto, G., Puopolo, G., Sonego, P., Moretto, M., Engelen, K., Viti, C., 2016. Complete genome sequence of *Bacillus amyloliquefaciens* subsp. plantarum S499, a rhizobacterium that triggers plant defences and inhibits fungal phytopathogens.

Journal of Biotechnology 238, 56–59. doi: 10.1016/j.jbiotec.2016.09.013

Nozaki, Y., Okonogi, K., Katayama, N., Ono, H., Harada, S., Kondo, M., Okazaki, H., 1984. Cephabacins, new cephem antibiotics of bacterial origin. IV. Antibacterial activities, stability to .BETA.-lactamases and mode of action. The Journal of Antibiotics 37, 1555–1565. doi:10.7164/antibiotics.37.1555

Ongena, M., Jacques, P., 2008. *Bacillus* lipopeptides: versatile weapons for plant disease biocontrol. Trends in Microbiology 16, 115-125. doi: 10.1016/j.tim.2007.12.009

Ongena, M., Jacques, P., Touré, Y., Destain, J., Jabrane, A., Thonart, P., 2005. Involvement of fengycin-type lipopeptides in the multifaceted biocontrol potential of *Bacillus subtilis*. Applied Microbiology Biotechnology 69, 29–38. doi: 10.1007/s00253-005-1940-3. S499

Park, J.H., Kim, R., Aslam, Z., Jeon, C.O., Chung, Y.R., 2008. *Lysobacter capsici* sp. nov., with antimicrobial activity, isolated from the rhizosphere of pepper, and emended description of the genus *Lysobacter*. International Journal of Systematic and Evolutionary Microbiology 58, 387–392. doi:10.1099/ijs.0.65290-0

Paulsen, I.T., Press, C.M., Ravel, J., Kobayashi, D.Y., Myers, G.S.A., Mavrodi, D.V., et al., 2005. Complete genome sequence of the plant commensal *Pseudomonas fluorescens* Pf-5. Nature Biotechnology 23, 873–878. doi: 10.1038/nbt1110

Postma, J., Scheper, R.W.A., Schilder, M.T., 2010. Effect of successive cauliflower plantings and *Rhizoctonia solani* AG 2-1 inoculations on disease suppressiveness of a suppressive and a conducive soil. Soil Biology and Biochemistry 42, 804–812. doi:10.1016/J.SOILBIO.2010.01.017

Postma, J., Schilder, M.T., 2015. Enhancement of soil suppressiveness against *Rhizoctonia solani* in sugar beet by organic amendments. Applied Soil Ecology 94, 72–79. doi:10.1016/j.apsoil.2015.05.002

Puopolo G., Tomada S., Sonego P., Moretto M., Engelen K., Perazzolli M., et al. 2016. The *Lysobacter capsici* AZ78 genome has a gene pool enabling it to interact successfully with phytopathogenic microorganisms and environmental factors. Frontiers in Microbiology 7, 96.

Puopolo, G., Cimmino, A., Palmieri, M.C., Giovannini, O., Evidente, A., Pertot, I., 2014a. *Lysobacter capsici* AZ78 produces cyclo(l -Pro- l -Tyr), a 2,5-diketopiperazine with toxic activity against sporangia of *Phytophthora infestans* and *Plasmopara viticola*. Journal of Applied Microbiology 117, 1168–1180. doi:10.1111/jam.12611

Puopolo, G., Giovannini, O., Pertot, I., 2014b. *Lysobacter capsici* AZ78 can be combined with copper to effectively control *Plasmopara viticola* on grapevine. Microbiological Research 169, 633–642. doi:10.1016/j.micres.2013.09.013

Puopolo, G., Tomada, S., Pertot, I., 2018. The impact of the omics era on the knowledge and use of *Lysobacter* species to control phytopathogenic micro-organisms. Journal of Applied Microbiology 124, 15–27. doi:10.1111/jam.13607

Qian, G., Xu, F., Venturi, V., Du, L., Liu, F., 2014. Roles of a Solo LuxR in the Biological Control Agent *Lysobacter enzymogenes* Strain OH11. Phytopathology 104, 224–231. doi:10.1094/PHYTO-07-13-0188-R

Robichaud, G., Garrard, K.P., Barry, J.A., Muddiman, D.C., 2013. MSiReader: An Open-Source Interface to View and Analyze High Resolving Power MS Imaging Files on Matlab Platform. Journal of The American Society for Mass Spectrometry

24, 718–721. doi:10.1007/s13361-013-0607-z

Roesch, L.F.W., Fulthorpe, R.R., Riva, A., Casella, G., Hadwin, A.K.M., Kent, A.D., Daroub, S.H., Camargo, F.A.O., Farmerie, W.G., Triplett, E.W., 2007. Pyrosequencing enumerates and contrasts soil microbial diversity. ISME Journal 1, 283–290. doi:10.1038/ismej.2007.53

Rosenzweig, N., Tiedje, J.M., Quensen, J.F., Meng, Q., Hao, J.J., 2012. Microbial communities associated with potato common scab-suppressive soil determined by pyrosequencing analyses. Plant Disease 96, 718–725. doi:10.1094/PDIS-07-11-0571

Ryu, C.-M., Farag, M.A., Hu, C.-H., Reddy, M.S., Wei, H.-X., Paré, P.W., Kloepper, J.W., 2003. Bacterial volatiles promote growth in *Arabidopsis*. Proceedings of the National Academy of Sciences of the United States of America 100, 4927–32. doi:10.1073/pnas.0730845100

Santos, J.A., Pereira, P.J.B., Macedo-Ribeiro, S. 2015. What a difference a cluster makes: The multifaceted roles of IscR in gene regulation and DNA recognition. Biochimica et Biophysica Acta - Proteins and Proteomics 1854(9), 1101-12, doi: 10.1016/j.bbapap.2015.01.010.

Schneider, C.A., Rasband, W.S., Eliceiri, K.W., 2012. NIH Image to ImageJ: 25 years of image analysis. Nature Methods 9, 671–5.

Schulz-Bohm, K., Zweers, H., de Boer, W., Garbeva, P., 2015. A fragrant neighborhood: Volatile mediated bacterial interactions in soil. Frontiers in Microbiology 6, 1–11. doi:10.3389/fmicb.2015.01212

Seccareccia, I., Kost, C., Nett, M., 2015. Quantitative analysis of *Lysobacter* predation.

Applied and Environmental Microbiology 81, 7098–105. doi:10.1128/AEM.01781-15

Shi, S., Nuccio, E.E., Shi, Z.J., He, Z., Zhou, J., Firestone, M.K., 2016. The interconnected rhizosphere: High network complexity dominates rhizosphere assemblages. Ecology Letters. doi:10.1111/ele.12630

Smyth, G.K. 2004. Linear models and empirical bayes methods for assessing differential expression in microarray experiments. Statistical Applications in Genetics and Molecular Biology 3, 3.

Su, C.C., Rutherford, D.J., Yu, E.W. 2007. Characterization of the multidrug efflux regulator AcrR from *Escherichia coli*. Biochemical and Biophysical Research Communications 361:85–90. doi:10.1016/j.bbrc.2007.06.175.

Su, Z., Chen, H., Wang, P., Tombosa, S., Du, L., Han, Y., Shen, Y., Qian, G., Liu, F. 2017. 4-Hydroxybenzoic acid is a diffusible factor that connects metabolic shikimate pathway to the biosynthesis of a unique antifungal metabolite in *Lysobacter enzymogenes*. Molecular Microbiology 104, 163–178. doi:10.1111/mmi.13619

Su, Z., Han, S., Fu, Z. Q., Qian, G., Liu, F. 2018. Heat-Stable Antifungal Factor (HSAF) biosynthesis in *Lysobacter enzymogenes* is controlled by the interplay of two transcription factors and a diffusible molecule. Applied and environmental microbiology 84(3), e01754-17. doi:10.1128/AEM.01754-17

Tasaki, S., Nakayama, M., Shoji, W., 2017. Self-organization of bacterial communities against environmental pH variation: Controlled chemotactic motility arranges cell population structures in biofilms. PLoS One 12, e0173195. doi: 10.1371/journal.pone.0173195

Tomada, S., Sonego, P., Moretto, M., Engelen, K., Pertot, I., Perazzolli, M. et al., 2017. Dual RNA–Seq of *Lysobacter capsici* AZ78 – *Phytophthora infestans* interaction shows the implementation of attack strategies by the bacterium and unsuccessful oomycete defense responses. Environmental Microbiology 19, 4113–4125.

Traxler, M.F., Watrous, J.D., Alexandrov, T., Dorrestein, P.C., Kolter, R., 2013. Interspecies interactions stimulate diversification of the *Streptomyces coelicolor* secreted metabolome. MBio 4, 1–12. doi:10.1128/mBio.00459-13

Tyc, O., de Jager, V.C.L., van den Berg, M., Gerards, S., Janssens, T.K.S., Zaagman, N., Kai, M., Svatos, A., Zweers, H., Hordijk, C., Besselink, H., de Boer, W., Garbeva, P. 2017. Exploring bacterial interspecific interactions for discovery of novel antimicrobial compounds. Microbial Biotechnology 10, 910–925. doi: 10.1111/1751-7915.12735

Tyc, O., Wolf, A.B., Garbeva, P., 2015. The effect of phylogenetically different bacteria on the fitness of *Pseudomonas fluorescens* in sand microcosms. PloS One 10, e0119838. doi:10.1371/journal.pone.0119838

Van Houdt, R., Aertsen, A., Michiels, C.W., 2007. Quorum-sensing-dependent switch to butanediol fermentation prevents lethal medium acidification in Aeromonas hydrophila AH-1N. Research in Microbiology 158, 379–385. doi:10.1016/J.RESMIC.2006.11.015

Vega, N.M., Allison, K.R., Khalil, A.S., Collins, J.J., 2012. Signaling-mediated bacterial persister formation. Nature Chemical Biology 8,431–3. doi: 10.1038/nchembio.915

Venturi, V., Keel, C., 2016. Signaling in the Rhizosphere. Trends in Plant Sciences

21,187–198. doi: 10.1016/j.tplants.2016.01.005

Wang, R., Zhang, H., Sun, L., Qi, G., Chen, S., Zhao, X., 2017. Microbial community composition is related to soil biological and chemical properties and bacterial wilt outbreak. Scientific Reports 7, 343. doi:10.1038/s41598-017-00472-6

Weinert, N., Piceno, Y., Ding, G.C., Meincke, R., Heuer, H., Berg, G., Schloter, M., Andersen, G., Smalla, K., 2011. PhyloChip hybridization uncovered an enormous bacterial diversity in the rhizosphere of different potato cultivars: Many common and few cultivar-dependent taxa. FEMS Microbiology Ecology 75, 497–506. doi:10.1111/j.1574-6941.2010.01025.x

Wu, L., Wu, H., Chen, L., Yu, X., Borriss, R., Gao, X., 2015. Difficidin and bacilysin from *Bacillus amyloliquefaciens* FZB42 have antibacterial activity against *Xanthomonas oryzae* rice pathogens. Scientific Reports 5. doi:10.1038/srep12975

Xiao, M., Zhou, X.-K., Chen, X., Duan, Y.-Q., Alkhalifah, D.H.M., Im, W.-T., Hozzein, W.N., Chen, W., Li, W.-J., 2019. *Lysobacter tabacisoli* sp. nov., isolated from rhizosphere soil of *Nicotiana tabacum* L. International Journal of Systematic and Evolutionary Microbiology 69, 1875–1880. doi:10.1099/ijsem.0.003164

Xie, Y., Wright, S., Shen, Y., Du, L., 2012. Bioactive natural products from *Lysobacter*. Natural Product Reports 29, 1277. doi:10.1039/c2np20064c

Yang, J., Caprioli, R.M., 2011. Matrix sublimation/recrystallization for imaging proteins by Mass Spectrometry at high spatial resolution. Analytical Chemistry 83, 5728–5734. doi:10.1021/ac200998a

Yu, F., Zaleta-Rivera, K., Zhu, X., Huffman, J., Millet, J.C., Harris, S.D., Yuen, G., Li, X.-C., Du, L., 2007. Structure and biosynthesis of heat-stable antifungal factor

(HSAF), a broad-spectrum antimycotic with a novel mode of action. Antimicrobial Agents and Chemotherapy 51, 64–72. doi:10.1128/AAC.00931-06

Yukl, E.T., Elbaz, M.A., Nakano, M.M., Moenne-Loccoz, P. 2008. Transcription factor NsrR from *Bacillus subtilis* senses nitric oxide with a 4Fe-4S cluster (dagger). Biochemistry 47, 13084–13092.

Zhang, J., Kobert, K., Flouri, T., and Stamatakis, A. 2014. PEAR: a fast and accurate Illumina Paired-End reAd mergeR. Bioinformatics 30, 614–620.

Zhang, W., Li, Y., Qian, G., Wang, Y., Chen, H., Li, Y.-Z., Liu, F., Shen, Y., Du, L., 2011. Identification and characterization of the anti-methicillin-resistant *Staphylococcus aureus* WAP-8294A2 biosynthetic gene cluster from *Lysobacter enzymogenes* OH11. Antimicrobial Agents and Chemotherapy 55, 5581–5589. doi:10.1128/AAC.05370-11

Zweerink, M.M., Edison, A., 1987. Difficidin and oxydifficidin: novel broad spectrum antibacterial antibiotics produced by *Bacillus subtilis*. III. Mode of action of difficidin. Journal of Antibiotics (Tokyo).40, 1692–1697. doi: 10.7164/antibiotics.40.1692

Figure legends

Figure 1. Visualization of *Lysobacter capsici* AZ78 macrocolony morphology developed during interaction with rhizosphere associated bacterial strains. Pictures show the cell monolayer outer ring of *Lysobacter capsici* AZ78 (AZ78) macrocolony grown alone and in the presence of *Pseudomonas protegens* Pf-5 (Pf-5) and *Bacillus amyloliquefaciens* subsp. *plantarum* S499 (S499). Bacterial cell suspensions were spot inoculated onto a thin layer of Rhizosphere-Mimicking Agar on glass slides and incubated at 25°C for 36 h. **A**, AZ78 grown alone; **B**, AZ78 grown in a two-way interaction with Pf-5; **C**, AZ78 monolayer outer ring facing Pf-5 in the three-way interaction; **D**, AZ78 grown in a two-way interaction with S499; **E**, AZ78 monolayer outer ring facing S499 in the three-way interaction. Observations were carried out using a phase-contrast microscope with a magnification X-100. The black bar corresponds to 10 nm.

Figure 2. Modulation of the inhibitory activity of *Lysobacter capsici* AZ78 during a two- and three-way interaction with rhizosphere associated bacterial strains. The impact of two and three-way interactions with *Bacillus amyloliquefaciens* subsp. *plantarum* S499 and *Pseudomonas protegens* Pf-5 on *Lysobacter capsici* AZ78 inhibitory activity was determined according to $[(Ac - Ai)/Ac] \times 100$, where A_c is *P. ultimum* growth area in presence of AZ78 grown alone and A_i is *P. ultimum* growth area in presence of AZ78 grown in two- and three-way interactions. Columns represent mean ± standard error. A one-way ANOVA revealed significant differences within

treatments ($p < 0.05$), different letters show significant differences according to Tukey's test ($\alpha = 0.05$).

Figure 3. Modulation of the inhibitory activity of *Lysobacter capsici* AZ78 during a two-way interaction with *Bacillus velezensis* FZB42 and its mutant derivatives. The impact of two-way interactions with *Bacillus velezensis* FZB42 and its mutants deficient for the production of lipopeptides, polyketides and Bacilysin (RS06), Bacillomycin (AK1), Fengycin (AK2), Surfactin (CH01), Bacillaene (CH06), Macrolactin (CH07), Difficidin (CH08) and Bacillibactin (CH39) on *L. capsici* AZ78 inhibitory activity was determined according to $[(Ac - Ai)/Ac] \times 100$

where A_c is *P. ultimum* growth area in presence of AZ78 grown alone and A_i is *P. ultimum* growth area in presence of AZ78 grown in two-way interactions. Columns represent mean ± standard error. A one-way ANOVA revealed significant differences within treatments ($p < 0.05$), different letters show significant differences according to Tukey's test ($\alpha = 0.05$).

Figure 4. Visualization of *Lysobacter capsici* AZ78 macrocolony morphology developed during during a two-way interaction with *Bacillus spp.* strains. Pictures show the cell monolayer outer ring of *Lysobacter capsici* AZ78 (AZ78) macrocolony grown alone and in the presence of *Bacillus amyloliquefaciens* subsp. *plantarum* S499 (S499), *Bacillus velezensis* FZB42 (FZB42) and its mutants CH08 and RS06. Bacterial cell suspensions were spot inoculated onto a thin layer of Rhizosphere-Mimicking Agar on glass slides and incubated at 25°C for 36 h. **A,** AZ78 grown alone; **B,** AZ78 grown

in a two-way interaction with S499; **C**, AZ78 grown in a two-way interaction with FZB42; **D**, AZ78 grown in a two-way interaction with CH08; **E**, AZ78 grown in a two-way interaction with RS06. Observations were carried out using a phase-contrast microscope with a magnification X-100. The black bar corresponds to 10 nm.

Figure 5. *Lysobacter capsici* AZ78 metabolic profiles during a two- and three-way interaction with rhizosphere associated bacterial strains.

The Venn Diagram shows the number of ions shared and specific between the metabolic profiles of *Lysobacter capsici* AZ78 grown alone (AZ78), AZ78 grown in a two-way interaction with *Pseudomonas protegens* Pf-5 (AZ78 *vs* Pf-5), AZ78 grown in a two-way interaction with *Bacillus amyloliquefaciens* subsp. *plantarum* S499 (AZ78 *vs* S499), AZ78 grown in a three-way interaction with Pf-5 and S499 (AZ78 *vs* Pf-5 *vs* S499). Pie charts show the distribution of the detected ions in the functional classesof antagonism, cell structure, primary metabolism, signals and unknown.

Figure 6. Spatial distribution of *Lysobacter capsici* AZ78 (AZ78) metabolites. MALDI TOF MSI images corresponding to the *m/z* values of 156.0 (A) 535.4 (B) and 1584.8 (C) ± 0.1 Th were normalized by Total Ion Count (TIC). The different treatments are shown in the columns: AZ78 grown alone (AZ78 alone), AZ78 grown in a two-way interaction with *Pseudomonas protegens* Pf-5 (AZ78 *vs* Pf-5), AZ78 grown in a two-way interaction with *Bacillus amyloliquefaciens* subsp. *plantarum* S499 (AZ78 *vs* S499), AZ78 grown in a three-way interaction with Pf-5 and S499 (AZ78 *vs* Pf-5 *vs* S499). Ion intensity is visualised as a heatmap.

Figure 7. *Lysobacter capsici* AZ78 (AZ78) Differentially Expressed Genes (DEGs).

The number of AZ78 DEGs up- and down-regulated for the two- and three-way interactions with *Bacillus amyloliquefaciens* S499 (S499) and *Pseudomonas protegens* Pf-5 (Pf-5) is reported (A). The Venn diagrams (B) show the number of DEGs (down-regulated and up-regulated) shared and specific for the transcriptomes of AZ78 grown in two- and three-way interactions with S499 and Pf-5.

Figure 8. Annotation of *Lysobacter capsici* AZ78 (AZ78) Differentially Expressed Genes (DEGs) shared in all two- and three-way interactions with *Bacillus amyloliquefaciens* S499 and *Pseudomonas protegens* Pf-5. DEGs were classified on the basis of NCBI gene description and Blast2GO description in functional classes. The number of DEGs for each functional category (except for the unknown function) is reported for AZ78 genes shared in all the interactions. Green, up-regulated DEGs; Orange, down-regulated DEGs. The total number of DEGs is shown for each functional class.

Figure S1. Experimental design for bacterial interactions. Drops (5 μl) of bacterial cell suspensions were inoculated in a stand-alone treatment, two-way interaction, three-way interaction to analyse the impact of interactions on the macrocolony structure and cell motility of *Lysobacter capsici* AZ78 (**A**) and on its inhibitory activity against *Pythium ultimum* (P.u., **B**).

Table 1. Bacterial strains used in this study

Bacterial strain	Growth medium[a]	Characteristics	Reference
Bacillus amyloliquefaciens subsp. *plantarum* S499	Nutrient Agar	Bacterial biocontrol agent able to produce antibiotics	Molinatto et al. 2016
Bacillus velezensis FZB42 (DSM 23117)[b]	Nutrient Agar	Bacterial biocontrol agent able to produce antibiotics	Fan et al. 2018
Lysobacter capsici AZ78	Nutrient Agar	Bacterial biocontrol agent able to produce antibiotics	Puopolo et al. 2016
Pseudomonas protegens Pf-5 (ATCC BAA477)	Nutrient Agar	Bacterial biocontrol agent able to produce antibiotics	Paulsen et al. 2005
Bacillus velezensis AK1	Nutrient Agar Em^1	FZB42 mutant deficient in synthesis of bacillomycin D	Koumoutsi et al.
Bacillus velezensis AK2	Nutrient Agar Cm^5	FZB42 mutant deficient in synthesis of fengycin	Koumoutsi et al.
Bacillus velezensis CH01	Nutrient Agar Em^1	FZB42 mutant deficient in surfactin synthesis	Koumoutsi et al.
Bacillus velezensis CH06	Nutrient Agar Cm^5	FZB42 mutant deficient in bacillaene synthesis	Chen et. al. 2006
Bacillus velezensis CH07	Nutrient Agar Cm^5	FZB42 mutant deficient in macrolactin synthesis	Chen et. al. 2006
Bacillus velezensis CH08	Nutrient Agar Em^1	FZB42 mutant deficient in difficidin synthesis	Chen et. al. 2006
Bacillus velezensis CH39	Nutrient Agar Cm^5	FZB42 mutant deficient in bacillibactin synthesis	Chen et. al. 2006
Bacillus velezensis RS06	Nutrient Agar Cm^5Em^1	FZB42 mutant deficient in secondary metabolite synthesis	Chen et. al. 2006

[a] Em^1= Erytromycin 1 mg/l; Cm^5: Chloramfenicol 5 mg/l

[b]ex *Bacillus amyloliquefaciens* subsp. *plantarum* FZB42

Table 2. Number of *Lysobacter capsici* AZ78 up- and down-regulated genes according to the interactions.

Interactions	Up-regulated	Down-regulated
Lysobacter capsici AZ78 × *Bacillus amyloliquefaciens* S499	686	787
Lysobacter capsici AZ78 × *Pseudomonas protegens* Pf-5	252	46
Lysobacter capsici AZ78 × *Bacillus amyloliquefaciens* S499 × *Pseudomonas protegens* Pf-5	783	625

Table S1. Treatments analysed. The table reports the two- and three-way interactions analysed in this study. The strains were spot-inoculated at 1 cm of distance according to the scheme reported in Figure S1.

Treatments	Interactions
Stand-alone	*Lysobacter capsici* AZ78
Two-way interactions	*Lysobacter capsici* AZ78 × *Bacillus amyloliquefaciens* S499 *Lysobacter capsici* AZ78 × *Bacillus velenzesis* FZB42 *Lysobacter capsici* AZ78 × *Bacillus velezensis* AK1 *Lysobacter capsici* AZ78 × *Bacillus velezensis* AK2 *Lysobacter capsici* AZ78 × *Bacillus velezensis* CH01 *Lysobacter capsici* AZ78 × *Bacillus velezensis* CH06 *Lysobacter capsici* AZ78 × *Bacillus velezensis* CH07 *Lysobacter capsici* AZ78 × *Bacillus velezensis* CH08 *Lysobacter capsici* AZ78 × *Bacillus velezensis* CH39 *Lysobacter capsici* AZ78 × *Bacillus velezensis* RS06 *Lysobacter capsici* AZ78 × *Pseudomonas protegens* Pf-5
Three-way interaction	*Lysobacter capsici* AZ78 × *Bacillus amyloliquefaciens* S499 ×*Pseudomonas protegens* Pf-5

Table S2. Composition of Rhizosphere Mimicking Agar.

Type	Ingredients[a]	Concentration (g/l)
Synthetic root exudates	Citric acid	0.010
	Fructose[b]	0.039
	Glucose	0.039
	Glutamic acid	0.019
	L-Alanine	0.019
	L-Serine	0.023
	Lactic acid	0.001
	Succinic acid	0.010
	Sucrose	0.037
Recalcitrant organic carbon sources	Cellulose	0.079
	Humic acids	0.033
	Lignin	0.065
	Starch	0.017
Salts	$CuSO_4$ $5H_2O$	0.005
	KCl	0.499
	KH_2PO_4	0.680
	$Fe_2(SO_4)_3$	0.031
	$MgSO_4$ $7H_2O$	0.493
	$MnSO_4$	0.001
	Na_2MoO_4 $2H_2O$	0.008
	$(NH_4)_2SO_4$	0.002

[a]The pH was adjusted to 6.5 and agar was added in a concentration of 1.6 % (w/v)

[b]Fructose, glucose and sucrose were added after autoclaving

Table S3. Distribution of *m/z* values in functional classes. Each *m/z* value was searched in an online database, "The Metabolomics Workbench" (http://www.metabolomicsworkbench.org/, 2019). The *m/z* putatively matching with metabolites were distributed in functional classes according to their function in the bacterial cell physiology.

Class name	Examples
Antagonism	*m/z* values matching with compounds involved in the competition between bacterial cells(e.g. antibiotics, siderophores)
Cell structure	*m/z* values matching with compounds included in bacterial cell structures (e.g. cell wall, peptidoglycan)
Primary metabolism	*m/z* values matching with compounds involved in the primary metabolism of bacterial cells (e.g. amino acids, sugars)
Signals	*m/z* values matching with compounds involved in the bacterial cell-cell signalling (e.g. homoserine lactones, volatile organic compounds)
Unknown	*m/z* values without any match in the database

Table S4. Presence/absence analysis of the ions found in the the metabolic profile of *Lysobacter capsici* AZ78 macrocolony. In blue are highlighted the *m/z* values of the ions found in the centre core and outer ring of *L. capsici* AZ78 macrocolony in each treatment: AZ78 alone (A), AZ78 in interaction with *Bacillus amyloliquefaciens* S499 (B), AZ78 in interaction with *Pseudomonas protegens* Pf-5 (C), AZ78 in a three-way interaction (D).

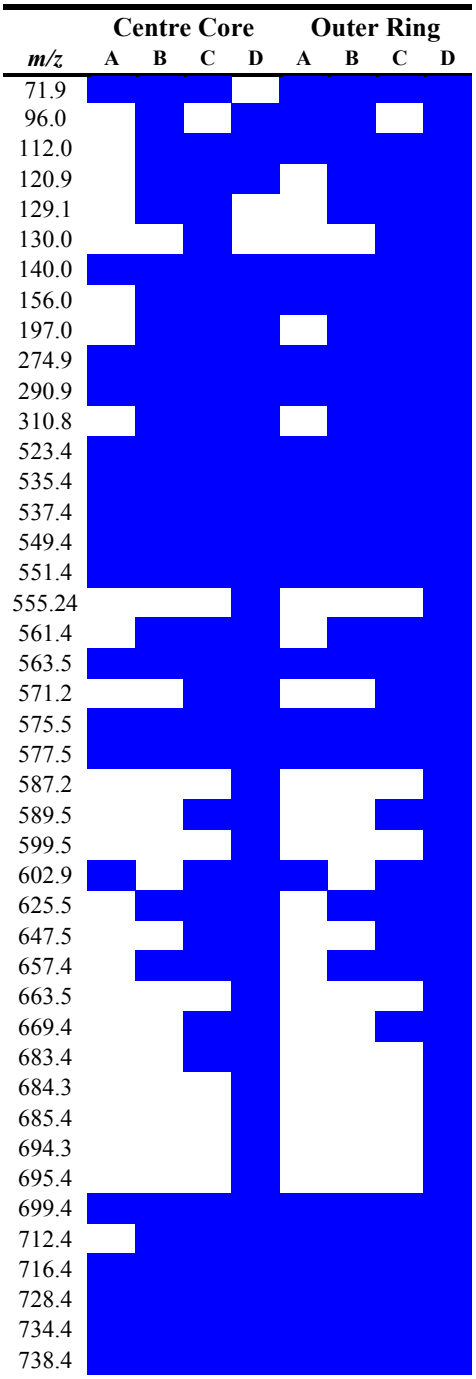

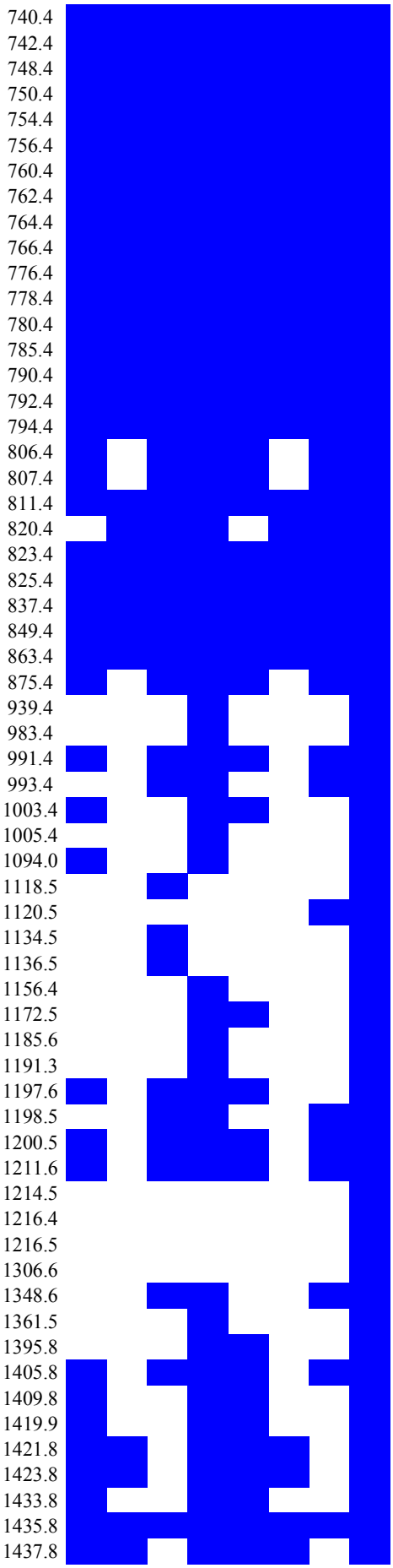
740.4
742.4
748.4
750.4
754.4
756.4
760.4
762.4
764.4
766.4
776.4
778.4
780.4
785.4
790.4
792.4
794.4
806.4
807.4
811.4
820.4
823.4
825.4
837.4
849.4
863.4
875.4
939.4
983.4
991.4
993.4
1003.4
1005.4
1094.0
1118.5
1120.5
1134.5
1136.5
1156.4
1172.5
1185.6
1191.3
1197.6
1198.5
1200.5
1211.6
1214.5
1216.4
1216.5
1306.6
1348.6
1361.5
1395.8
1405.8
1409.8
1419.9
1421.8
1423.8
1433.8
1435.8
1437.8

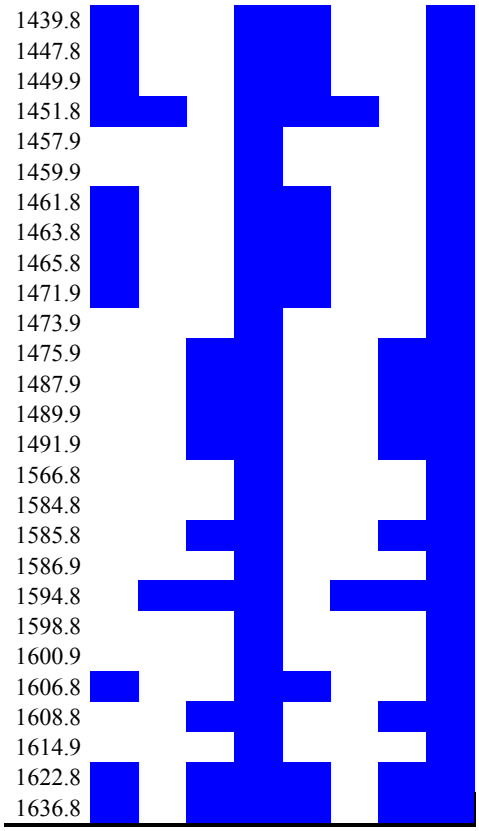
1439.8
1447.8
1449.9
1451.8
1457.9
1459.9
1461.8
1463.8
1465.8
1471.9
1473.9
1475.9
1487.9
1489.9
1491.9
1566.8
1584.8
1585.8
1586.9
1594.8
1598.8
1600.9
1606.8
1608.8
1614.9
1622.8
1636.8

Figure 1

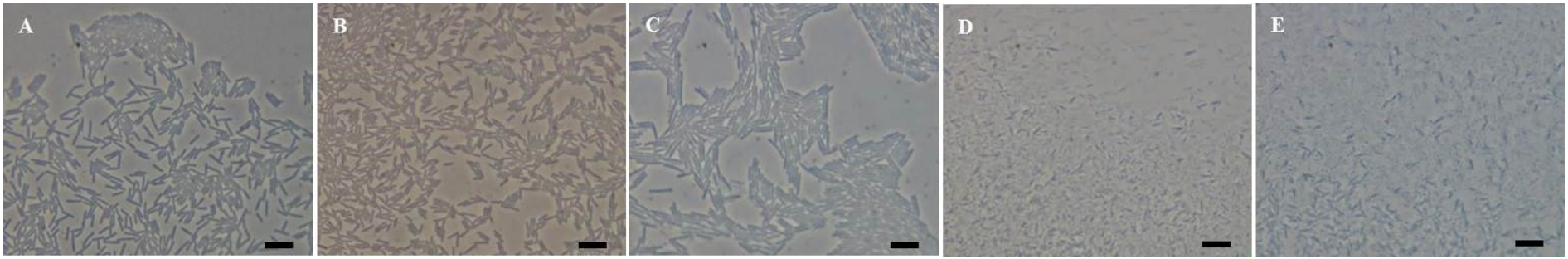

Figure 2

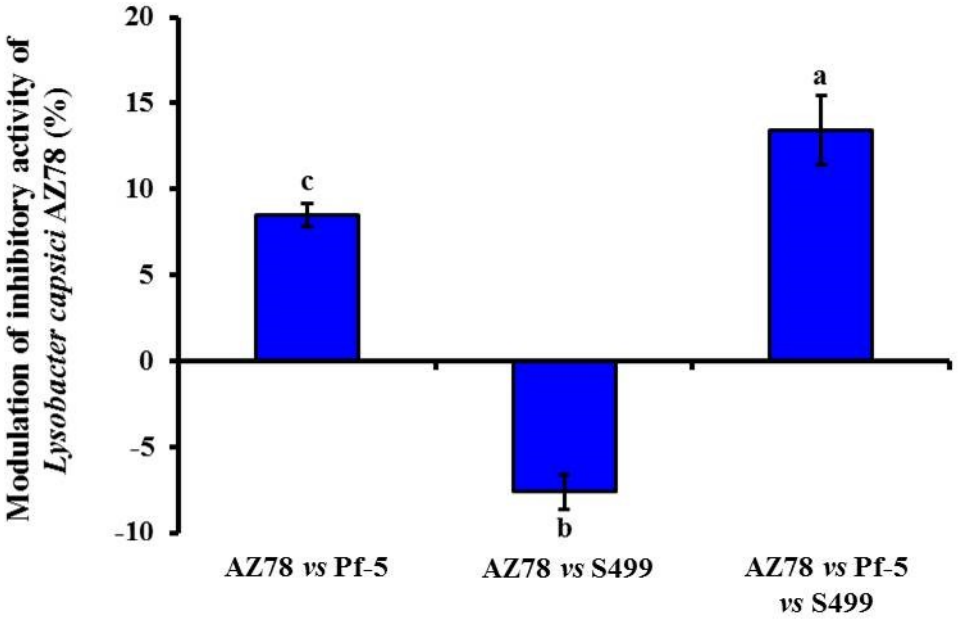

Figure 3

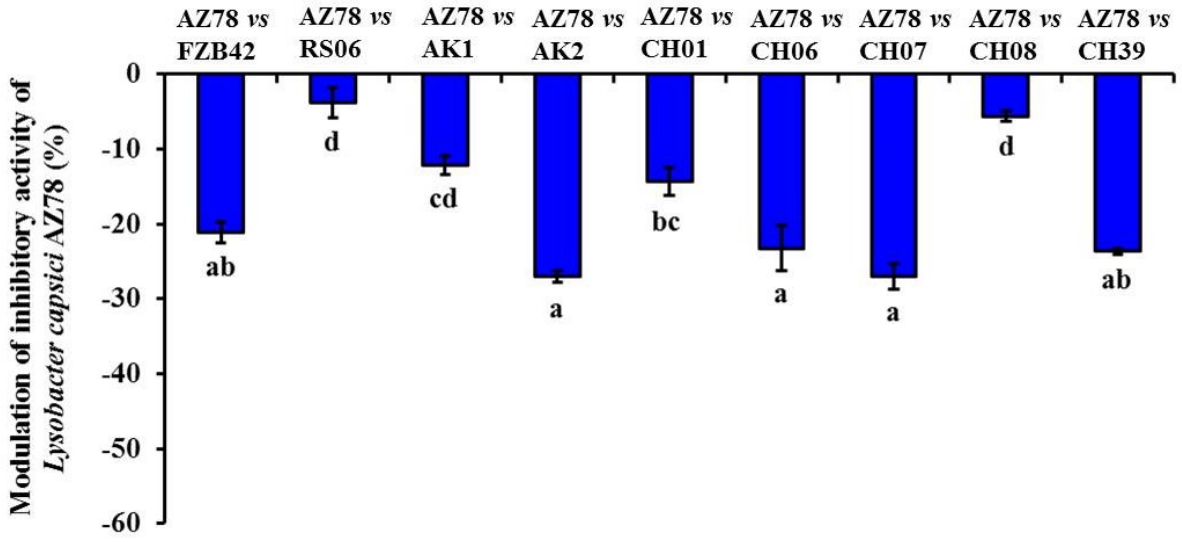

Figure 4

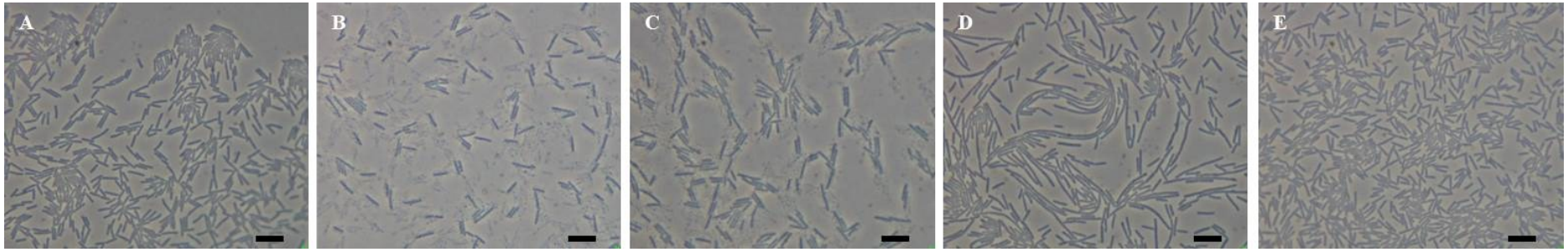

Figure 5

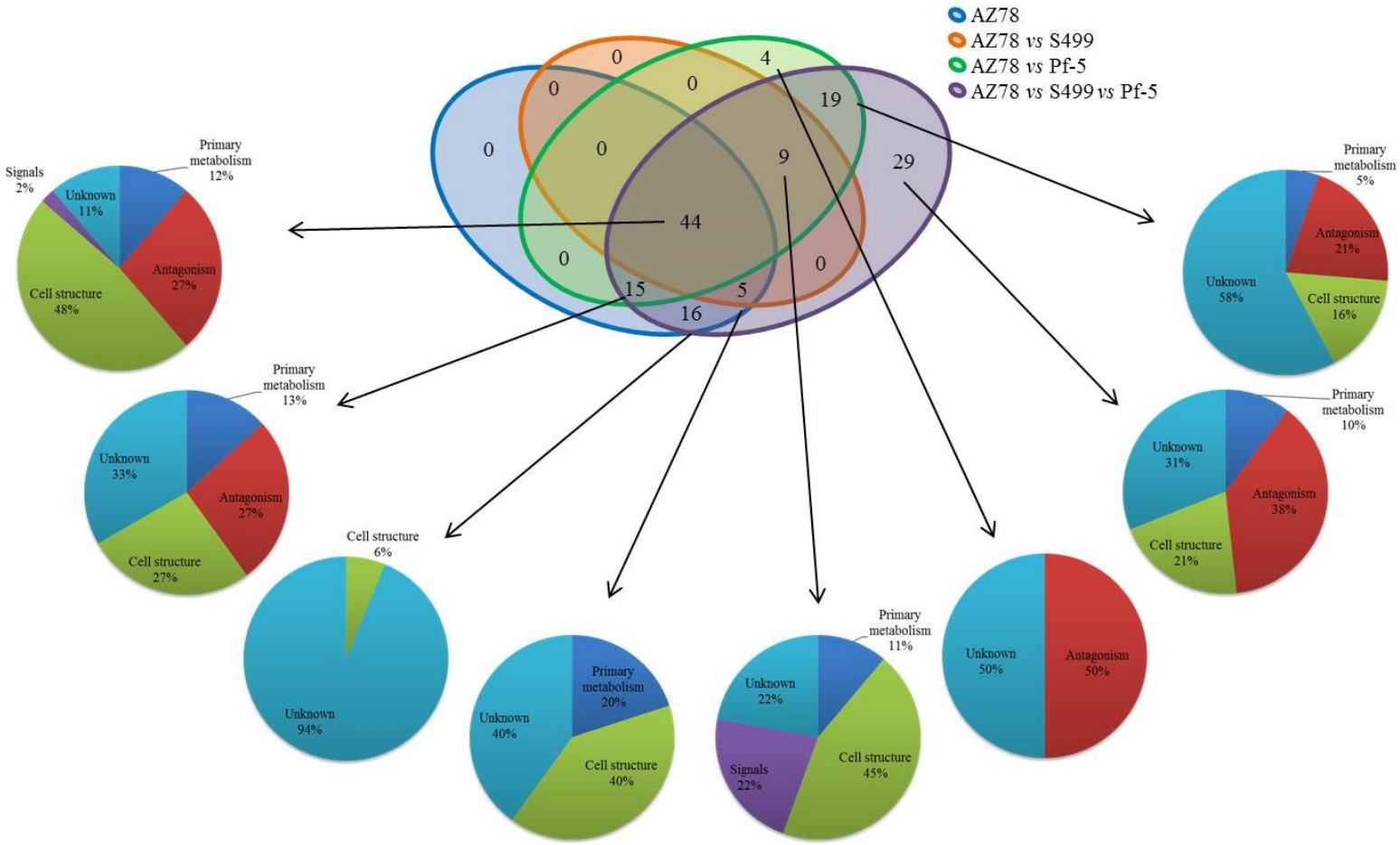
AZ78
AZ78 vs S499
AZ78 vs Pf-5
AZ78 vs S499 vs Pf-5
0
0
0
4
19
0
0
9
29
44
0
0
15
5
16
Primary metabolism 12%
Antagonism 27%
Cell structure 48%
Unknown 11%
Signals 2%
Primary metabolism 5%
Antagonism 21%
Cell structure 16%
Unknown 58%
Primary metabolism 13%
Antagonism 27%
Cell structure 27%
Unknown 33%
Cell structure 6%
Unknown 94%
Primary metabolism 20%
Cell structure 40%
Unknown 40%
Primary metabolism 11%
Cell structure 45%
Signals 22%
Unknown 22%
Unknown 50%
Antagonism 50%
Primary metabolism 10%
Antagonism 38%
Cell structure 21%
Unknown 31%

Figure 6

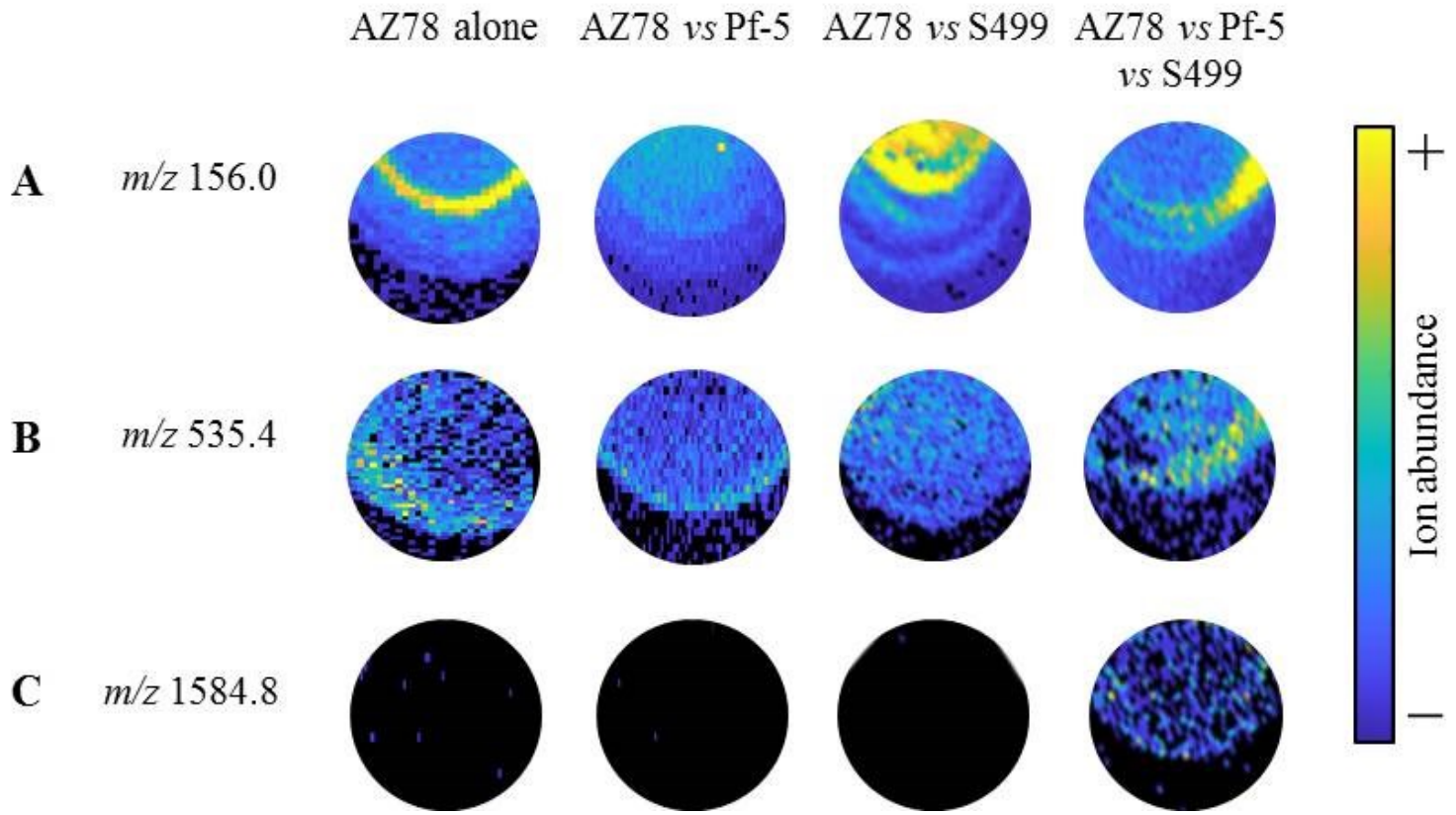

Figure 7

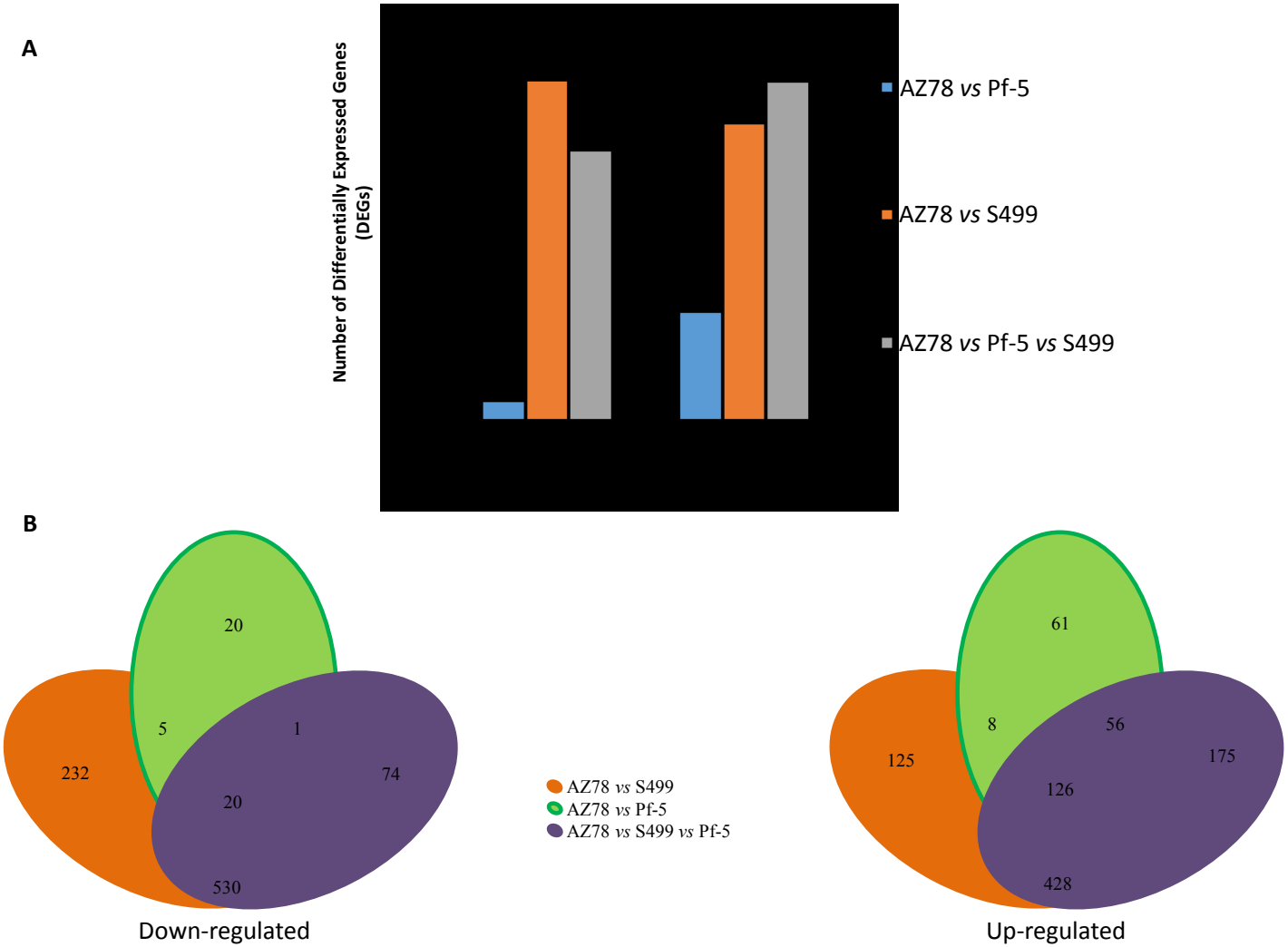
A
Number of Differentially Expressed Genes (DEGs)
AZ78 vs Pf-5
AZ78 vs S499
AZ78 vs Pf-5 vs S499
B
20
5
1
232
74
20
530
AZ78 vs S499
AZ78 vs Pf-5
AZ78 vs S499 vs Pf-5
Down-regulated
61
8
56
125
175
126
428
Up-regulated

Figure 8

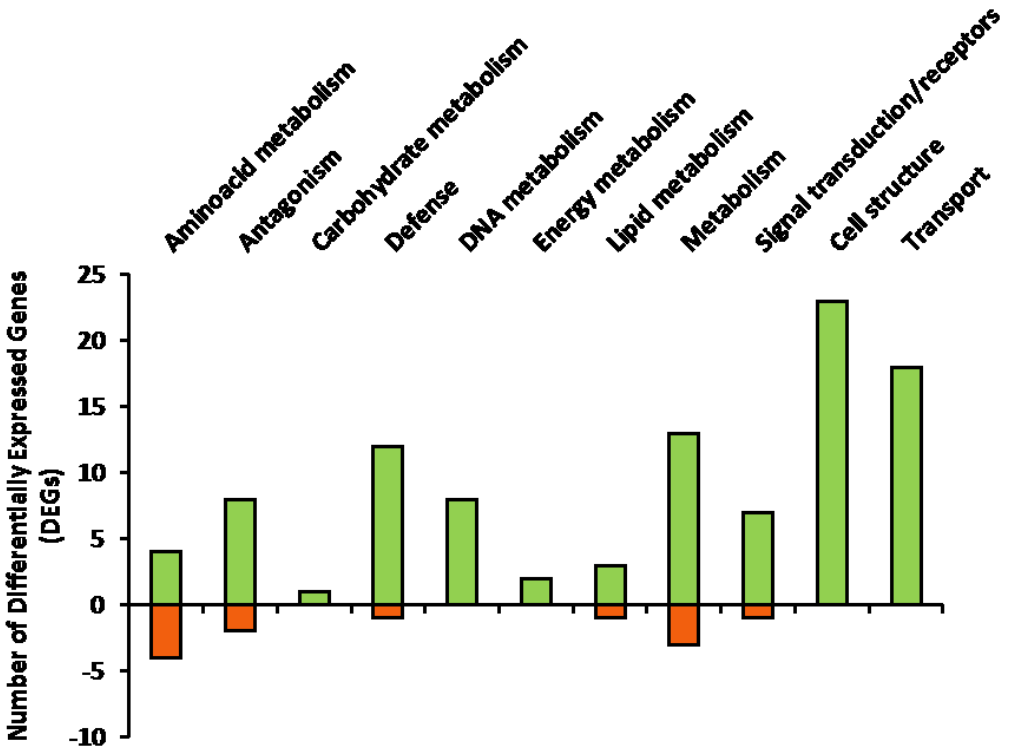
Aminoacid metabolism
Antagonism
Carbohydrate metabolism
Defense
DNA metabolism
Energy metabolism
Lipid metabolism
Metabolism
Signal transduction/receptors
Cell structure
Transport
Number of Differentially Expressed Genes (DEGs)
25
20
15
10
5
0
-5
-10

Figure S1

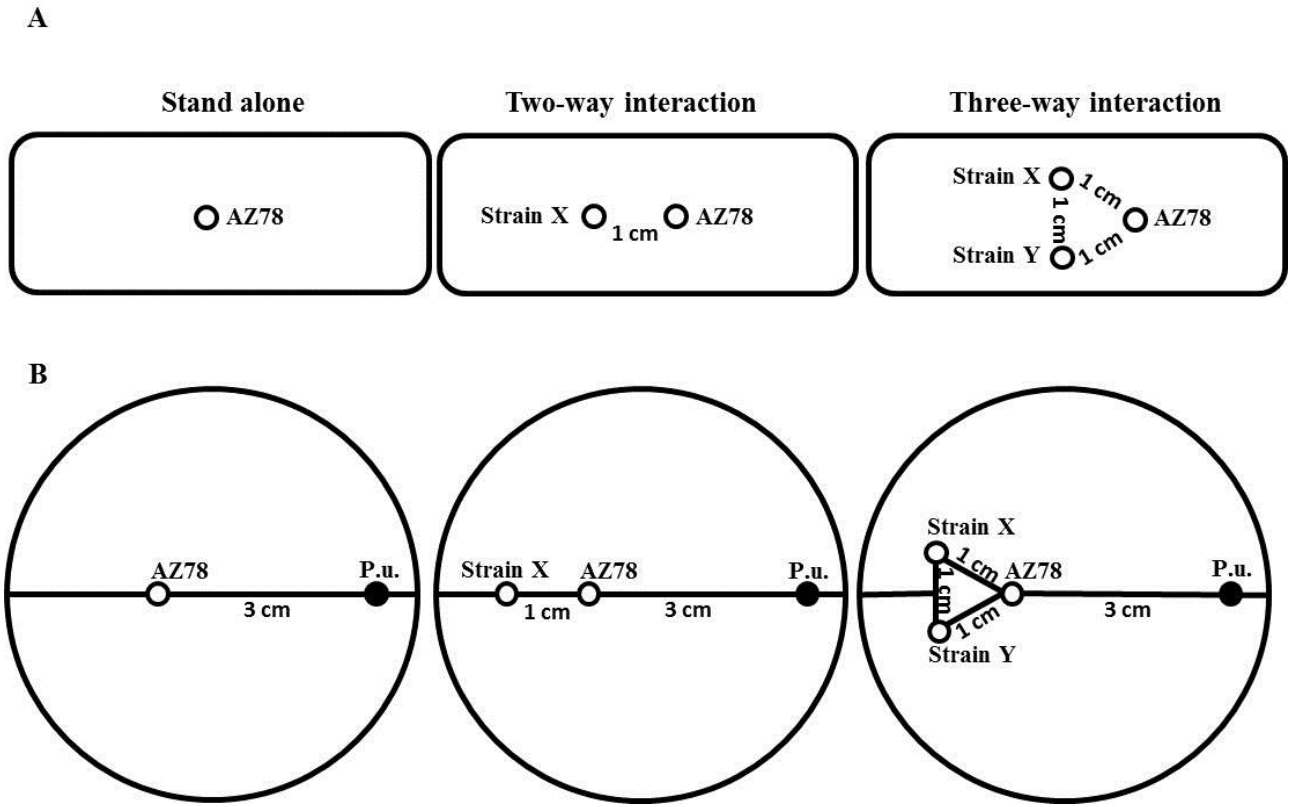
A
Stand alone
Two-way interaction
Three-way interaction
AZ78
Strain X
1 cm
AZ78
Strain X
1 cm
1 cm
1 cm
Strain Y
AZ78
B
AZ78
P.u.
3 cm
Strain X
AZ78
P.u.
1 cm
3 cm
Strain X
1 cm
1 cm
1 cm
AZ78
P.u.
3 cm
Strain Y

Chapter 4

The inhibitory activity of the biocontrol agent *Lysobacter capsici* AZ78 is negatively modulated by *Bacillus* spp. isolated from grapevine leaves

Francesca Brescia[1,2], Lisa Ioriatti[1], Oscar Giovannini[1], Gerardo Puopolo[1], Ilaria Pertot[1,3]

[1]Department of Sustainable Agro-Ecosystems and Bioresources, Research and Innovation Centre, Fondazione Edmund Mach (FEM), San Michele all'Adige, Italy; [2]Department of Agricultural, Food, Environmental and Animal Sciences, University of Udine, Udine; [3]Center Agriculture, Food, Environment, University of Trento, San Michele all'Adige, Italy

Email: francesca.brescia@guests.fmach.it

The bacterial genus *Lysobacter* includes different species that can produce molecules and lytic enzymes with activity against fungi and oomycetes (Panthee et al., 2016). For example, *L. capsici* AZ78 (AZ78) produces antibiotics that have a toxic effect on *P. viticola* sporangia (Puopolo et al., 2014a) and effectively controls *P. viticola*, both if used alone and in combination with copper (Puopolo et al., 2014b).

Since bacterial communities may modulate the antibiotic activity of biocontrol agents (De Boer, 2017), our aim was to determine how the interactions with phyllosphere-dwelling bacteria can influence AZ78 biocontrol activity in a simplified model system.

We recovered 47 bacterial isolates from leaves of *Vitis vinifera* L. cv. Pinot gris and Goldtraminer and identified them at species level by 16S rDNA phylogenetic analysis. To assess the impact of the 47 bacterial isolates on the in vitro inhibitory activity of AZ78, we designed experiments where the bacterial isolates and AZ78 were coinoculated on Luria Bertani Agar (LBA). Briefly, five µl of bacterial cell suspension ($\approx 10^9$ cells/ml) of AZ78 and bacterial isolates were spot-inoculated on LBA plates at 1 cm of distance. Once dried under laminar flow, LBA plates were incubated at 25°C.

After 48 h incubation, the plates were inoculated with 5 mm plugs of *Pythium ultimum* at 2.5 cm from AZ78 developed macrocolony. The controls consisted of LBA plates inoculated with *P. ultimum* alone, as well as *P. ultimum* inoculated with only AZ78 (2.5 cm of distance) and *P. ultimum* inoculated with only one bacterial isolate (3.5 cm of distance). After seven days incubation at 25°C, the growth area of *P. ultimum* was measured. To determine whether modulation of AZ78 inhibitory activity was due to changes in its viability, AZ78 viable cells were counted after 48 h of interaction with the bacterial isolate that had the most negative effect.

Most of the bacteria isolated from grapevine leaves were Gram-negative belonging to the γ-Proteobacteria, while the Gram-positive bacterial isolates belonged to Actinobacteria and Firmicutes (Figure 1). The interactions tests carried out in vitro revealed that most of the bacterial strains evaluated had a positive effect on AZ78 ability to inhibit *P. ultimum* growth (Figure 2). On the contrary, bacterial strains belonging to *Bacillus* spp. showed a negative effect on AZ78 inhibitory activity. In particular, the bacterial strain that had the most negative effect was *Bacillus* sp. L30 that reduced of the 18.8 ± 0.7% the ability of AZ78 to inhibit *P. ultimum* growth (Figure 3). However, there was one bacterial strain belonging to the genus *Bacillus* that was increasing of the AZ78 inhibitory activity against *P. ultimum, Bacillus* sp. L29 (Figure 3).

Although there was a significant decrease of viable cells when AZ78 was co-inoculated with L30 (8.90 ± 0.07 log10 cells/macrocolony) compared to the control (9.46 ± 0.04 log10 cells/macrocolony), this reduction was not enough to fully explain the drop in *P. ultimum* growth inhibition. Conversely, it is likely that AZ78 invested more energy in the protection against toxic secondary metabolites produced by *Bacillus* sp. L30 rather than the release of secondary metabolites active against *P. ultimum*.

These results show that the interactions among biocontrol agents and the natural microbiome are an important factor to be considered in evaluating their efficacy, since they can modify the inhibitory activity either in a positive or in a negative way. In light of that, more studies are required to consider the variation in AZ78 gene expression, taking into account the plant response as well.

Keywords

***Lysobacter*, *Bacillus*, inhibitory activity, biocontrol agents, microbial interactions**

References

De Boer, W. 2017: Upscaling of fungal-bacterial interactions: from the lab to the field. Curr. Opin. Microbiol. 37: 35-41.

Felsenstein, J., 1985. Confidence limits on phylogenies: an approach using the Bootstrap. Evolution 39, 783–791.

Kimura, M. 1980. A simple method for estimating evolutionary rates of base substitutions through comparative studies of nucleotide sequences. J. Mol. Evol. 16, 111–120.

Kumar, S., Stecher, G., Tamura, K. 2016. MEGA7: Molecular Evolutionary Genetics Analysis Version 7.0 for Bigger Datasets. Mol. Biol. Evol. 33, 1870–1874.

Panthee, S., Hamamoto, H., Paudel, A. & Sekimizu, K. 2016: Lysobacter species: a potential source of novel antibiotics. Arch. Microbiol. 198: 839-845.

Puopolo, G., Cimmino, A., Palmieri, M.C., Giovannini, O., Evidente, A. & Pertot, I. 2014a: Lysobacter capsici AZ78 produces cyclo(L-Pro-L-Tyr), a 2,5-diketopiperazine

with toxic activity against sporangia of Phytophthora infestans and Plasmopara viticola. J. Appl. Microbiol. 117: 1168-1180.

Puopolo, G., Giovannini, O. & Pertot, I. 2014b: Lysobacter capsici AZ78 can be combined with copper to effectively control Plasmopara viticola on grapevine. Microbiol. Res. 169: 633-642.

Saitou, N., Nei, M. 1987. The neighbor–joining method: a new method for reconstructing phylogenetic trees. Mol. Biol. Evol. 4, 406–25.

Figure legends

Figure 1. Phylogenetic analysis of the phyllosphere bacterial isolates.

Phylogenetic tree resulting from analysis of the 16S rRNA gene sequences of phyllosphere bacterial isolates. GenBank was used to collect genes encoding 16S rRNA from type strain bacteria. Once aligned by ClustalW, the alignment profile was used to construct the optimal phylogenetic tree using the Neighbour-Joining method (Saitou and Nei, 1987) and the evolutionary distances were computed using the Kimura's two-parameter model (Kimura, 1980). Bootstrap values (1000 replicates) higher than 70 are shown next to the branches (Felsenstein, 1985). All the phylogenetic analyses were carried out using MEGA7 (Kumar et al., 2016).

Figure 2. Modulation of the inhibitory activity of *Lysobacter capsici* AZ78 during a two-way interaction with the phyllosphere bacterial strains. The impact of two-way interactions with each phyllosphere bacterial isolate on *L. capsici* AZ78 inhibitory activity was determined according to $[(A_c - A_i)/A_c] \times 100$

where A_c is *P. ultimum* growth area in presence of AZ78 grown alone and A_i is *P. ultimum* growth area in presence of AZ78 grown in two-way interactions. Columns represent mean ± standard error.

Figure 3. Modulation of the inhibitory activity of *Lysobacter capsici* AZ78 during a two-way interaction with *Bacillus thuringiensis* L29 and *Bacillus pumilus* L30. The impact of two-way interactions with *Bacillus thuringiensis* L29 and *Bacillus pumilus* L30 on *L. capsici* AZ78 inhibitory activity was determined according to $[(A_c - A_i)/A_c] \times 100$

where A_c is *P. ultimum* growth area in presence of AZ78 grown alone and A_i is *P. ultimum* growth area in presence of AZ78 grown in two-way interactions. Columns

represent mean ± standard error. The asterisk indicate values that differ significantly according to Student's t-test ($\alpha = 0.05$).

Figure 1

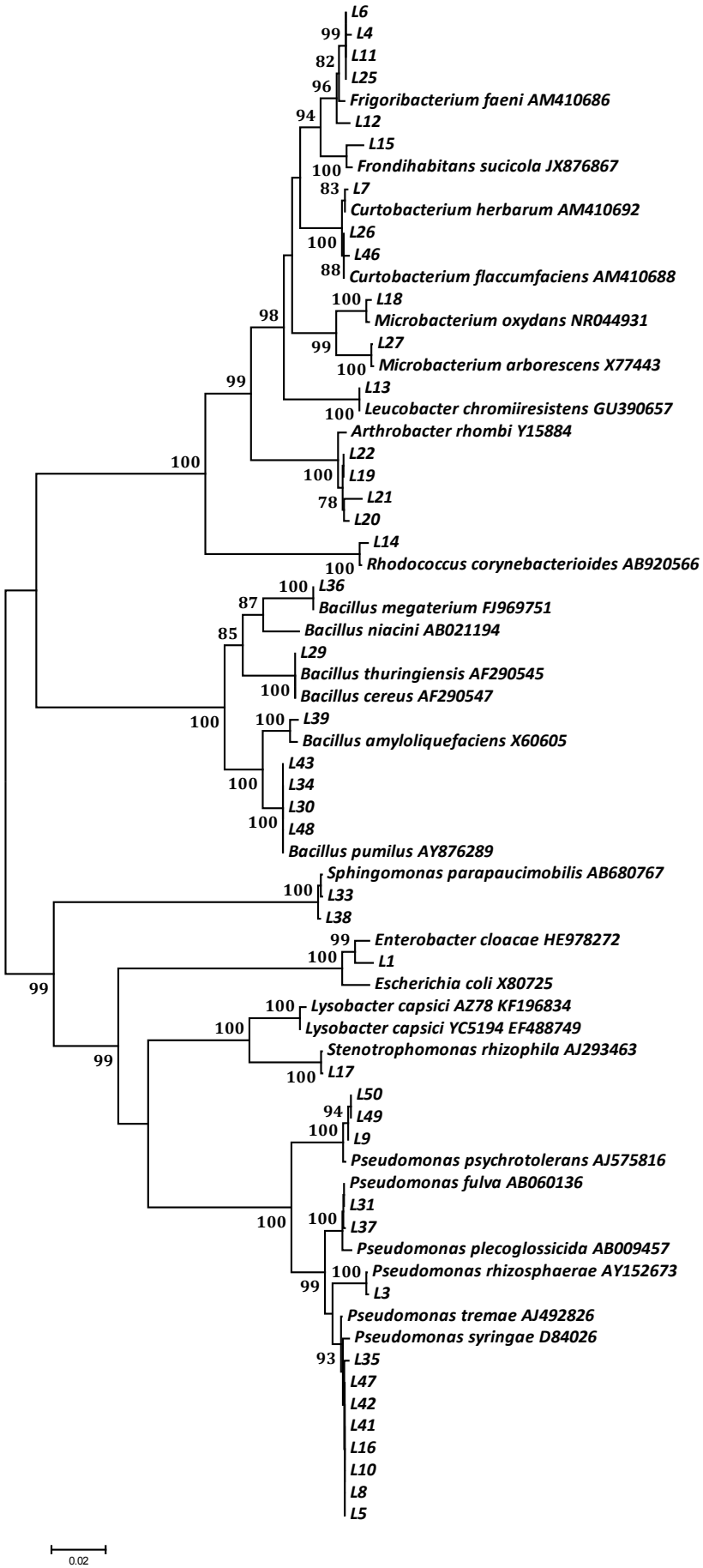
L6
99
L4
82
L11
L25
96
Frigoribacterium faeni AM410686
94
L12
L15
100
Frondihabitans sucicola JX876867
83
L7
Curtobacterium herbarum AM410692
L26
100
L46
88
Curtobacterium flaccumfaciens AM410688
100
L18
98
Microbacterium oxydans NR044931
99
L27
100
Microbacterium arborescens X77443
99
L13
100
Leucobacter chromiiresistens GU390657
Arthrobacter rhombi Y15884
100
L22
100
L19
78
L21
L20
L14
100
Rhodococcus corynebacterioides AB920566
100
L36
87
Bacillus megaterium FJ969751
Bacillus niacini AB021194
85
L29
Bacillus thuringiensis AF290545
100
Bacillus cereus AF290547
100
100
L39
Bacillus amyloliquefaciens X60605
L43
100
L34
L30
100
L48
Bacillus pumilus AY876289
Sphingomonas parapaucimobilis AB680767
100
L33
L38
99
Enterobacter cloacae HE978272
100
L1
99
Escherichia coli X80725
100
Lysobacter capsici AZ78 KF196834
100
Lysobacter capsici YC5194 EF488749
Stenotrophomonas rhizophila AJ293463
99
100
L17
L50
94
L49
100
L9
Pseudomonas psychrotolerans AJ575816
Pseudomonas fulva AB060136
L31
100
100
L37
Pseudomonas plecoglossicida AB009457
100
Pseudomonas rhizosphaerae AY152673
99
L3
Pseudomonas tremae AJ492826
Pseudomonas syringae D84026
93
L35
L47
L42
L41
L16
L10
L8
L5
0.02

Figure 2

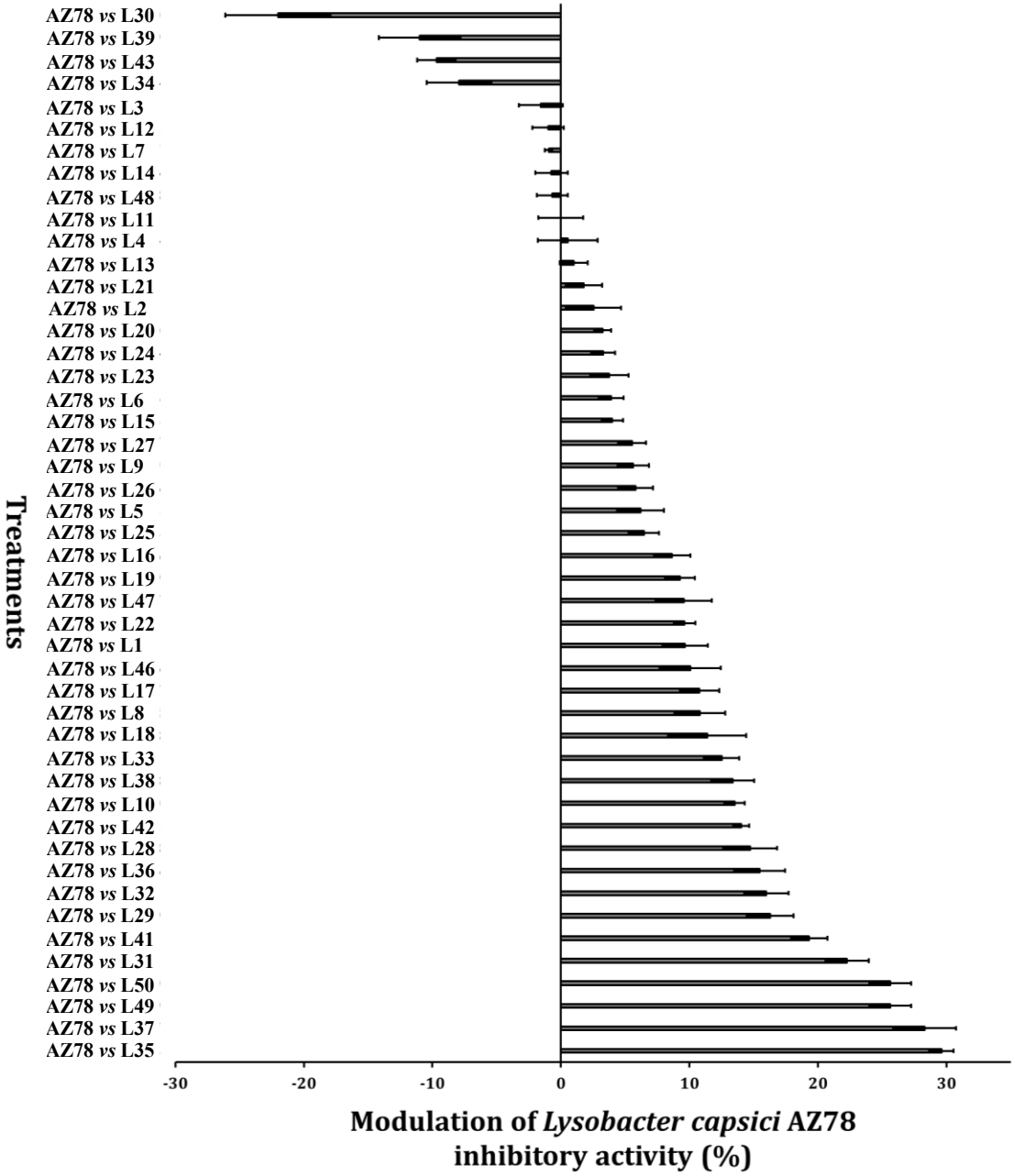
AZ78 vs L30
AZ78 vs L39
AZ78 vs L43
AZ78 vs L34
AZ78 vs L3
AZ78 vs L12
AZ78 vs L7
AZ78 vs L14
AZ78 vs L48
AZ78 vs L11
AZ78 vs L4
AZ78 vs L13
AZ78 vs L21
AZ78 vs L2
AZ78 vs L20
AZ78 vs L24
AZ78 vs L23
AZ78 vs L6
AZ78 vs L15
AZ78 vs L27
AZ78 vs L9
AZ78 vs L26
AZ78 vs L5
AZ78 vs L25
AZ78 vs L16
AZ78 vs L19
AZ78 vs L47
AZ78 vs L22
AZ78 vs L1
AZ78 vs L46
AZ78 vs L17
AZ78 vs L8
AZ78 vs L18
AZ78 vs L33
AZ78 vs L38
AZ78 vs L10
AZ78 vs L42
AZ78 vs L28
AZ78 vs L36
AZ78 vs L32
AZ78 vs L29
AZ78 vs L41
AZ78 vs L31
AZ78 vs L50
AZ78 vs L49
AZ78 vs L37
AZ78 vs L35
Treatments
-30
-20
-10
0
10
20
30
Modulation of Lysobacter capsici AZ78 inhibitory activity (%)

Figure 3

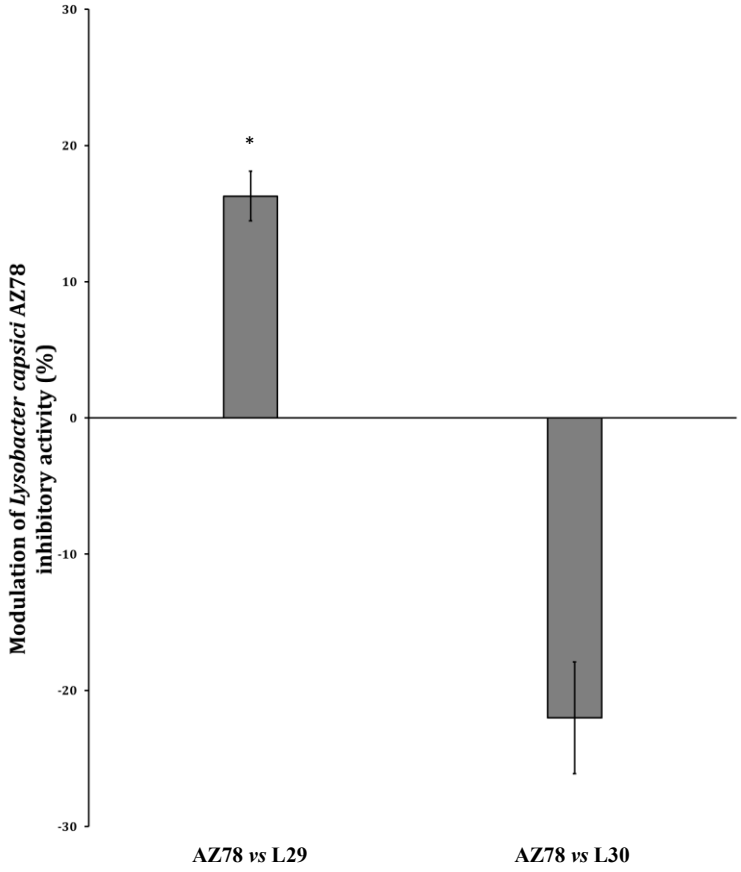
30
20
10
0
-10
-20
-30
*
Modulation of Lysobacter capsici AZ78 inhibitory activity (%)
AZ78 vs L29
AZ78 vs L30

Conclusions

During this PhD thesis, the effects of rhizosphere nutrients and the interactions with the rhizosphere and phyllospere-associated microbiota in shaping *Lysobacter capsici* AZ78 (AZ78) behaviour were dissected by using a multitechnique approach. A growth medium formulated to mimic the rhizosphere niche was a valid tool to analyse AZ78 physiological traits in a controlled and reproducible set-up. Traits that play a key role in the rhizosphere colonisation, such as cell motility, biofilm formation and biosynthesis of bioactive secondary metabolites, were activated when AZ78 was grown on this growth medium, confirming the AZ78 ability to successfully colonise and persist in the plant rhizosphere.

However, the effective colonisation of the plant rhizosphere may also depend on the interactions that occur between the rhizosphere inhabitants. Indeed, this ecological niche is densely populated and is characterised by an intense competition for resources. The study of the impact of the two rhizosphere-associated bacterial strains, *Bacillus amyloliquefaciens* S499 and *Pseudomonas protegens* Pf-5, on AZ78 behaviour in the rhizosphere brought the complexity of microbial interactions. In fact, AZ78 motility, a fundamental trait to colonise favourable environments before competitors, was impaired by the presence of the other strains. However, the effect of Pf-5 differed from S499, inducing the increase of both AZ78 production of broad-spectrum antagonism metabolites and inhibitory activity against the phytopathogenic oomycete *Pythium ultimum*. Drastic negative effects on AZ78 physiology and inhibitory activity were due to the presence of S499, negatively modulating its secondary metabolite production. Intriguingly, the outcome of the three-way interaction was even different, with a mitigation of the negative effect of S499 due to the presence of Pf-5. During all the

interactions considered, AZ78 activated a defence response against oxydative stress and for the detoxyfication from antibiotics produced by competitors. The resuts obtained suggested that an intense competition for resources was occurring among the strains of this simplified model system.

Interestingly, the study of the influence of phyllosphere associated bacteria on the AZ78 antagonism activity was consistent with the trends registered for the interactions in the rhizosphere niche. Indeed, the bacterial strains having the most negative effect on AZ78 inhibitory activity were *Bacillus* spp.. Conversely, the majority of the Gram-negative strains, most of them belonging to the genus *Pseudomonas*, was increasing AZ78 antagonism activity, consistently with the results obtained for the rhizosphere niche.

The results achieved in this PhD thesis show that the nutrient conditions and the interactions occurring between *Lysobacter* spp. and the plant-associated microbiota are important factors to be considered in the study of this genus. It is increasingly clear that the plant microbiota is strictly linked with plant health, thus the study of microbial interactions is fundamental for the protection of crop plants, as they influence the establishment of beneficial microorganisms in plant-related ecological niches.

The study of microbial interactions in plant niches may lead to the formulation of a biocontrol consortium combining the biocontrol ability of different strains active against different pests. However, in the future more studies will be required to consider a more complex interaction-network involving also the plant, focussing for instance on the induction of resistance mechanisms.

Funding

The PhD project has been funded with support from Fondazione Edmund Mach.

Part of the project has been funded with a STSM COMULIS (Correlated Multimodal Imaging in Life Sciences) COST Action CA17121.

Aknowledgments

At the end of this PhD work, I can say that I have profoundly changed and grown wiser. It wasn't easy, it wasn't at all, but if I'm here now, it is also because of all the people who accompanied and supported me throughout this tortuous path.

All my gratitude and respect go to Prof. Gerardo Puopolo, my mentor. I will never thank him enough for conveying to me his passion for research, for his constant and precious support, for trusting me and for his wise guidance through the years. Without him, all this would not be possible.

I thank Prof. Martina Marchetti-Deschmann not only for giving me the opportunity to be a visiting PhD student in her lab at the Technical University of Vienna for 7 months and learn the complex technique of MALDI TOF MSI, but also for her supervision and for her trust and encouragement when I felt that I was drowning in too much data.

I thank Prof. Michele Perazzolli, for his precious suggestions and guidance, especially with the molecular biology part of my work, and for his constant support during the doctoral work.

I thank Prof. Rita Musetti for passionately introducing me to the fascinating world of Electron Microscopy.

I thank Samuele Zoratto for introducing me to MALDI TOF MSI and for his support in managing the instrument. Especially, I thank him for giving me a warm welcome in Vienna and for being a supportive friend. I also thank all my colleagues at the Vienna TU for including me in their nice group and for their friendly support during my work there.

A special thanks goes to all my colleagues, friends and companions of adventures at FEM for accompanying me with cheerfulness during my work, for sharing the joys and the sad moments with me, and for making me feel at home, even if I was far from my parents and my family. Especially, I want to thank Carmela Sicher, Oscar Giovannini, Lisa Ioriatti and Romane Hellec that gave me a great help with part of the microbiology experiments.

And, eventually, I thank my parents and my family for their constant support in all my choices, even if they brought me far from home, for their daily help and for their love.